33106

INVESTIGATION AND PERFORMANCE OF CONCRETE LIGHT-WEIGHT SANDWICH CONSTRUCTION

PANAYIOTIS SPYRIDON ARMPIS

A Thesis

in

The Faculty

of

Engineering

Presented in Partial Fulfillment of the Requirements for
the Degree of Master of Engineering at
Concordia University
Montreal, Quebec, Canada

September, 1976

© Panayiotis Spyridon Armpis 1977

To my Mother and

in memory of my Father

ABSTRACT

Panayiotis Spyridon Armpis

INVESTIGATION AND PERFORMANCE OF CONCRETE LIGHT-WEIGHT SANDWICH CONSTRUCTION

The Constant Module (CM) System utilizes a single element composed of a 3½' x 10' panel with two integral corner posts 4' in height. Four such elements are assembled to form an enclosure which can function as a shipping container for wheat, or as part of a house.

The dual function holds novel promise as means of distributing grain to developing countries with housing as a secondary benefit.

In developing the structural element (CM Panel) the prime requirement was for low cost lightweight sandwich panel suitable for mass production in any part of the world. The program of development and testing was aimed at finding a novel combination of materials which best satisfied the criteria of strength, weight and cost. The work described deals with panels composed of 1/4" thick skins of Latex Modified Concrete (LMC) using lightweight aggregate with steel mesh or glass cloth reinforcement in conjunction with cores of pre-expanded polystyrene beads, bonded with Portland cement and Latex, or Kraft paper honeycomb.

ACKNOWLEDGEMENTS

The author wishes to express his thanks to his supervisor, Professor Cedric Marsh for his encouragement and advice, to the Trebron Holdings Ltd., where the CONSTANT MODULE SYSTEM concept originates, to the Federal Department of Housing and Transportation of Canada for providing the research funds, and to the personnel of Albert E. Sargent Memorial Structures Laboratories of Sir George Williams Campus at Concordia University.

TABLE OF CONTENTS

PAGE

LIST OF TABLES

LIST OF FIGURES

FIGURES PAGE

NOMENCLATURE

f'_c, ε_c	=	Compressive strength, Compressive strain
f_t, ε_t	=	Tensile strength, Elongation of figure-eight specimens
E, E_f, E_c	=	Modulii of elasticity, f = face material, c = core material
σ_f, σ_c	=	Flexural stresses in faces and core respectively
G	=	Modulus of rigidity
τ	=	Shear stress
γ	=	Shear strain
ρ_f, ρ_c	=	Density of face and core materials respectively
Q	=	First moment of area.
x, y, z	=	Cartesian coordinates with z normal to the faces and positive downwards. In a beam x lies along the principal axis of the member
b	=	Width of beam
t	=	Face thickness
d	=	Distance between centre-lines of faces = $\frac{h + c}{2}$
h	=	Total thickness of sandwich
L	=	Span
I_f	=	Sum of moments of inertia of faces about their own separate axes
I_o	=	Total moment of inertia of both faces about the beam's centroidal axis
D	=	Bending stiffness of sandwich beam (EI)
q	=	Distributed transverse load, per unit length
W	=	Point load
V	=	Shear force

M = Bending moment

Δ = Deflection at mid-span or mid-point

$A = \frac{bd^2}{c}$

CHAPTER 1

INTRODUCTION

CHAPTER 1

INTRODUCTION

In this research work the performance of lightweight sandwich construction using concrete as a face material, along with the use of styropor-filled lightweight concrete and paper honeycomb as core materials is investigated.

In order for concrete to be used in the small thicknesses required for this type of sandwich construction its mechanical properties have to be improved. Furthermore, the nature and use of sandwich panels in the building industry demand improved physical properties of the concrete, such as hardness, water penetration resistance, sound absorption, fire protection, etc.

The improvement of mechanical and physical properties of concrete through the addition of polymer latexes is investigated.

Core materials in sandwich construction, apart from the special function of stabilizing the faces in their planes with respect to each other, are required to provide thermal insulation.

Two types of core materials are proposed, namly an extremely light-weight type of concrete using expanded polystyrene beads as aggregate (styropor) and kraft paper honeycombs.

The influence on properties of various formulations, and mixing techniques for the styropor core; and the shear strengths of kraft paper honeycombs are studied.

The applicability of the theory of sandwich construction is explained in order to interpret the experimental results on complete panels.

There is a requirement to join panels such that their full moment capacity can be developed. Several variations are studied.

CHAPTER 2

LATEX MODIFIED CONCRETES AS FACE MATERIAL

CHAPTER 2

LATEX MODIFIED CONCRETES AS FACE MATERIAL

2.1 INTRODUCTION

Concrete and cement mortars perform well in compression, however, they are poor in tension and wear and hence, require modification for special areas of application.

The use of ordinary concrete or cement mortars as a sole thin face material in sandwich construction is not acceptable. However, the addition of polymer Latexes in mortars can improve the mechanical properties of these systems and permit them to be used for this special application. In this investigation, the polymer styrene butadiene[1] was used throughout the laboratory work.

2.2 POLYMER LATEXES

Synthetic latexes are polymer (plastic) particles dispersed in water. They have very good compatibility with Portland cement and can greatly improve the mechanical and physical properties of concrete and mortars such as bond, tensile, compressive and flexural strength, toughness and hardness. The durability of these systems is also greatly improved (freeze-thaw and chemical resistance). Table 2.1 shows some typical latex properties.

The advantages of Latex Modified Concrete (LMC) are easily appreciated from the histograms shown in Figure 2.1

TABLE 2.1

BASIC LATEX PROPERTIES[1]

Polymer Type	Styrene Butadiene Emulsion	Saran Emulsion
Stabilizer type	Non-Ionic	Non-Ionic
Percent solids	48%	50%
Specific gravity (25 °C)	1.01	1.23
Weight per Gallon (lbs at 25 °C)	8.4	10.25
pH	10.5	2.0
Particle size range (angstrome)	2000	1400
Surface tension at 25 °C (Dynes/square centimeter)	32	33
Freeze-thaw stability	5 cycles (-15°C to 25°C)	none
Specific gravity of latex solids	1.03	1.60
Film forming (25 °C) (4 °C)	yes yes	yes no
Self time	> 2 years	6 months

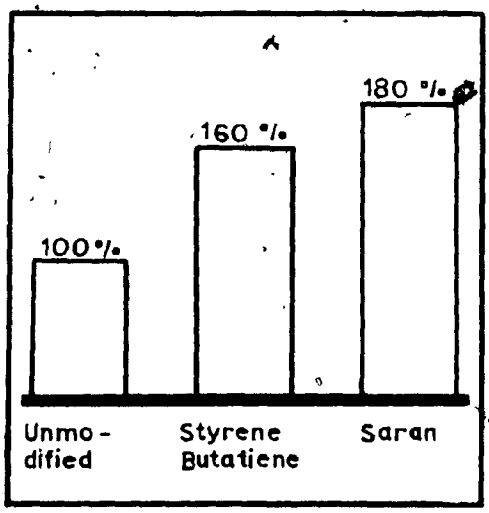

Typical Compressive Strength

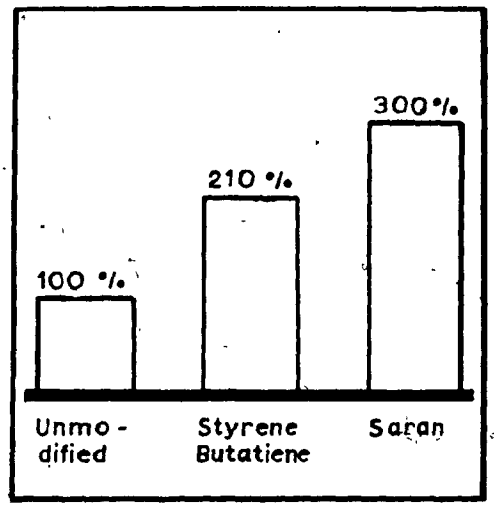

Typical Tensile Strength

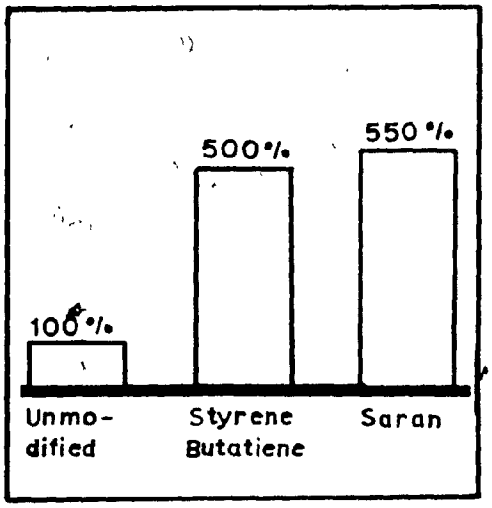

Typical Shear Bond Strength

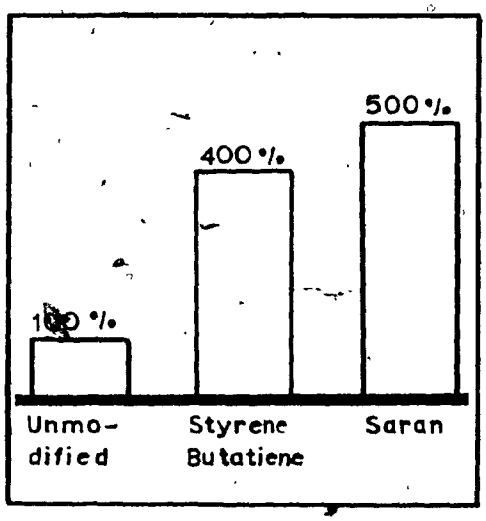

Typical Flexural Strength

FIG. 2.1 TYPICAL MORTAR PROPERTY IMPROVEMENT USING POLYMER LATEXES, DOW LATEX 460 (STYRENE BUTADIENE) AND DOW LATEX 464 (SARAN)

for two different types of latexes. More figures for comparison of mechanical properties are listed in Appendix "A".

2.3 FORMULATIONS AND MIXING

Any type of Portland cement may be used except the air-entrained ones (Type 1A, 2A, or 3A). White Portland cement, waterproof Portland cement and aluminite cement can also be used for special applications.

Styrene butadiene and saran latexes can be used efficiently and economically at a latex solids-to-cement ratio of 0.10 to 0.20 and 0.15 to 0.30, respectively, based on the weight of Portland cement.

Both of these latexes when used with Portland cement react to produce millions of tiny gas bubbles, resulting in an air-entrained system. Although this contributes greatly to the workability of the mix, it also reduces its strength and quality. In order to minimize the air content of latex mortars, antifoamers are used. The antifoamer ANTIFOAM B[1] was used in this investigation from .3% to .4% of the weight of Latex solids. It is capable of limiting the air content of latex mortars to the range of 3% to 10% by volume, depending on the formulation and the type of mixing used.

---

[1] A product of Dow Corning Corporation.

In addition, there is no limit to the number of additives that can be used with the basic ingredients in order to change some of the properties of the concrete and mortars. For example, diethylene glycol, a humectant, acts as a retarder and it can also slow down the differential setting on the surface of LMC mortar, with respect to the inside.

Any mechanical mixer can be used and the materials can be proportioned by either weight or volume. A recommended sequence of mixing operations is as follows:

(i) Add antifoamer and stir into the latex
(ii) Pour latex into the mixer (with antifoamer)
(iii) Add one half the mixing water
(iv) Add sand
(v) Add Portland cement
(vi) Add diethylene glycol, if used
(vii) Add the remainder of the mixing water

It is essential that the mixer should run during the addition of all ingredients and most important, the total mixing time should not exceed five minutes. However, a somewhat different mixing procedure was adopted in the laboratory work conducted and the author claims consistently better results than the average published ones [1] with the same proportioning and type of latex, air-curing conditions and weaker aggregates (expanded shale). The main difference

in mixing was that the surface saturated sand Mel-lite aggregates were first thoroughly mixed with the Portland cement and then the combined latex-water-antifoamer solution was added at an initially faster rate. It is noted here that in the development of styropor-filled lightweight concrete different mixing procedures were adopted, as explained in Chapter 3.

2.4 FEASIBILITY TESTS ON LMC MORTARS

2.4.1 Types of Tests and Test Procedures

Compressive strength tests (ASTM C109-70 T) with 3" diameter by 6" cylinders, and 2" cubes, and direct tensile strength tests (ASTM C190-70) with figure-eight specimens of 1, 1/2 and 1/4 square inch cross-sections were conducted (Figure 2.2).

The static modulus of elasticity was obtained from the stress-strain curve in compression. Toughness was considered as the area under the stress strain curve between zero and the maximum compressive stress.

A Tinius-Olsen testing machine was used on which a recording device was attached so that the load vs. compression-elongation was recorded in a graph form.

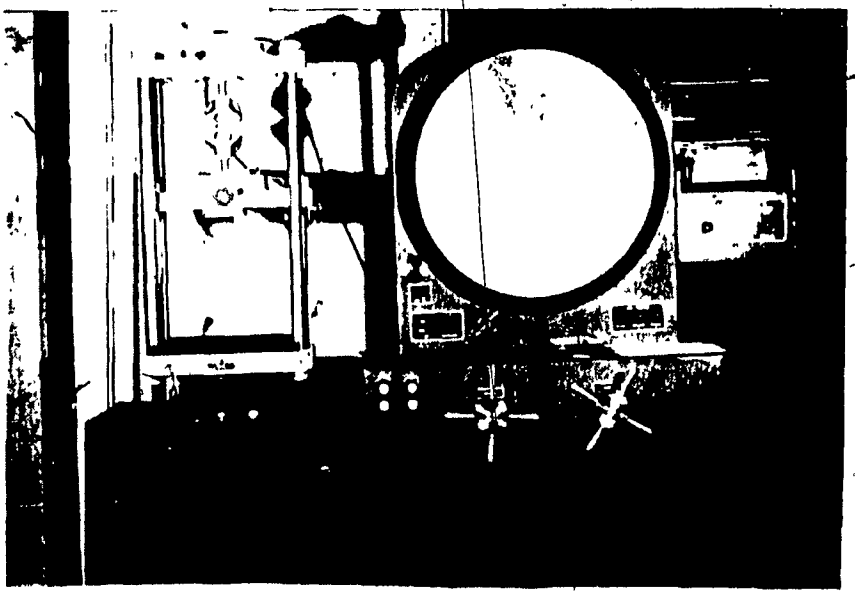

(a)

(b)

FIG. 2.2 (a) TENSION TEST (ASTM C190-70) WITH FIGURE-EIGHT SPECIMENS

(b) TESTED COMPRESSION SPECIMENS (ASTM C109-70T)

#4-0 SIEVE SIZE MEL-lite AGGREGATE (LEFT), WASHED SAND (RIGHT)

2.4.2 Materials and Specimens

Two types of aggregates were used; MEL-lite[2], 1/4"-0 in size aggregates, and washed sand. Type III Portland cement was used with a saturated surface aggregate-to-cement ratio of 3:1 by weight, along with styrene-butadiene emulsion (Dow Latex 460).

The specimens were cured in the air at laboratory temperatures for 14 days. Latex and water contents were varied. Note that in one of the series of test specimens, Mel-lite aggregates passing sieve #12 were used. The gradation was checked and found to be:

Sieve	% Passing
# 12	100
# 16	75
# 30	39
# 50	8
# 100	1.5

having a fineness modulus of 2.76, medium sand.

---

[2]Rotary kiln expanded shale aggregate, a product of Avon Aggregates Ltd., Moncton, N.B., Canada.

2.5 MECHANICAL AND PHYSICAL PROPERTIES OF LMC MORTARS - TEST RESULTS

2.5.1 Compressive Strength (f'_c) and Modulus of Elasticity (E_c)

The use of lightweight aggregates produced lightweight concrete mortars of comparable strength to normal mortars. Compressive strength and modulus of elasticity are decreased as the latex content is increased. Table 2.2 lists some results of a series of tests. Compressive strengths as high as f'_c = 7530 psi (530 kgf/cm^2) were obtained from specimens in series C1 at 90 days. The range of $\frac{w}{c}$ ratio between .30 and .40 does not seem to influence the f'_c of LMC mortars. In Fig. 2.3, some characteristic compressive stress-strain cures are plotted.

The static secant modulus at the point of $\frac{1}{3} f'_c$ on the stress-strain curve was taken as the value of E_c. A maximum reduction of E_c equal to 45% was estimated from all series of specimens.

2.5.2 Compressive Strength (f'_c) and Direct Tensile Strength (f_t)

The ratio of f_t to f'_c was estimated in the range of $\frac{1}{5}$ to $\frac{1}{9}$ for both expanded shale and sand aggregates, as compared to the range of $\frac{1}{9}$ to $\frac{1}{15}$ for unmodified mortars.

Typical tensile stress-elongation curves are reproduced

TABLE 2.2 (1)

MECHANICAL PROPERTIES OF LMC MORTARS AT 14 DAYS WITH TYPE III CEMENT

Specimen Series	Type of Aggregate (Passig Sieve)	Pol. Solids / Cement Ratio by Weight	W/C Ratio by Weight	Unit Weight of Mortar (W_c) lb/ft^3 (kg/m^3)
C1	MEL-lite (#4-0)	.15	.40	109(1746)
C2	MEL-lite (#4-0)	.20	.40	111(1778)
C3	MEL-lite (#12-0)	.15	.40	120(1922)
C4	MEL-lite (#12-0)	.20	.40	123(1970)
C5	Sand	.15	.30	135(2163)
C6	Sand	.15	.40	130(2083)
C7	MEL-lite (#8-0) and Sand	.15*	.30	115(1842)

* No Antifoam used.

Elongation at Maximum Strength: 0.13 to 0.23 in(.33 to .58 cm.)

(continued) TABLE 2.2 (2)

Specimen Series	Compressive Strength (f'_c) psi(kgf/cm^2)	Tensile Strength (f_t) psi(kgf/cm^2)	Modulus of Elasticity (E) psi x 10^6 (kgf/cm^2)	Compressive Strain at Max. Strength x 10^{-3} in/in(cm/cm)
C1	6300(443)	675(47.5)	2.068(.145)	4.35
C2	5700(400)	540(38)	1.714(.120)	5.7
C3	6000(422)	1042(73.3)	2.00(.140)	4.8
C4	5140(362)	750(53)	1.92(.135)	5.5
C5	5370(378)	770(54)	1.84(.129)	6.0
C6	6000(422)	610(43.0)	1.87(.131)	5.5
C7	5530(389)	1000(70.3)	-	4.10
Elongation at Maximum Strength: 0.13 to 0.23 in(.33 to .58 cm.)				

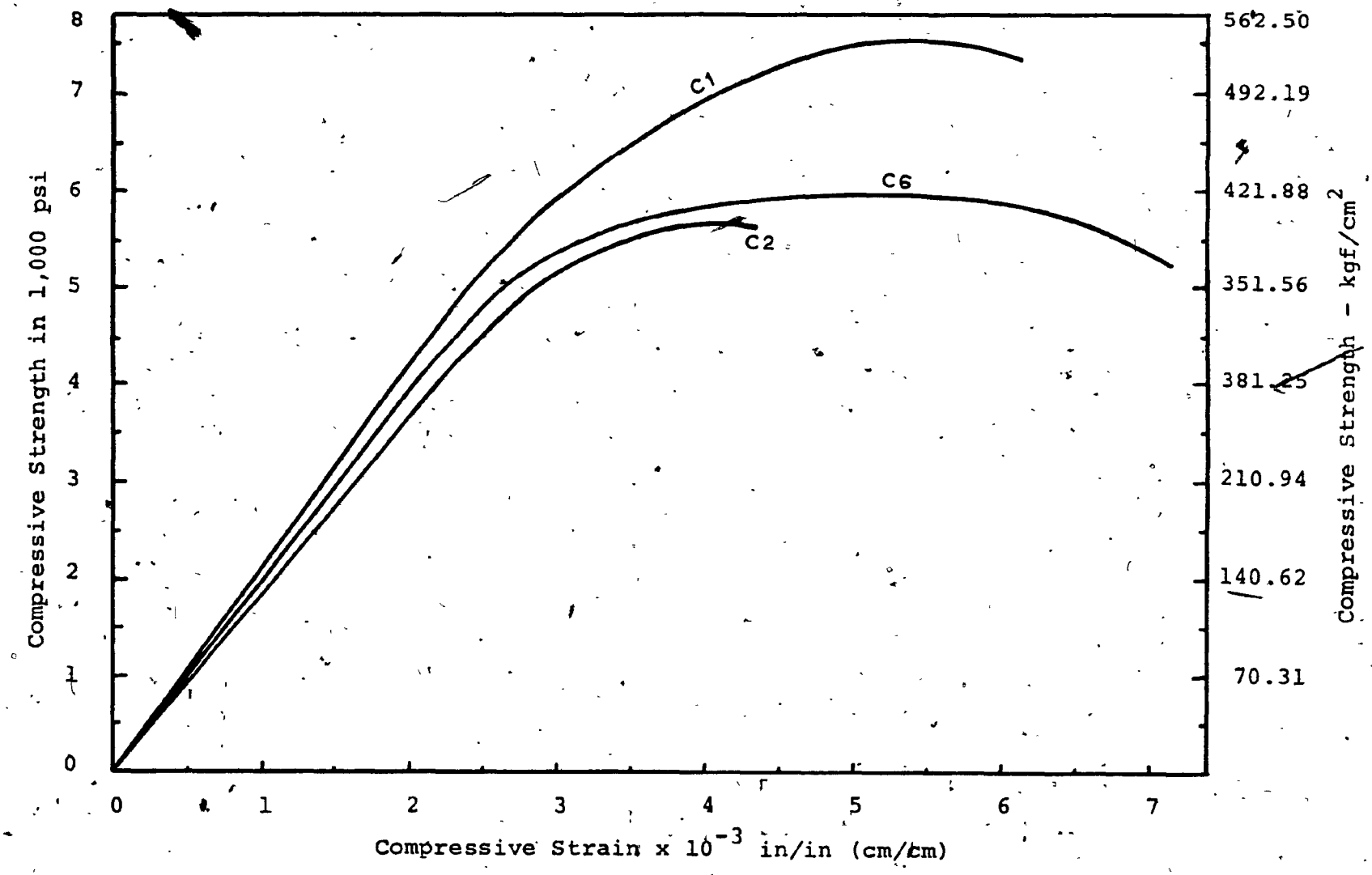

FIG. 2.3 CHARACTERISTIC COMPRESSIVE STRESS-STRAIN CURVES FOR LMC MORTARS

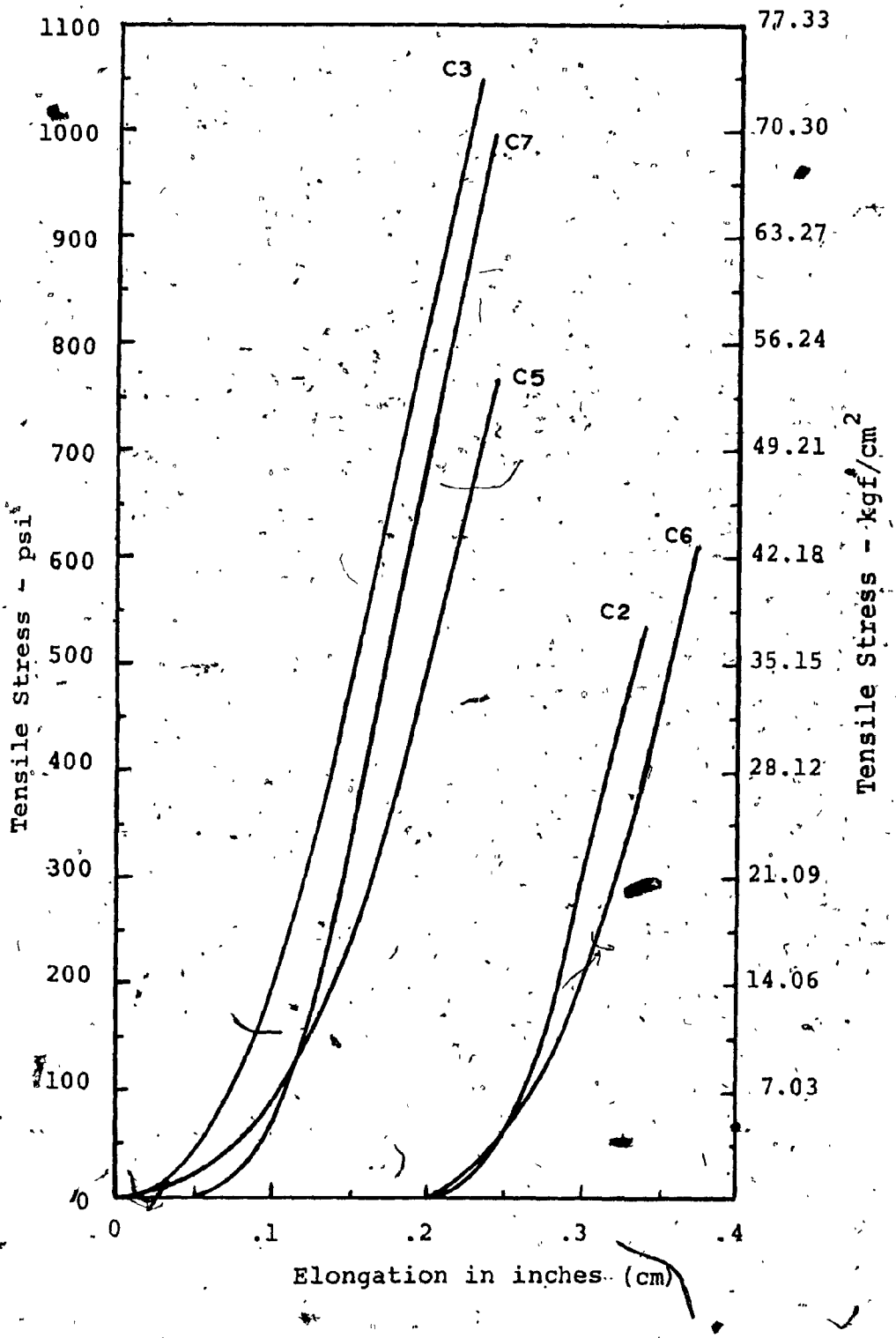

FIG. 2.4 TYPICAL TENSILE STRESS - ELONGATION CURVES FOR LMC MORTARS

in Figure 2.4. Tensile strength values were ranging from 650 psi (45.70 kgf/cm^2) to as high as 1050 psi (73.83 kgf/cm^2).

2.5.3 Strains at Maximum Stresses

Compressive and tensile strains are greatly increased with the addition of polymer latexes. These strains are proportional to the polymer content.

Typical values at ultimate loads are listed in Table 2.2. It is noted that unlike unmodified concretes, which fail in a brittle manner, LMC mortars undergo a ductile failure and the amount of ductility is increased with the increase of polymer content. This, in fact, permits the stress-strain curve to cover a region beyond the maximum loading (Fig. 2.3).

2.6 WATER VAPOUR TRANSMISSION RESISTANCE

The LMC mortars have great water vapour resistance than the unmodified mortars.

The test (ASTM E96-63T, PROCEDURE E) to determine the water vapour transmission rate described in Reference [1],

The test (ASTM E96-63T, PROCEDURE E) to determine the water vapor transmission rate described in Reference [1], involves casting $\frac{1}{4}$ inch thick specimens and curing them for 14 days at 73°F (23 °C) and 50% relative humidity. Then, the specimens are sealed in Pyrex crystallizing dishes which contain measured amounts of calcium chloride ($CaCl_2$). After the samples are weighed, they are placed in controlled environment of 100 °F(38 °C) and 95% relative humidity. Then the specimens are weighed periodically until a constant gain in weight is obtained.

The unit of Water Vapor Transmission Rate is defined as:

> ... *The rate of water vapor transmission through a specimen caused by the vapor pressure difference across the specimen* ...

or

$$1 \text{ Perm} = \frac{\text{gain}}{\text{hr. x sq.ft. x in.Hg}}$$

The results of the above test are listed in Table 2.3. This Table shows the best WVTR for Dow Latex 460 and Dow Latex 464, which is at the level of 15% latex solids. Further tests indicated that as the content of Dow Latex 464 is increased, the WVTR of mortars decreases.

TABLE 2.3

WATER VAPOR TRANSMISSION RATE OF LATEX MODIFIED MORTARS

Formulation	Dow Latex	WVTR in Perms.
Control[4]	None	20-30
Styrene Butadiene	15%-460	2-5
Saran	15%-464	6-9

2.7 BOBTEX GLASS FIBRE REINFORCED CONCRETE

The Bobtex Fibre Glass, Fig.2.5a is a specially made reinforcing material. The glass fibre strands, with approximately 200-230 fibres per strand, are coated with polypropylene to which cotton fibres adhere, forming a protective cover against the alkaline attack of concrete. These threads are then woven to a 4 ft. wide cloth, with a thread density of 8 x 8 to 12 x 12 threads per inch.

The strength of the material is between 180-300 lbs. per inch in tension, depending on the number of threads per inch.

---

[4] Control mortar was wet cured 7 days at 73 °F(23 °C) followed by 7 days dry cured at 73 °F(23 °C) and 50% relative humidity.

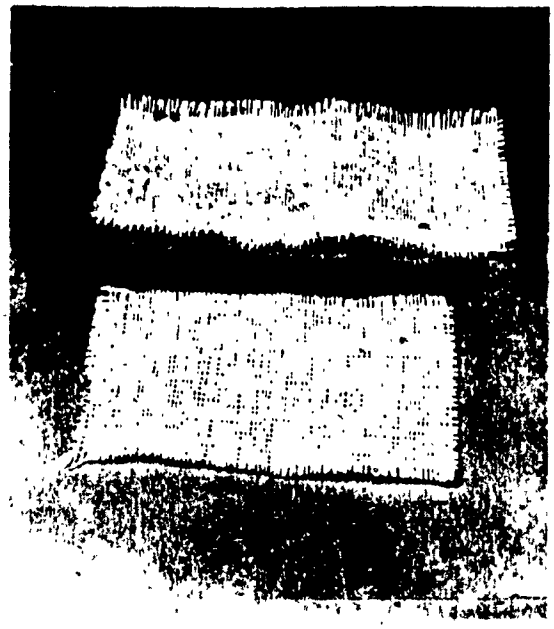

(a)

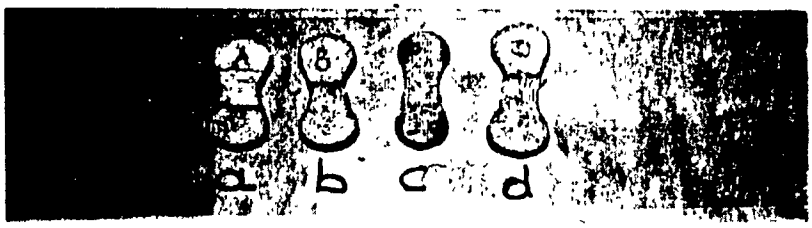

(b)

FIG. 2.5 (a) BOBTEX FIBRE GLASS (B.F.G.) "CLOTH": 12 x 12 THREADS PER INCH (TOP); 8 x 8 THREADS PER INCH (BOTTOM)

(b) TESTED 1/4"-THICK BFG REINFORCED SPECIMENS

The ASTM C190-70 tension test with several figure-eight $\frac{1}{4}$ - inch thick specimens was performed. The strength and toughness were investigated with respect to reinforcement location.

Typical tensile stress-elongation curves for three different reinforcement locations are shown in Fig. 2.6. In specimens "A", (LMC mortar and no antifoams with f'_c = 5500 psi (386.7 kgf/cm^2) and f_t = 700 psi (49.2 kgf/cm^2) was used), two layers of 11 threads each were placed at the center of the $\frac{1}{4}$ - inch thick by 1 - inch wide specimens at $\frac{1}{16}$ - inches apart.

The behaviour of these specimens under direct tensile load is shown by the "A" curve, which suggests that although its ultimate tensile strength is 345 x 4 = 1380 psi, (97.03 kgf/cm^2), the materials did not perform as an integrated unit.

In specimens "B" the two layers of reinforcement, 12 threads each, were placed eccentrically into the specimen. The tensile behaviour of this arrangement is curve "B".

An ultimate of 1630 psi (114.61 kgf/cm^2) tensile strength was reached, and in this case, the reinforcement acted more integrally with the concrete mortar.

Specimens "C" had the reinforcement (2 layers of 12 threads each) on the outside, one layer on each face. At failure, 1210 psi (85.07 kgf/cm^2), only one layer of rein-

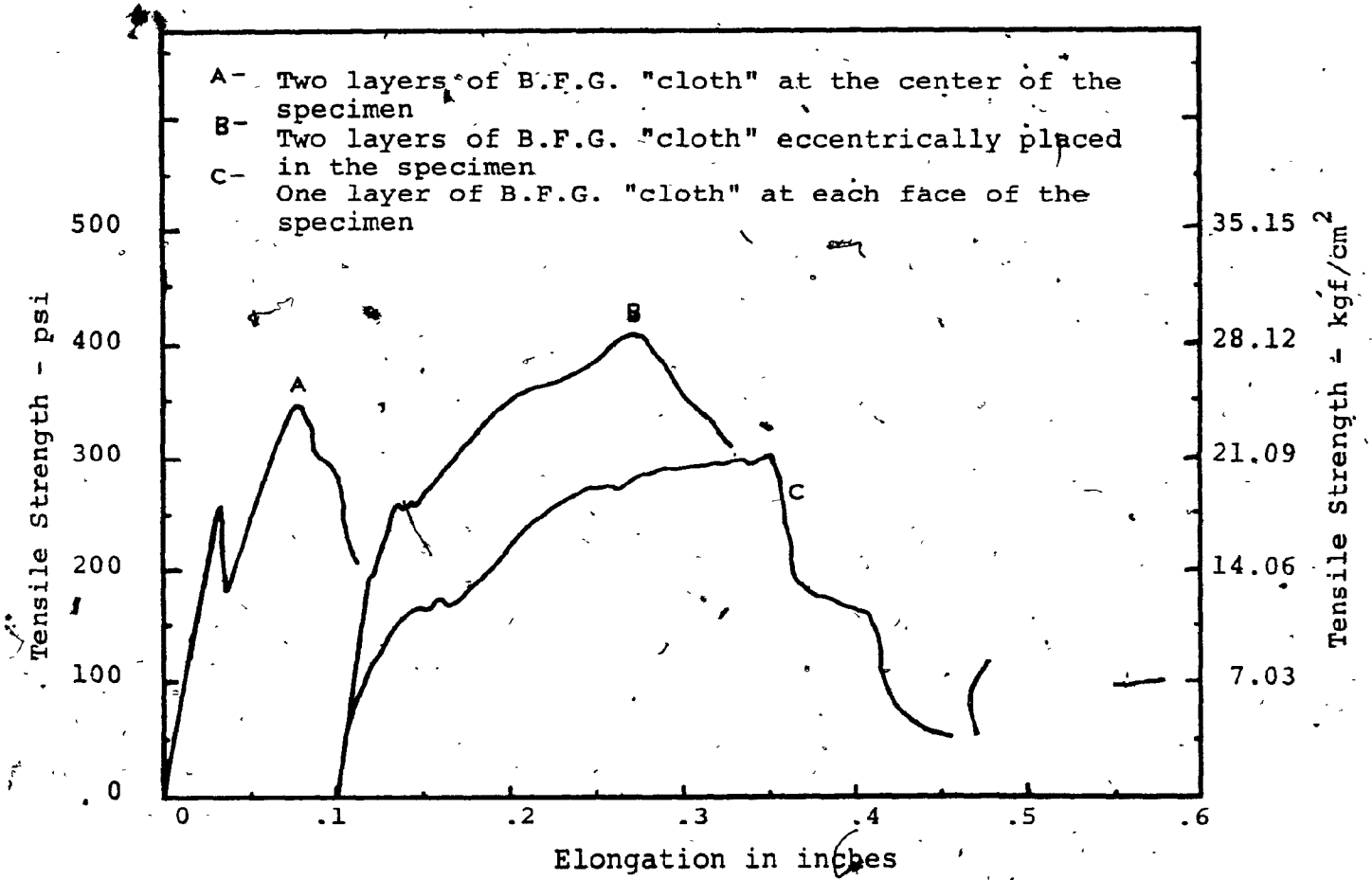

FIG. 2.6 STRESS-ELONGATION CURVES FOR 1/4 in^2 IN CROSS-SECTION B.F.G. REINFORCED MORTAR AT 14 DAYS

forcement was completely failed. The other one was untouched. In both "B" and "C" series, the improved toughness and ductility was apparent from the areas under their respective curves, and the fact that the specimens failed long after they reached their maximum strengths.

Although the three different patterns of reinforcement showed substantial difference in their behaviour under tensile loads, it is believed that if the fibre cloth reinforcement is properly stretched when is placed, the strengths of cement mortar and "cloth" can be added.

Curves A and B suggest that tensile strengths higher than 700 psi (49.20 kgf/cm^2) were obtained. This is explained by the fact that no antifoam was used, therefore the $\frac{1}{4}$ - inch thick specimens, due to better compaction and escape of the gas bubbles, show higher strengths than the 1 - inch thick ones. A set of tested Bobtex Fibre Glass reinforced specimens is shown in Fig. 2.5b.

2.8 OBSERVATIONS AND COMMENTS

- Optimum (efficient and economical) latex content was found to be in the range of 15 - 18% solids. Note that the emulsion water was considered in the total water content.

- Higher percentages reduce the compressive strength (f'_c) and modulus of elasticity (E) of concrete. It does however, increase the strains (ductility), toughness, hardness, flexibility and shear bond strength. It was also

observed that LMC mortars had an increased flexural strength while being more flexible.

- If antifoam is not used in mechanically mixed LMC mortars, it produces a foamed or cellular concrete, and the air content can be as high as 30 percent by volume. This may be desirable if light-weight and air-entrained concrete is the objective. However, it reduces appreciably the compressive, tensile and bond strengths and results in a poorer water resistant material.

- Both sizes of Mel-lite lightweight aggregates (#4-0 and #12-0) produced mortars with higher compressive and tensile strength than sand aggregates. This was due to the superior gradation and cleanliness of the Mel-lite particles. The best overall and most consistent results were obtained for the passing sieve #12-0 sizes. In addition, $\frac{1}{4}$ inch thick tensile specimens gave higher tensile strengths than the 1-inch thick ones, especially when antifoam was not used.

In Appendix A, additional information on the mechanical and physical properties of LMC mortars is presented from Reference [1]. It is observed from Table A-2 in the Appendix, that the use of Type III cement gives slightly better results than Type I cement, at 28 days.

Finally, the higher the polymer content, the more difficult it is to finish the surface.

The improved mechanical and physical properties of latex modified concrete mortars, especially their tensile strength, toughness and hardness, suggested their use as a face material in sandwich construction.

CHAPTER 3

STYROPOR-FILLED EXTRA LIGHTWEIGHT CONCRETE AS A CORE MATERIAL

CHAPTER 3

STYROPOR-FILLED EXTRA LIGHTWEIGHT CONCRETE AS A CORE MATERIAL

3.1 INTRODUCTION

Expanded polystyrene beads as aggregate produce lightweight concretes of various densities. Densities from 50 lb/ft^3 (815 kg/m^3) to 142 lb/ft^3 (2270 kg/m^3) [5] with compressive strengths of 180 psi (12.6 kgf/cm^2) [5] to 6900 psi (485 kgf/cm^2) respectively, have been obtained for structural and insulating applications.[2]

In order to use cellural concretes as core material in lightweight sandwich construction, the compressive and shear strengths of extra lightweight concretes of densities in the region of 12-25 lb/ft^3 (192-400 kg/m^3) were investigated.

The results were very satisfactory and are presented in this Chapter.

3.2 EXPANDED POLYSTYRENE BEADS

Cellular concretes so far have been produced either by

---

[5] These normal weight concretes, included river sand and 3/8 - inch river gravel.

the injection of air into the mix or by the use of chemicals, such as aluminum powder, which react with the cement and generate millions of tiny gas bubbles. However, in the use of these techniques the thickness of a slab or panel is difficult to control.

The use of expanded polystyrene beads (Fig. 3.1a) produces similar concrete products as the above-mentioned techniques, with controlled dimensions.

The pre-expanded beads have a closed cellural form and can be mixed conventionally with little difficulty.

Polystyrene beads expand as much as 50 times their original volume. Varied degrees of expansion produce beads with varied volumes and the same weight (since they come from the same unit.) This coupled with the fact that these beads are extremely light .75 to 1.0 lb/ft^3(12 to 16 kg/m^3), can cause segregation on mixing especially when there are large differences in particle size. Another disadvantage during mixing is that polystyrene beads are hydrophobic, and coating of particles with adhesive substances prior to mixing is necessary, or bonding admixtures should be used.

In all, the series of experiments performed in this investigation, the polymer latex styrene-butadiene was used successfully. Other bonding agents such as epoxy resins (though expensive), or polyvinyl proprionate emulsion (Propriofan) may be used. However, Propriofan appears to have

(a)

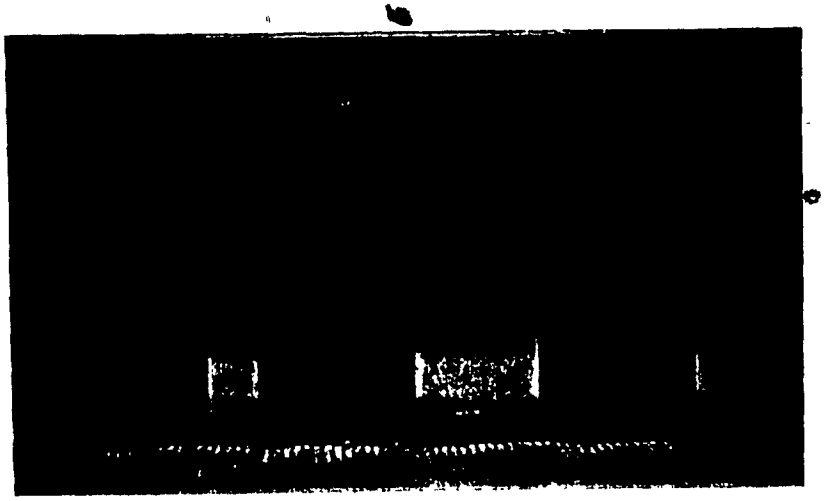

(b)

(c)

FIG. 3.1 (a) UNEXPANDED POLYSTYRENE CRYSTALS (TOP), EXPANDED POLYSTYRENE BEADS (BOTTOM)

(b) STYROPOR-FILLED LIGHTWEIGHT CONCRETE, 3"-DIA. BY 6", SPECIMENS (12-25 lb/ft^3)

(c) TESTED SPECIMENS

deleterious effect on the properties of the cement paste, and this has not been given yet any attention, as far as Badische Aniln-and Soda Fabric A.G. (BASF) Company, which has done considerable research on polystyrene concrete, is concerned.[2]

3.3 FORMULATIONS AND MIXING

Mainly, three different aggregate gradations were used:

Gradation "A"		Gradation "B"		Gradation "C"	
Sieve	% Retained	Sieve	% Retained	Sieve	% Retained
#4	0.0	#4	0.0	#12	0.0
#8	40.0	#8	41.5	#16	12.57
#12	50.0	#12	41.0	#30	77.14
#16	10.0	#16	2.2	#50	10.29
		#30	13.5		
		#50	1.8		

In proportioning the materials, polystyrene beads were measured by volume. The formula $C_xL_yW_z$ means that in 1 cubic foot of beads, there are x pounds of cement for which the corresponding latex solids to cement ratio and water to cement ratio is y% and z% respectively, based on the weight of cement.

The mixing procedure adopted is as follows, after the required quantities in each case are measured.

(i) One half the required water was mixed with the latex emulsion.

(ii) One quarter of the above solution was poured in a prewetted mixing pan with the beads and mixed until all beads were coated.[6]

(iii) The cement was poured while mixing was continued.

(iv) The remaining latex solution was added with the rest of the water into it, and mixed until all beads were evenly coated with the cement paste.

It is very <u>important to note</u> that pouring water, after all latex emulsion has been used, washes away any existing paste from the surface of the beads, and longer mixing is required.

The best method in the above mixing procedure is to use latex emulsion without any added water to coat the beads first, leave them to dry for approximately 10-15 minutes (no longer), and then pour the cement and latex with the required water in it, while continuously stirring. However, this last mixing technique requires more latex.

---

[6] As a matter of fact, it was very difficult to check the degree of coating, because beads and latex are milk white.

3.4 MECHANICAL PROPERTIES OF LATEX MODIFIED STYROPOR-FILLED LIGHTWEIGHT CONCRETE

Due to the fact that most of the test specimens never failed completely, the ultimate load was established at a compressive strain of $\varepsilon_c = .05$. Table 3.1 lists the mechanical properties of a series of specimens for various cement contents and two different Polymer/cement ratios, using Gradation "A".

Tables 3.2, 3.3 and 3.4 list the variation in properties using Gradations "B" and "C" at constant cement content and different P/C ratios. Typical stress-strain curves are plotted in Fig. 3.2.

It is understood that compressive strength depends on the degree to which the interstices between the aggregates are filled with cement paste. For the beads/cement ratios used in this investigation, the interstices were never filled with paste completely (except maybe regionally). Therefore, the quality of the material, depends on how the paste is distributed and how well the beads are coated. Specimens before and after testing are shown in Fig. 3.1b and C, respectively. The modes of failure illustrate perfectly the problems of segregation, coating and the effect of the amount of latex.

The compressive strength and modulus of elasticity are almost direct functions of the unit weight of the material, as it is shown in Fig. 3.3. In Fig. 3.4, the effect of the polymer content on the compressive strength is shown. One has to

TABLE 3.1

MIX PROPORTIONS AND MECHANICAL PROPERTIES USING GRADATION "A", AT 14 DAYS AND COMPRESSIVE STRAIN OF ε_c=.05

Specimen[1]	Unit Weight[2] lb/ft^3(kg/m^3)	Compressive Strength[2] (f') psi(kgf/cm^2)	Modulus of Elasticity (E) psi(kgf/cm^2)	Shear Strengh (τ) psi(kgf/cm^2)
$C_{15}L_{15}W_{30}$	25(400	168(11.8)	6500(457)	55(3.86)
$C_{14}L_{15}W_{30}$	24(384)	145(10.2)	5100(358)	53(3.72)
$C_{13}L_{15}W_{30}$	21.2(340)	120(8.5)	3100(218)	51(3.58)
$C_{12}L_{15}W_{30}$	16.8(269)	109(7.7)	2700(190)	54(3.79)
$C_{11}L_{15}W_{30}$	15.4(247)	82(5.7)	2600(183)	53(3.72)
$C_{10}L_{15}W_{30}$	14.3(229)	78(5.5)	2500(176)	49(3.44)
$C_{15}L_{15}W_{30}$	22.2(355)	156(11.0)	3500(246)	45(3.16)
$C_{14}L_{15}W_{30}$	20.7(331)	109(7.7)	3100(218)	38(2.67)
$C_{13}L_{15}W_{30}$	18.6(298)	90(6.3)	2550(179)	35(2.46)

[1] Type III Portland Cement was used

[2] Is the average of 3 specimens

TABLE 3.2

MECHANICAL PROPERTIES USING GRADATION "B" FOR $C_{10}L_{25}W_{30}$ SPECIMENS AT 14 DAYS AND ϵ_c = .05 COMPRESSIVE STRAIN

Specimen	Unit Weight lb/ft^3 (kg/m^3)	Compressive Strength (f'_c) psi (kgf/cm^2)	Modulus of Elasticity (E) psi (kgf/cm^2)
1	18.41(295)	103(7.24)	5140(362)
2	17.69(283)	85(5.97)	4000(281)
3	18.41(295)	95(6.68)	4100(288)
4	18.23(292)	76(5.34)	3900(274)
5	17.61(282)	87(6.11)	4280(301)
Average	18.07(289)	89.2(6.27)	4285(301)

TABLE 3.3

MECHANICAL PROPERTIES USING GRADATION "B" FOR $C_{10}L_{20}W_{30}$ SPECIMENS AT 14 DAYS AND ε_c=.05 COMPRESSIVE STRAIN

Specimen	Unit Weight lb/ft^3 (kg/m^3)	Compressive Strength (f'_c) psi (kgf/cm^2)	Modulus of Elasticity (E) psi (kgf/cm^2)	Shear Strength (τ) psi (kgf/cm^2)
1	15.81(253)	87(6.11)	3025(213)	50(3.51)
2	16.26(260)	95(6.68)	4110(289)	53(3.7)
3	16.89(270)	115(8.08)	6050(425)	58(4.08)
4	16.17(259)	90(6.33)	3680(259)	51(3.58)
5	16.08(257)	102(7.17)	5140(361)	55(3.86)
Average	16.2 (260)	97.8(6.87)	4400(310)	53.4(3.75)

TABLE 3.4

MECHANICAL PROPERTIES USING GRADATION "C"
AT 14 DAYS AND COMPRESSIVE STRAIN $\varepsilon_c = .05$

Formulation $C_{10}L_{70}W_{76}$	Unit Weight lb/ft^3 (kg/m^3)	Compressive Strength (f'_c) psi (kgf/cm^2)	Modulus of Elasticity (E) psi (kgf/cm^2)
1	20.03(321)	154.3(10.85)	6430(452)
2	20.12(322)	164.3(11.55)	8570(603)
3	20.21(323)	156.0(11.0)	7900(555)
Average	20.12(322)	158.2(11.33)	7630(537)
Formulation $C_{10}L_{25}W_{42}$			
1	16.71(267)	110(7.73)	6430(452)
2	16.80(269)	108(7.59)	7350(517)
3	16.89(270)	107(7.52)	4200(295)
Average	16.8(268)	108.5(7.61)	6000(422)

TABLE 3.5

TENSILE STRENGTH USING GRADATION "C"
FOR $C_{10}L_{70}W_{76}$ SPECIMENS AT 14 DAYS

Specimen	Unit Weight lb/ft^3 (kg/cm^3)	Tensile Strength - psi (kgf/cm^2) at		
		Yield	ε_t = .07 in	Failure
1	20.03(321)	56(3.94)	60(4.22)	110(7.73) (ε_t=(7.73)
2	20.12(322)	75(5.27)	80(5.62)	115(8.08) (ε_t=(8.08)
3	20.21(323)	90(6.33)	95(6.68)	115(8.08) (ε_t=(8.08)
Average	20.12(322)	73(5.2)	78(16.52)	113(7.96)

ε_t = the elongation in this case

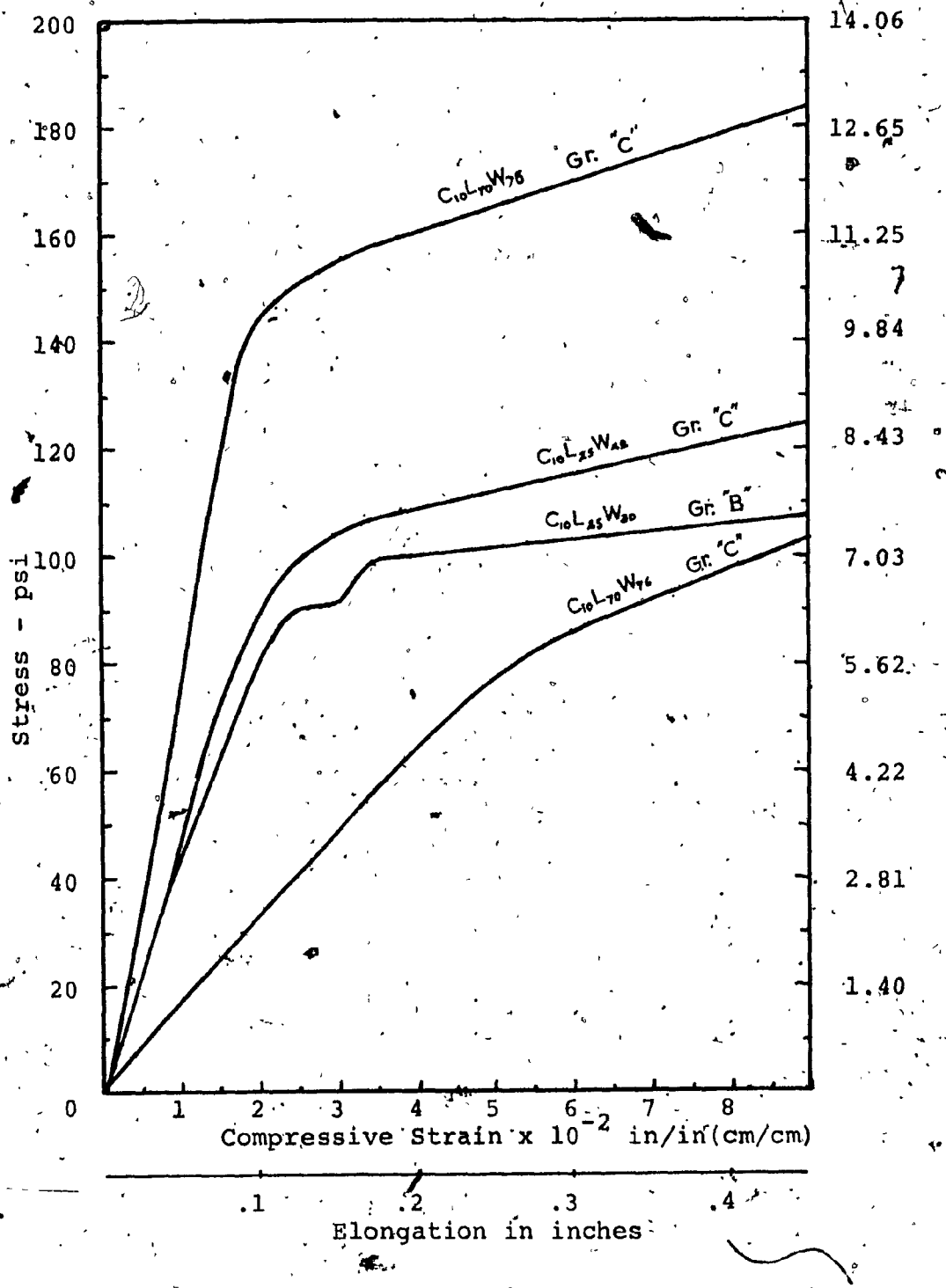

FIG. 3.2 STRESS-STRAIN CURVES FOR COMPRESSION (TOP OF THREE CURVES) AND TENSION (BOTTOM CURVE) STYROPOR-FILLED CONCRETE SPECIMENS

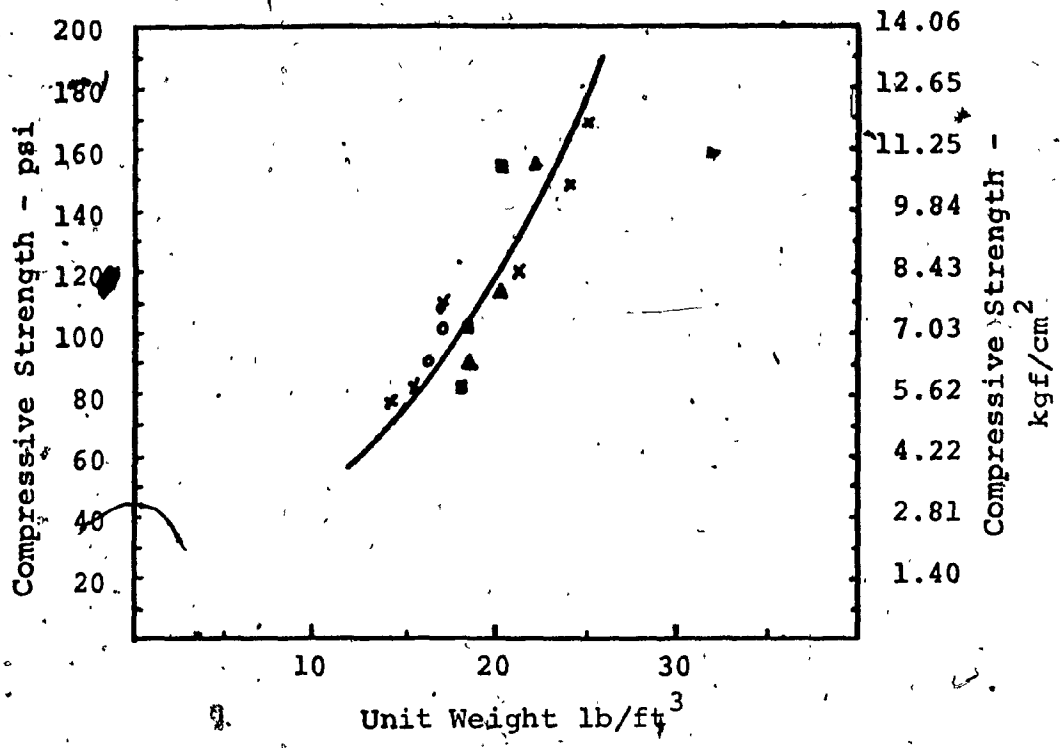

FIG. 3.3 RELATION BETWEEN COMPRESSIVE STRENGTH AND UNIT WEIGHT FOR DIFFERENT LATEX-WATER/CEMENT RATIOS

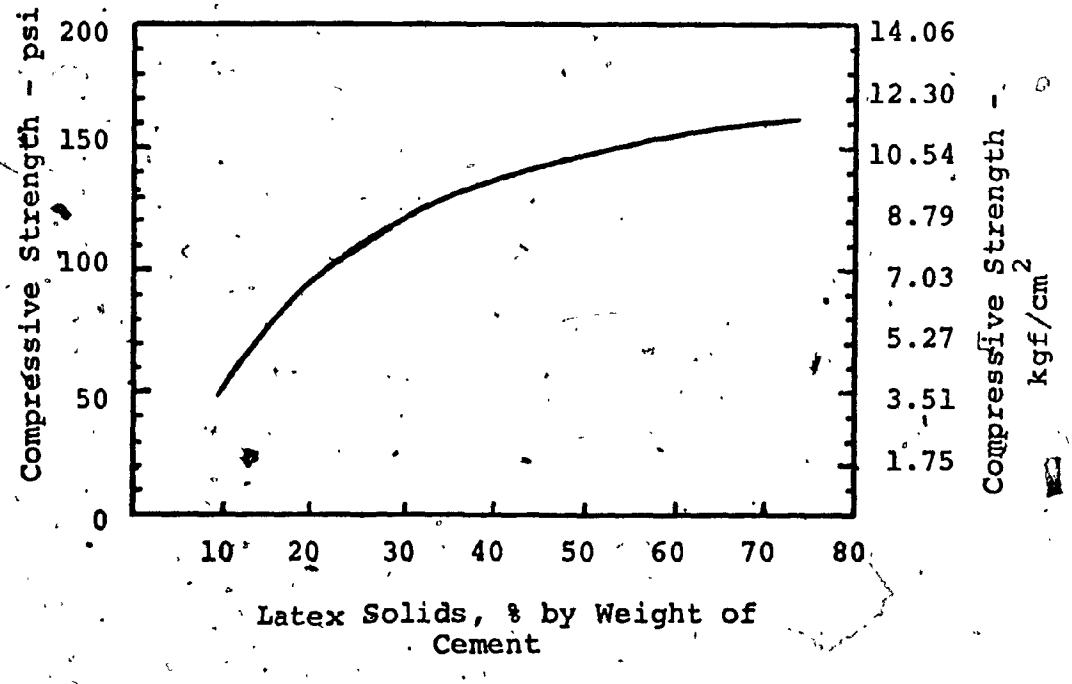

FIG. 3.4 COMPRESSIVE STRENGTH AS RELATED TO LATEX CONTENT FOR 10 LBS (4.53 kg) OF CEMENT PER CUBIC FOOT OF BEADS

realize the difficulties involved when working in these small ranges of strength and unit weight.

For a high latex content (70%), the tensile strength at yield, at an elongation ε_t = .07 in. and at failure are given in Teble 3.5. The tensile strength of these specimens is over 70% of their compressive strength.

3.5 STYROPOR-FILLED LIGHTWEIGHT CONCRETE SHEAR TESTS

Two different double shear tests were performed, in order to compare the results. In the first test, the 3" dia. by 6" compression cylinders were used in double shear, as shown in Fig. 3.5a. The results of these tests are the ones in Table 3.1 and Table 3.3.

The arrangement for the double-block shear test using material with the same formulation as in the cylinder double shear test is shown in Fig. 3.5b. From this test, both the shear strength (τ) and shear modulus of rigidity (G), were calculated. The average value for τ was 43.75 psi (3.07 kgf/cm^2), and G = 2,450 psi(172 kgf/cm^2) is the slope of the stress (τ) vs. strain (γ) curve shown in Fig. 3.6.

The shear strength from this test is approximately 10 psi (.70 kgf/cm^2) lower than the average values of the first

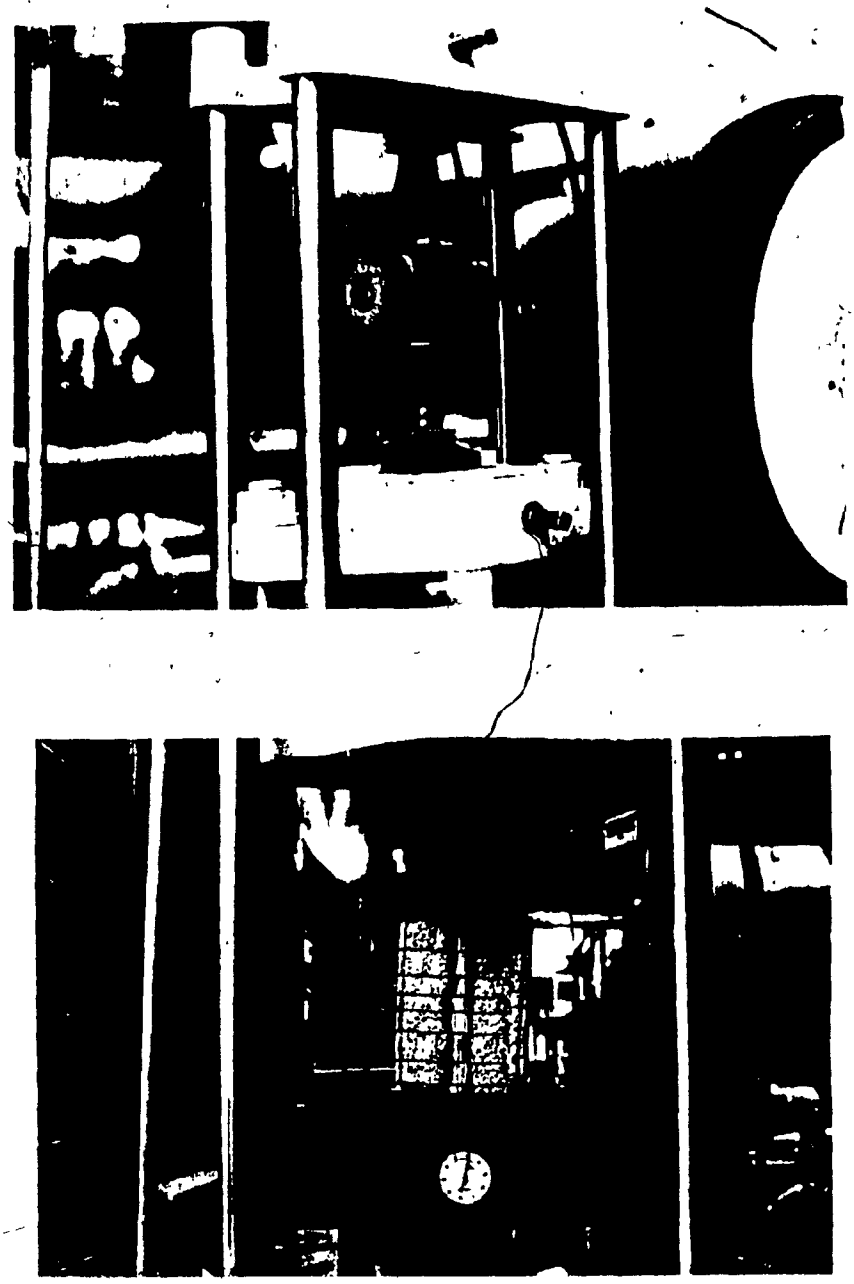

(a)

(b)

FIG. 3.5 DOUBLE-SHEAR TEST ARRANGEMENTS.

(a) 3" x 6" CYLINDER IN DOUBLE-SHEAR

(b) THE DOUBLE-BLOCK SHEAR TEST

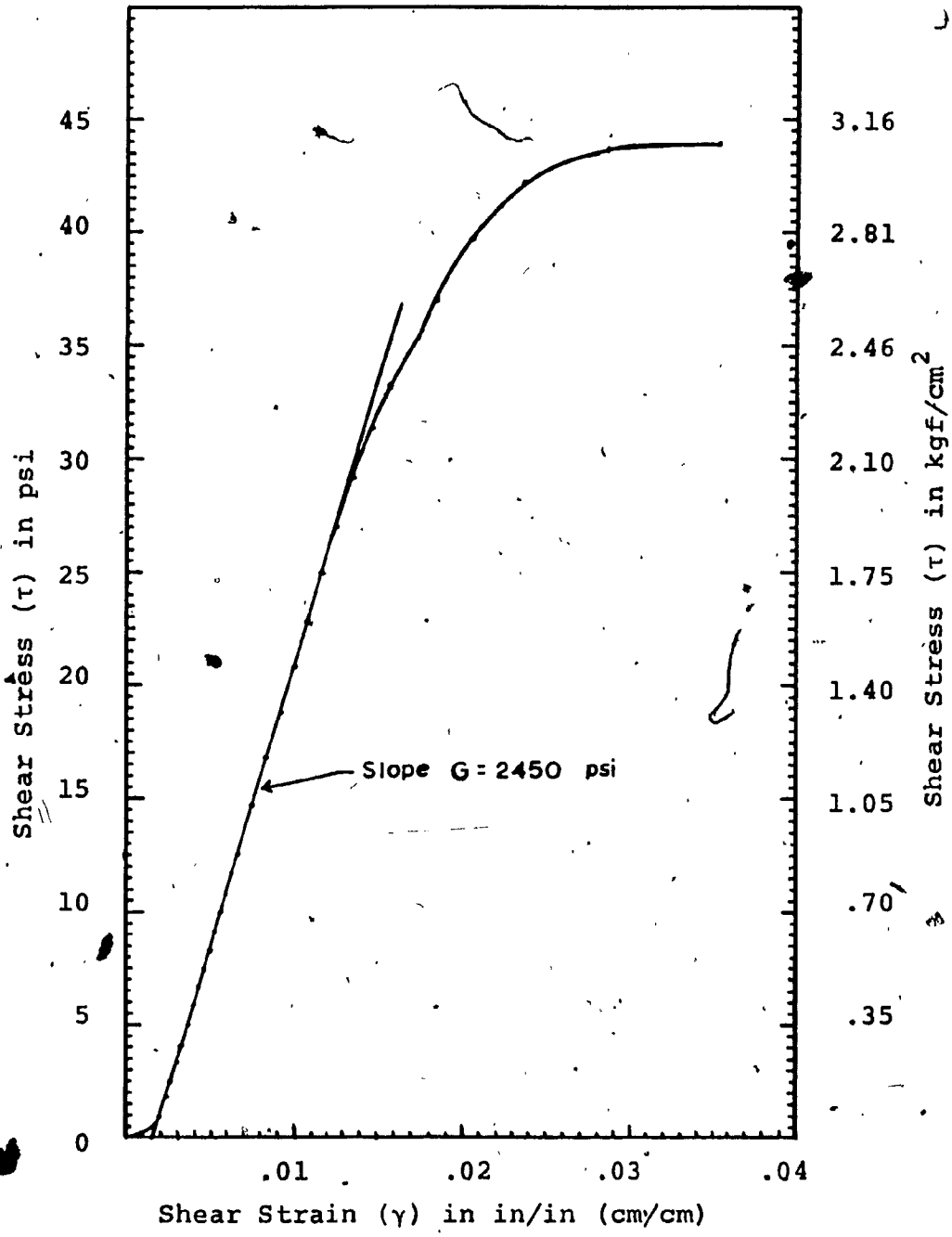

FIG. 3.6 DOUBLE-BLOCK SHEAR TEST: STRESS-STRAIN CURVE FOR STYROPOR-FILLED LIGHTWEIGHT CONCRETE

test. This is due to the difference in specimen preparation and the fact that no provision was made for carrying the complementary shear stress at the ends of the specimen.[7]

However, clamping forces were provided near the bottom supports. Under these conditions, it seemed that failure was initiated at the top free ends.

3.6 HONEYCOMB CORE COMPRESSION AND SHEAR TESTS

Two types of honeycomb core were tested in compression and shear. The first type shown in Fig. 3.7a is a 1"-cell size kraft paper honeycomb. The second is a 3/8"-cell size Cormat, type of honeycomb, as shown in Fig. 3.7b. The basic difference of these honeycombs other than in the cell size and construction is the quality of the paper, which in the first type is thicker and hence stronger and more stable than the second. Also, since it was received unexpanded and due to the lack of expanding equipment, expansion had to be done manually. This produced dimension problems after expansion and created local variation in stiffness. The average cell size was estimated to be 3/4". Honeycomb by construction is less stiff and weaker in shear in the direction of "expansion" than in the transverse direction. The problems of expansion and definition of directions (planes) are illustrated in Fig. 3.7.

---

[7]Because at both ends the core is completely free, the shear stress must be zero. Therefore, the assumption of uniform shear across the edge does not hold.

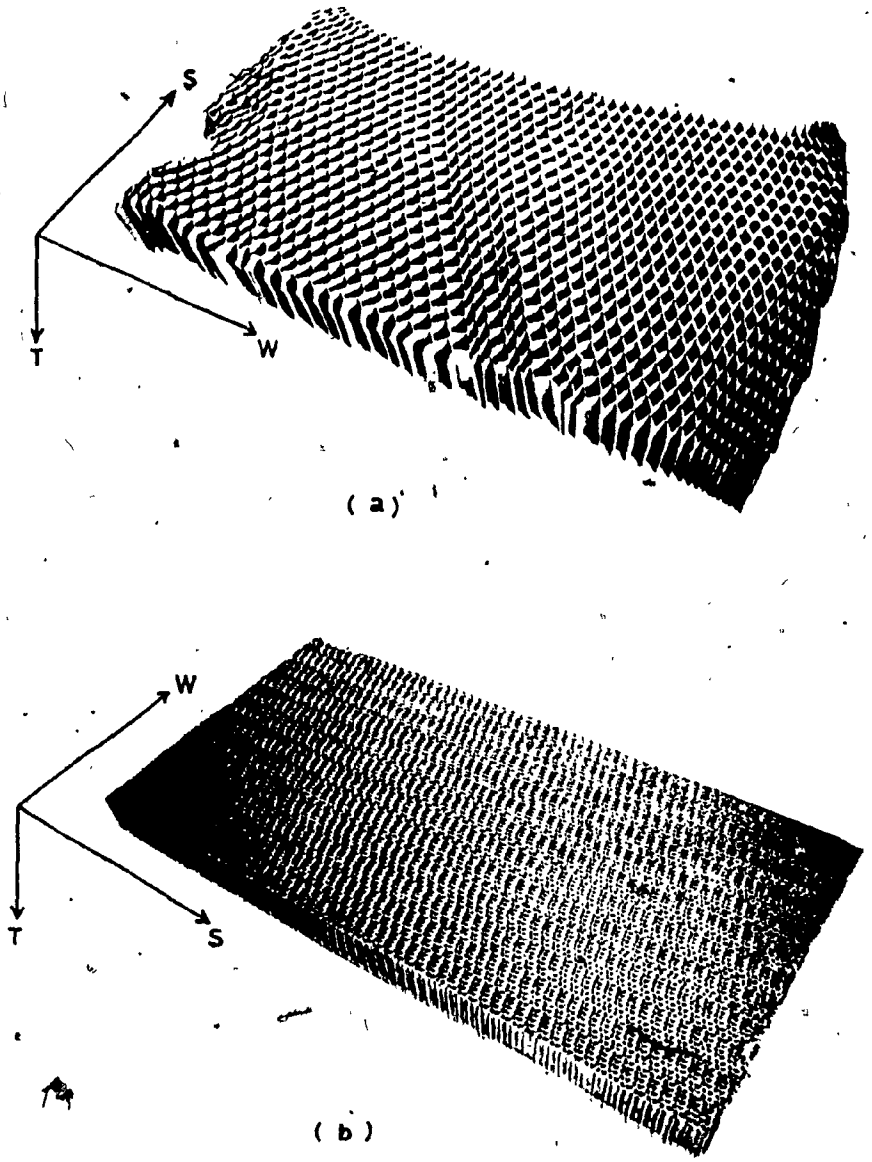

FIG. 3.7 TYPES OF HONEYCOMB AND DEFINITION OF DIRECTIONS

(a) 1"-CELL SIZE KRAFT PAPER HONEYCOMB

(b) 3/8"-CELL SIZE CORMAT PAPER

W = WEAK DIRECTION, S = STRONG DIRECTION

T = DIRECTION PERPENDICULAR TO WS-PLANE

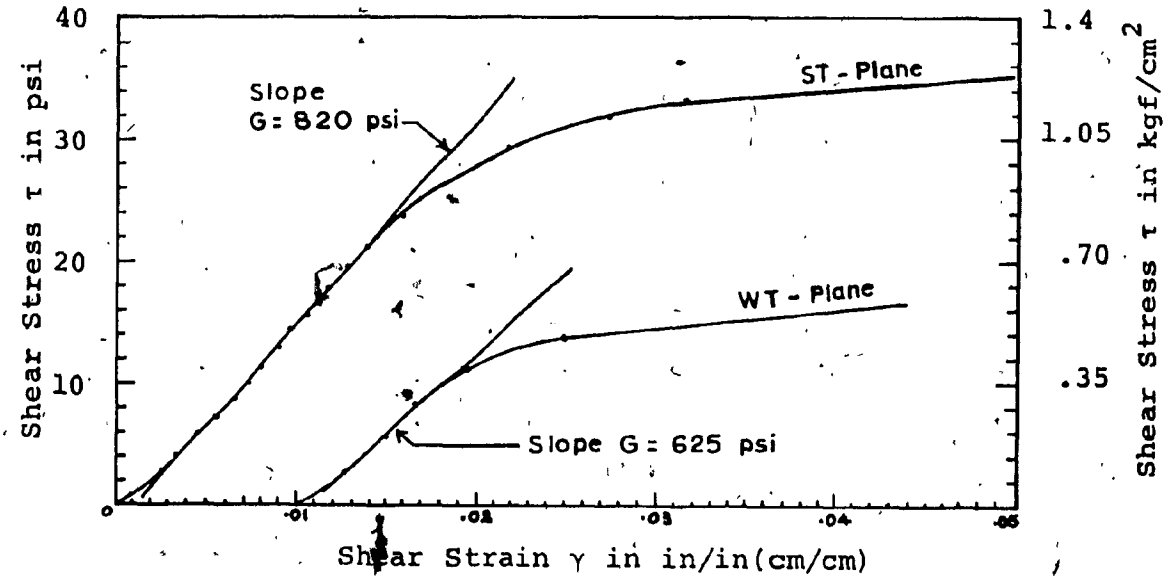

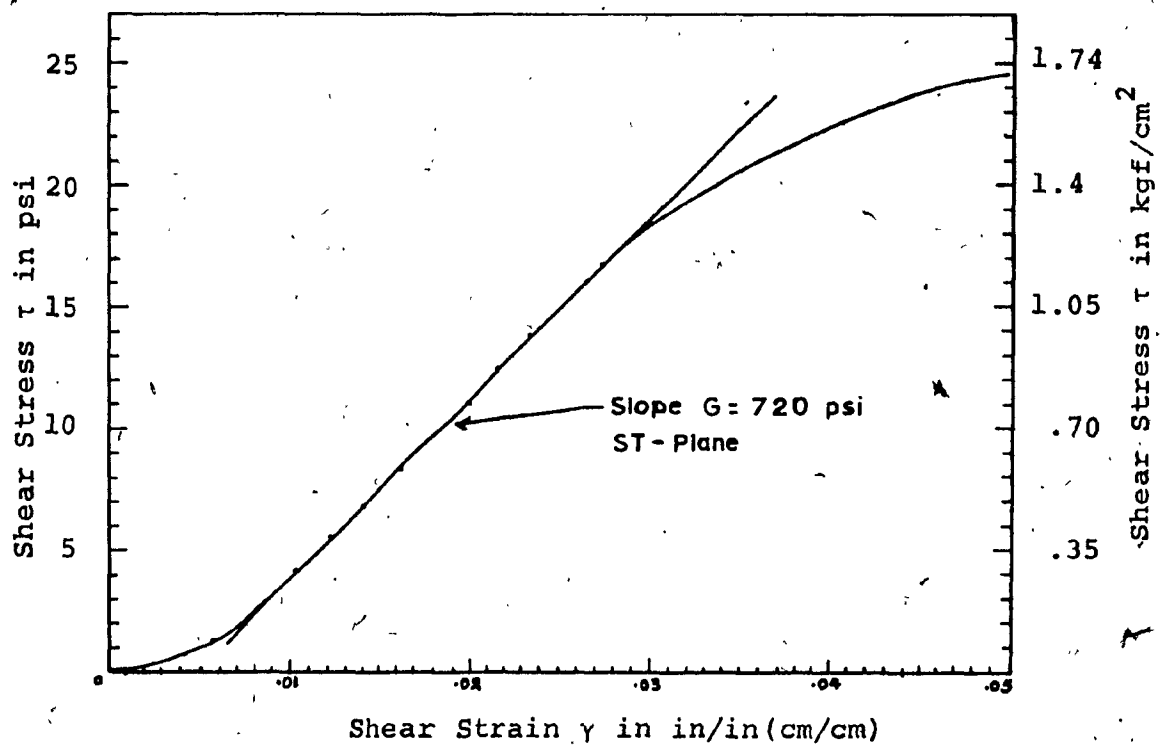

FIG.3.8 THE DOUBLE-BLOCK SHEAR TEST: STRESS-STRAIN CURVES

(a) 3/4"-CELL HONEYCOMB

(b) 3/8"-CELL CORMAT

TABLE 3.6

PROPERTIES OF CORE MATERIALS INVESTIGATED

(All Units in psi (kgf/cm^2)

Material	E	f'_c	τ_{WT}	G_{WT}	τ_{ST}	G_{ST}	Density pcf (kg/m^3)
Styropor-Filled Lightweight Concrete $C_{10}L_{15-20}W_{30}$ Gradation "B"	4400(310)	100(7.03)	43.75(3.07)	2450(172)	43.75(3.07)	2450(172)	17(272)
3/4"-Cell Size Paper Honeycomb	2100(147)	28(1.96)	8.0 (.56)	625(44)	17.6(1.23)	820(57.6)	1.2(19.2)
3/8"-Cell Size Cormat Paper	1300(91.4)	25(1.75)	-	-	25(1.75)	720(50.6)	2.4(38.4)

The double-block shear test was used to determine the shear strength and modulus of rigidity of these cores. The test specimens were directly glued to the shear plates or exposed to the compression head in the compression test. The stress (τ) vs. strain (γ) curves for both types of honeycomb are plotted in Fig. 3.8 were the difference in behavior under shear is illustrated. Table 3.6 summarizes the properties of the core materials investigated.

3.7 OBSERVATIONS AND COMMENTS

Cement paste is many times heavier than the beads, and tends to accumulate at the lower levels of the batch especially when excessive water or shaking is used.

- It seemed that the very small aggregate particles were more difficult to coat.

- It is very important how, and how well the material is compacted, because both of these factors control greatly the weight and strength of the material.

- Swelling and shrinkage deformations are somewhat high (20-25%) for these low densities of concrete[2]. However, as a core material for sandwich panel construction, these values do not present serious problems.

- Poisson's ratio was extremely difficult to estimate from the specimens in Fig. 3.1c.

Manual expansion of the honeycomb resulted in weaker ST and especially WT - planes. As compared to honeycomb, styro-

por-filled light-weight concrete is more than four times stronger in compression (f'_c) and has three times higher shear strength (τ) and shear modulus (G) in at least one direction.

CHAPTER 4

ANALYSIS OF SANDWICH BEAMS

CHAPTER 4

ANALYSIS OF SANDWICH BEAMS

4.1 SANDWICH CONSTRUCTION

A sandwich is a composite system which basically consists of two thin, dense and strong sheets (faces) held firmly to a thick layer of weaker, light and less stiff material (core).

The three parts are held together by adhesives, rivets or anything that can resist the shear forces that are expected to develop at the interfaces.

The form of the sandwich construction is the key to resisting forces and to excellent performance with respect to the element's weight.

The main functions of the core are to give the desired panel thickness, to transmit shear forces and to stabilize the skins. This is achieved by the stiffness of the core in shear perpendicular to the faces.

The core apart from its required mechanical properties can also have other qualities such as thermal insulation, low sound transmission, incombustibility, etc. Metal foil, aluminum or steel, plastic or kraft paper resin-impregnated honeycombs are commonly used in sandwich construction. "*Solid*" cores such as perforated chipboard, balsa

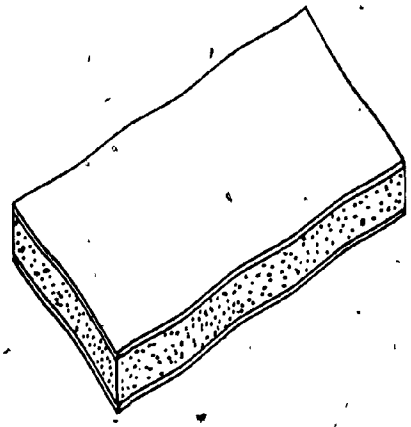

(a)

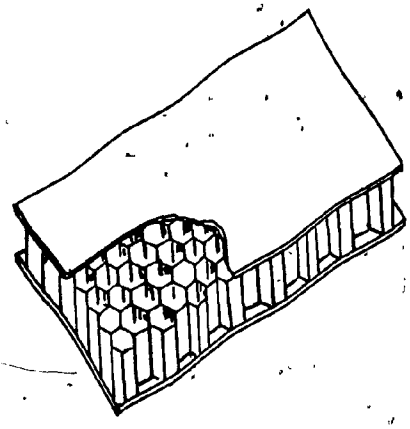

(b)

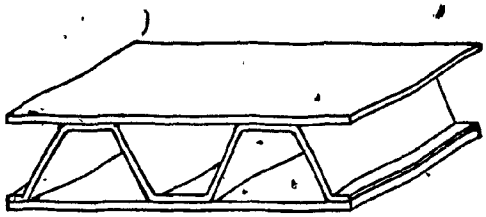

(c)

FIG. 4.1 TYPICAL SANDWICH PANELS WITH (a) POLYSTYRENE FOAM CORE, (b) HONEYCOMB CORE, (c) CORRUGATED CORE

wood, expanded plastics, and lightweight concrete are also used. Three basic forms of a sandwich panel are shown in Fig. 4.1.

The faces have to be strong enough to take compression and tension. Other desirable properties of a face material are impermeability, durability, hardness and incombustibility. Furthermore, depending on the intended use, core and face materials should have additional qualities.

Metal or aluminum sheets of various gauges have been used consistently, especially in sandwich panels for aircraft structures. In building industry, the panels must be cheap, so that materials such as asbestos-cement, plywood and hardboard are often used for semi-structural panels.

The selection of the adhesive is also important. High strength, and durability are some of its essential properties.

Analysis of deflections, stresses and buckling loads are very important in sandwich construction. However, details such as stiffeners and inserts to distribute concentrated loads, the nature of edge members, splices and joints are equally important. Temperature and moisture content differences may cause differential expansion of the faces (in asbestos cement, for example), which may lead to undesirable transverse deflections. All of the above factors

are very important design considerations in any sandwich construction.

4.2 APPLICATION OF ORDINARY BEAM THEORY

A particularly good introduction to the application of ordinary beam theory in sandwich beams, is given by Allen[3] and most of the analysis which follows is based on his book.

According to the ordinary beam theory, for a homogeneous material the stresses and deflections are found, using the assumption that cross-sections remain plane and perpendicular to the principal (longitudinal) axis of the unloaded beam after bending. Based on the above assumption, the bending moment (M), and curvature ($\frac{1}{R}$) are related as follows:

$$\frac{M}{EI} = -\frac{1}{R} \qquad (4.1)$$

where (EI) is the flexural rigidity of the beam.

The above relationship is based on the sign convention shown in Fig. 4.2.

For a sandwich beam such as the one shown by Fig.4.3, the stresses and deflections can be found to a good approximation by the use of the above-stated assumption, further assuming that both faces and core are isotropic. [3]

The flexural rigidity D, replacing EI by D, for

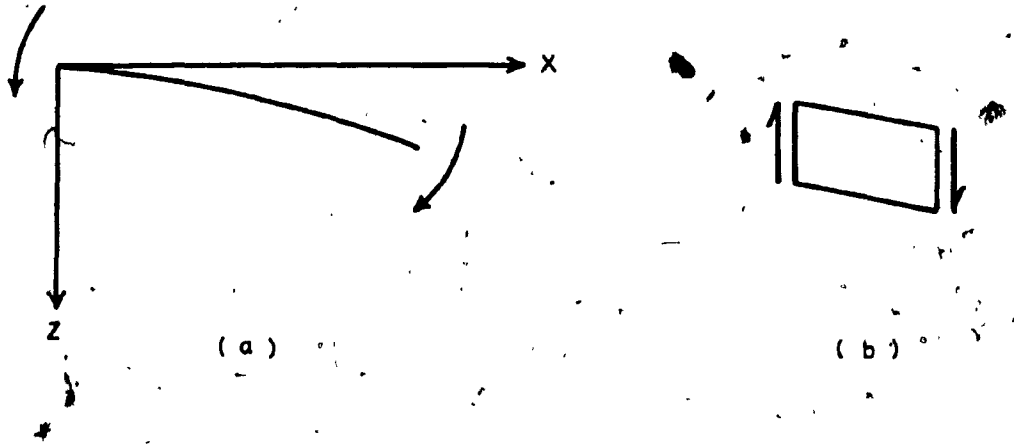

FIG. 4.2 SIGN CONVENTIONS (a) DEFLECTION, SLOPE AND CURVATURE ARE POSITIVE, BENDING MOMENT IS NEGATIVE (b) SHEAR FORCE, SHEAR STRESS AND SHEAR STRAIN ARE NEGATIVE

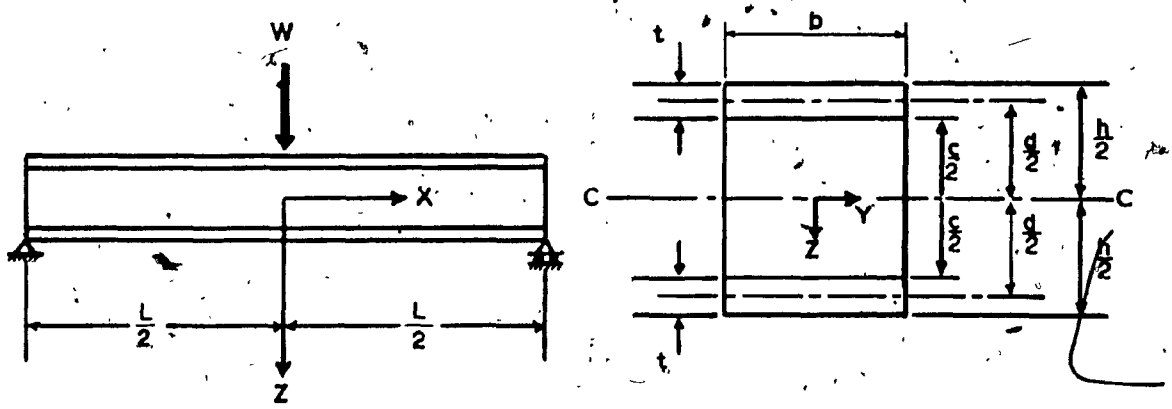

FIG. 4.3 SIMPLY SUPPORTED CENTRALLY LOADED SANDWICH BEAM (LEFT) WITH TYPICAL CROSS-SECTION (RIGHT)

convenience of a composite beam such as the sandwich beam in Fig. 4.3 is:

$$D = E_f I_o + E_c I_c \ , \quad I_o = I_f + 2A_f\left(\frac{d}{2}\right)^2$$

or

$$D = \left(E_f \frac{bt^3}{6} + \frac{E_f\, btd^2}{2}\right) + \frac{E_c\, bc^3}{12} \qquad (4.2)$$

where

E_f = modulus of elasticity of face material

E_c = modulus of elasticity of core material

I_f = sum of moments of inertia of facings about their own separate axes

I_o = total moment of inertia of both facings about the beam's centroidal axis c-c

which is the sum of the flexural rigidities of the faces (first term), and the core (second term) about the neutral axic c-c of the cross-section.

The first of the two in parentheses term, represents the flexural rigidity of the faces about their own separate axes. However, when

$$\frac{d}{t} > 6.0 \qquad (4.3)$$

the first term is less than 1% of the second and can be neglected.

The last term in equation (4.2) represents the flexural rigidity of the core about c-c. This term is less than 1% of the second in parentheses term when

$$\frac{E_f}{E_c}\frac{t}{c} > 17 \qquad (4.4)$$

and usually can be neglected.

The flexural stresses, in the faces and the core can be found by using the flexural strain formula

$$\varepsilon = \frac{Mz}{D} \qquad (4.5)$$

which gives the strain at a point of distance z from the centroidal axis c-c (Fig. 4.3).

Thus, by multiplying the strain by the appropriate elasticity modulus we obtain the stresses for the faces and core, respectively

$$\sigma_f = E_f \frac{Mz_f}{D}, \quad \frac{c}{2} \leq z_f \leq \frac{h}{2}; \; -\frac{h}{2} \leq z_f \leq -\frac{c}{2} \qquad (4.6a)$$

$$\sigma_c = E_c \frac{Mz_c}{D}, \quad -\frac{c}{2} \leq z_c \leq \frac{c}{2} \qquad (4.6b)$$

For a homogeneous beam, the shear stress (τ) at a distance z below the centroid of the cross-section is:

$$\tau = \frac{VQ}{Ib} \qquad (4.7)$$

where

V = the shear force at the section where the stress is to be evaluated

Q = the first moment of area of that section that lies between the level at which the stress is to be found and the nearest extreme fibre.

However, to apply equation (4.7) to a composite beam, such as a sandwich beam, the different moduli of elasticity of the elements of the cross-section must be considered. Thus for a sandwich beam equation (4.7) becomes

$$\tau = \frac{V}{Db} \Sigma(QE) \qquad (4.8)$$

where $\Sigma(QE)$ is the sum of the products of Q and E of all parts of the section between the level at which τ is calculated and the nearest extreme fibre.

Now assume that the shear stress at level z in the core is required. In order to use equation (4.8)

$$\Sigma(QE) = E_f \frac{btd}{2} + \frac{E_c b}{2} \left(\frac{c}{2} - z\right)\left(\frac{c}{2} + z\right)$$

$$= E_f \frac{btd}{2} \quad \frac{E_c b}{2} \left(\frac{c^2}{4} - z^2\right)$$

Therefore, the shear stress in the core is

$$\tau = \frac{V}{D} \left[E_f \frac{td}{2} + \frac{E_c}{2}\left(\frac{c^2}{4} - z^2\right)\right] \qquad (4.9)$$

$$\text{for } z = 0, \qquad \tau_{max} = \frac{V}{2D}\left(E_f\, td + \frac{E_c c^2}{4}\right)$$

$$\text{for } z = \frac{c}{2}, \qquad \tau_{min} = \frac{V}{2D} E_f td$$

and

$$\frac{\tau_{max}}{\tau_{min}} = \left(1 + \frac{E_c}{4E_f}\frac{c^2}{td}\right) \tag{4.10}$$

For a weak core we may assume $E_c = 0$. This implies from equation (4.10) that the shear stress distribution across the core section is constant. Thus, further assuming that condition (4.3) applies, i.e., that the flexural rigidity of the faces about their own separate axes is small we obtain from equations (4.2) and (4.9), respectively,

$$D = E_f \frac{btd^2}{2} \tag{4.11}$$

$$\tau = \frac{V}{D}\frac{E_f td}{2} \tag{4.12}$$

From the last two equations, the shear stress in the core is

$$\tau = \frac{V}{bd} \tag{4.13}$$

Equation (4.10) is close to unity with a maximum 1% error provided

$$\frac{E_f}{E_c}\frac{td}{c^2} > 25 \tag{4.14}$$

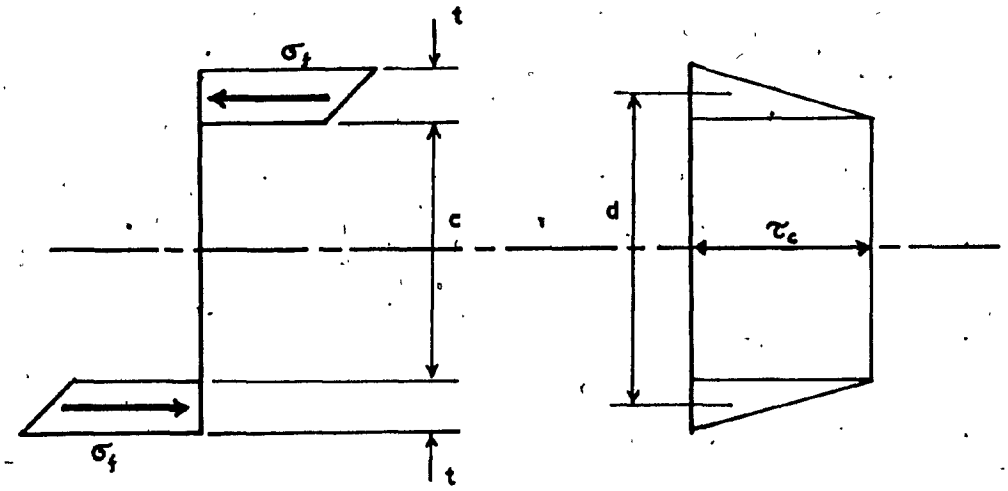

FIG. 4.4 BENDING (LEFT) AND SHEAR (RIGHT) STRESS DISTRIBUTIONS IN A SANDWICH BEAM WITH A WEAK CORE. THE LOCAL BENDING STIFFNESSES OF THE FACES ARE NEGLECTED

Therefore, whenever the core is too weak to contribute to the flexural rigidity of the sandwich, the shear stress distribution may be assumed constant.

Therefore, with the assumptions made previously, the bending stress distribution (considering equation (4.6) (a) and (b)), and the shear stress distribution over the depth of the cross-section of a sandwich beam are, for practical purposes, as illustrated in Fig. 4.4.

A sandwich section resisting stresses in a manner illustrated in Fig. 4.4 is said to have an idealized core in which the modulus of elasticity in planes parallel with the faces is zero, but the shear modulus in planes perpendicular to the faces is finite. Such a core makes no contribution to the bending stiffness of the beam. Kraft paper honeycomb cores fall closely into this category.

4.3 SIMPLY SUPPORTED SANDWICH BEAMS, DEFLECTION AND FACE THICKNESS DEFINITION

Although lightweight and weak materials have high enough shear modulus, and can be used as cores in lightweight sandwich construction, these materials exhibit significant shear deformations, that have to be considered when deflections are calculated.

The bending and shear deformations of a centrally loaded sandwich beam are illustrated in Fig. 4.5b and c respectively.

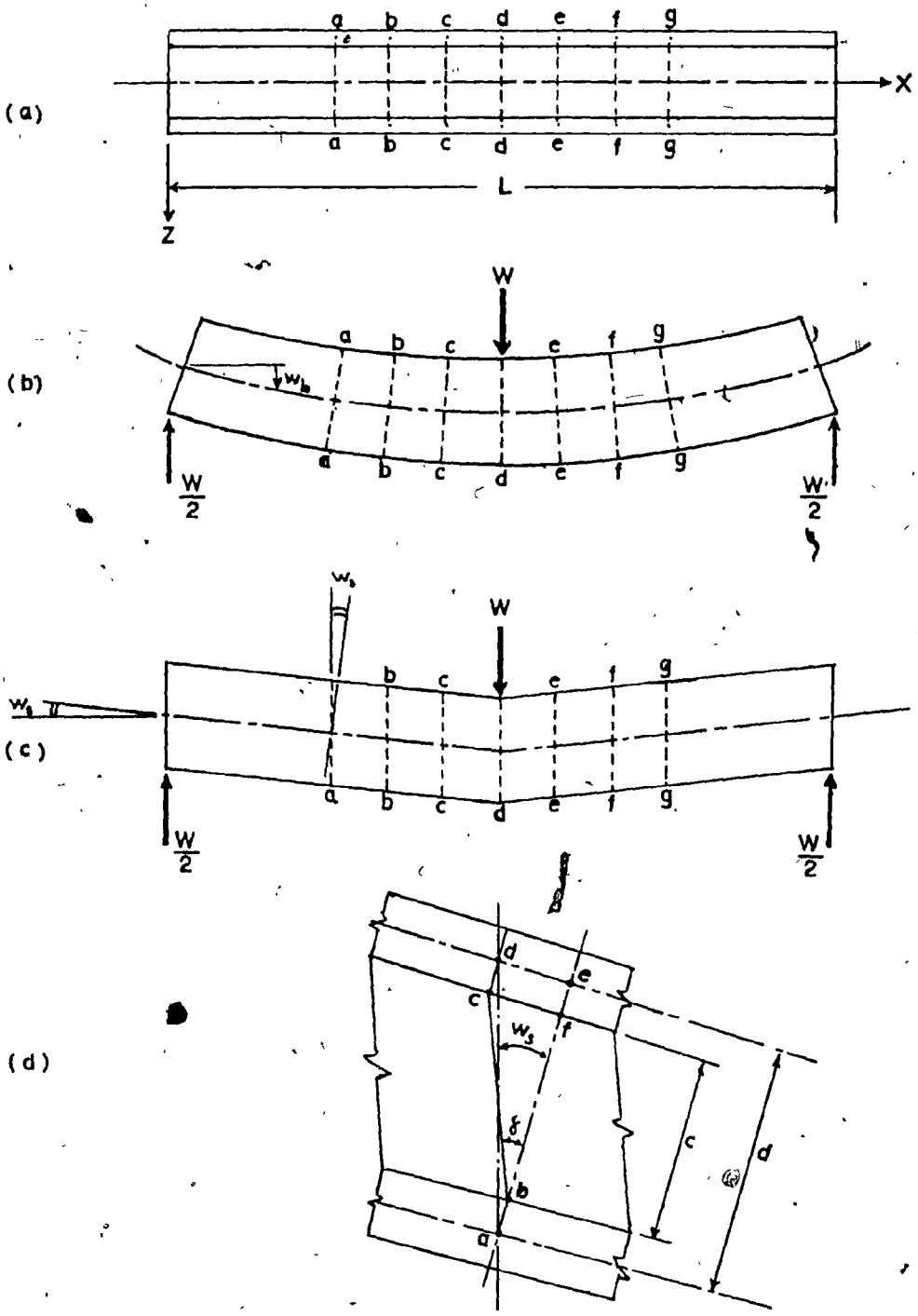

FIG. 4.5 DEFLECTION OF A SANDWICH BEAM (b) DEFORMATION DUE TO BENDING (c) DEFORMATION DUE TO SHEAR (d) SEGMENT FROM THE DEFORMED BEAM IN (c) WITH THIN FACES

The points a,b,c, ... lie on the centre-lines of the faces and the cross-sections aa, bb, cc, ... remain perpendicular to the principal x-axis of the beam after bending. Since however, the shear stress in the core at any section is constant (equation (4.13)), the shear strain (γ) will also be constant over the same sections of the core

$$\gamma = \frac{V}{Gbd} \tag{4.15}$$

where

G = the shear modulus of the core material

These constant shear strains displace the planes aa, bb, ... vertically by an amount w_s. The faces however, and the centre-line of the beam tilt at a slope of dw_s/dx.

The total deflection of a simply supported sandwich beam is therefore the bending (w_b) and shear (w_s) deflections superimposed

$$w = w_b + w_s \tag{4.16}$$

The relation between the slope of the beam dw_s/dx due to shear strain, and the core shear strain is found from using Fig. (4.5d). The distance (de) is equal to $d.(dw_s/dx)$. Assuming that the shear strains in the faces can be neglected, (de) is also equal to (cf), which in turn, is equal to (γ.c). Therefore

$$d.\frac{dw_s}{dx} = \gamma.c$$

Substituting γ from Equation (4.15)

$$\frac{dw_s}{dx} = \gamma \cdot \frac{c}{d} = \frac{V}{Gbd} \cdot \frac{c}{d} = \frac{V}{AG} \tag{4.17a}$$

and

$$A = \frac{bd^2}{c} \tag{4.17b}$$

A is the effective cross-sectional area of the beam and AG is the shear stiffness of the sandwich.

By integrating equation (4.17a) over the left half of any sandwich beam such as in Figure 4.3, the deflection due to shear stress is:

$$w_s = \frac{V}{AG} \cdot x + \text{constant} \qquad 0 \leq x \leq \frac{L}{2}$$

The constant vanishes because at $x = 0$, $w_s = 0$. Therefore, substituting for $V = +W/2$ and $x = \frac{L}{2}$, the maximum deflection is

$$\Delta_s = \frac{WL}{4AG} \tag{4.18}$$

The maximum deflection due to bending, at center is:

$$\Delta_b = \frac{WL^3}{48D} \tag{4.19}$$

The total central deflection Δ is therefore

$$\Delta = \Delta_b + \Delta_s = \frac{WL^3}{48D} + \frac{WL}{4AG} \tag{4.20}$$

Considering that Equation (4.18) may be written as

$$\Delta_s = \frac{M}{AG}$$

The total central deflection Δ, for a simply supported beam, loaded with a uniformly distributed load q may be written:

$$\Delta = \Delta_b + \Delta_s = \frac{5}{384}\frac{qL^4}{D} + \frac{M}{AG}$$

or

$$\Delta = \frac{5}{384}\frac{qL^4}{D} + \frac{qL^2}{8AG} \qquad (4.21)$$

The shear stiffness of the sandwich beam was found to be

$$AG = G\frac{bd^2}{c} \qquad (4.22)$$

If

$$\frac{d}{c} \approx 1 \text{ and } \frac{d}{t} > 100 \qquad (4.23)$$

the shear stiffness may be written

$$AG = Gbd \qquad (4.24)$$

The last expression means that when considering the geometry of the deformation of a sandwich under the conditions (4.23), the thickness of the faces are neglected.

On the basis of conditions (4.3) and (4.23) we may define the following terms:

"Very Thin" facing: $\frac{d}{t} > 100$; $A = bd$: neglect I_f

"Thin" facing: $100 > \frac{d}{t} > 6.0$; $A = \frac{bd^2}{c}$; neglect I_f

"Thick" facing: $\frac{d}{t} < 6.0$; $A = \frac{bd^2}{c}$; include I_f

CHAPTER 5

DESIGN AND TESTING IN SANDWICH CONSTRUCTION

CHAPTER 5

DESIGN AND TESTING IN SANDWICH CONSTRUCTION

5.1 INTRODUCTION

The trial and error process of design is usually the most effective. At the same time, it is advantageous to have methods of design that can check and roughly indicate where the trials should begin. The basic design approach for a required strength when core and face materials are specified is to determine the face and core thicknesses for minimum weight or cost.

In the next article the process of determining the core and face thicknesses for minimum weight is explained.

For common materials used in sandwich construction, such as steel and aluminum, is not difficult to obtain information about their strength and stiffness. For other materials however, accurate information on their properties must be obtained by tests. Common tests on sandwich beams include the three-point load test, the four-point and five-point load tests. These tests can be used to determine the flexural and shear rigidities.

It is important that deflections are small so that the horizontal component of inclined reactions does not introduce a significant bending moment.

5.2 OPTIMUM DESIGN OF PANEL FOR MINIMUM WEIGHT DETERMINATION OF CORE AND FACE THICKNESS

There are two approaches in optimizing face and core thickness in sandwich construction. The first is based on the bending strength of a sandwich beam, and the second on the bending stiffness.

Suppose that the limiting stress σ is specified, as are the face and core materials to be used. The maximum moment that can be resisted by a section of unit width is

$$M = \sigma t d \tag{5.1}$$

The total weight[1] of the beam per unit area is

$$W = 2t\rho_f + \rho_c d \tag{5.2}$$

where ρ_f = unit weight of face material

ρ_c = unit weight of core material

d = core thickness[2]

---

[1] The weight of adhesive and face reinforcement is not considered.

[2] The faces have been assumed thin.

The task is to minimize W subject to the stress requirement (5.1).

Let

$$\frac{M}{\sigma} = td = B$$

and

$$t = \frac{B}{d} \tag{5.3}$$

Substitute (5.3) into (5.2) and

$$W = 2\frac{B}{d}\rho_f + \rho_c d$$

Minimize W with respect to d, and solving for d we obtain the optimum core thickness:

$$\frac{dw}{dd} = -\frac{2B\rho_f}{d^2} + \rho_c = 0$$

$$d = \sqrt{2B(\rho_f/\rho_c)} \tag{5.4}$$

From expression (5.3) we obtain the optimum face thickness

$$t = \sqrt{B/2(\rho_c/\rho_f)} \tag{5.5}$$

The ratio of the weight of the combine faces to the core is a measure of the efficiency of a sandwich construction.

$$\frac{W_f}{W_c} = \frac{2t\rho_f}{\rho_c d} = \frac{2\rho_f}{\rho_c d}\sqrt{B\,\rho_c/2\,\rho_f}$$

$$\frac{W_f}{W_c} = \frac{1}{d}\sqrt{2B(\rho_f/\rho_c)} = 1 \qquad (5.6)$$

Therefore, the efficiency ratio is 1 and if a sandwich has a different ratio, the construction is not so economical based on its bending strength.

Should the bending stiffness D be specified along with the face and core materials, equation (5.7) must be satisfied and at the same time t and d must provide a minimum weight W in (5.8).

$$D = \frac{E_f b t d^2}{2} \qquad (5.7)$$

$$W = 2\rho_f t + \rho_c d \qquad (5.8)$$

Solving equation (5.7) for t and substituting in (5.8) we get

$$t = \frac{\sqrt{2D}}{E_f b d^2} \qquad (5.9)$$

$$W = \frac{4\rho_f D}{E_f b d^2} + \rho_c d \qquad (5.10)$$

Minimizing the weight by setting dw/dd = 0, the optimum core depth is

$$d^3 = \frac{8D}{bE_f}\left(\frac{\rho_f}{\rho_c}\right) \qquad (5.11)$$

The efficiency ratio w_f/w_c is

$$\frac{2t\rho_f}{\rho_c d} = \frac{4D}{E_f b d^3}\left(\frac{\rho_f}{\rho_c}\right) = \frac{1}{2} \qquad (5.12)$$

Therefore, when designing in terms of bending stiffness, the combined weight of the faces must be half that of the core.

5.3 THE THREE-POINT LOAD TEST

Any new form of sandwich construction should be subjected to tests in order to determine, the strength limits, and by analyzing and studying the behaviour under various loading conditions and restraints.

The three-point load test is usually employed in order to determine the flexural and shear rigidities of a particular sandwich construction. In Section 4.3, the total deflection (equation (4.20)) under a central point load was found to be

$$\Delta = \Delta_b + \Delta_s = \frac{WL^3}{48D} + \frac{WL}{4AG} \qquad (5.13)$$

For practical purposes, G is the shear modulus of the core and $A = bd^2/c$. The arrangement for the test is shown schematically in Fig. 5.1. Large deflections should be avoided in order to reduce the influence of the horizontal components of the inclined reactions; otherwise the central

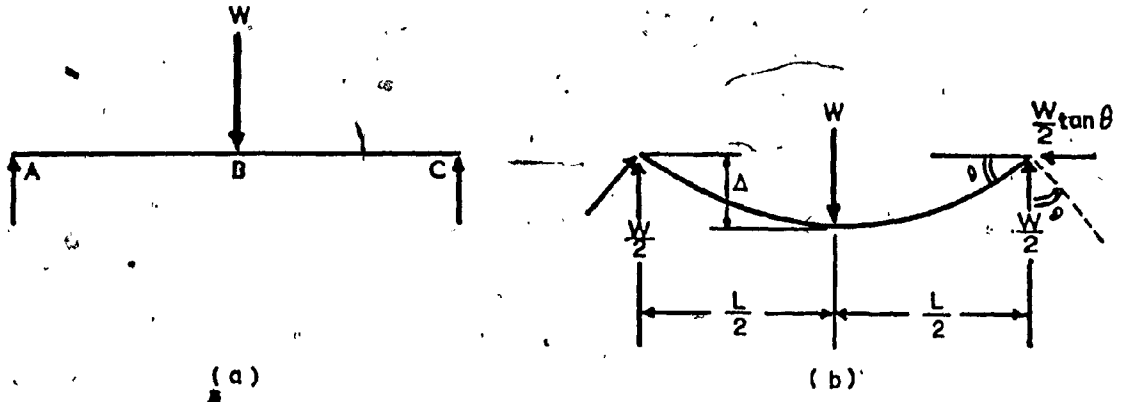

FIG. 5.1 (a) THREE POINT LOAD TEST (b) EFFECT OF EXCESSIVE DEFLECTION

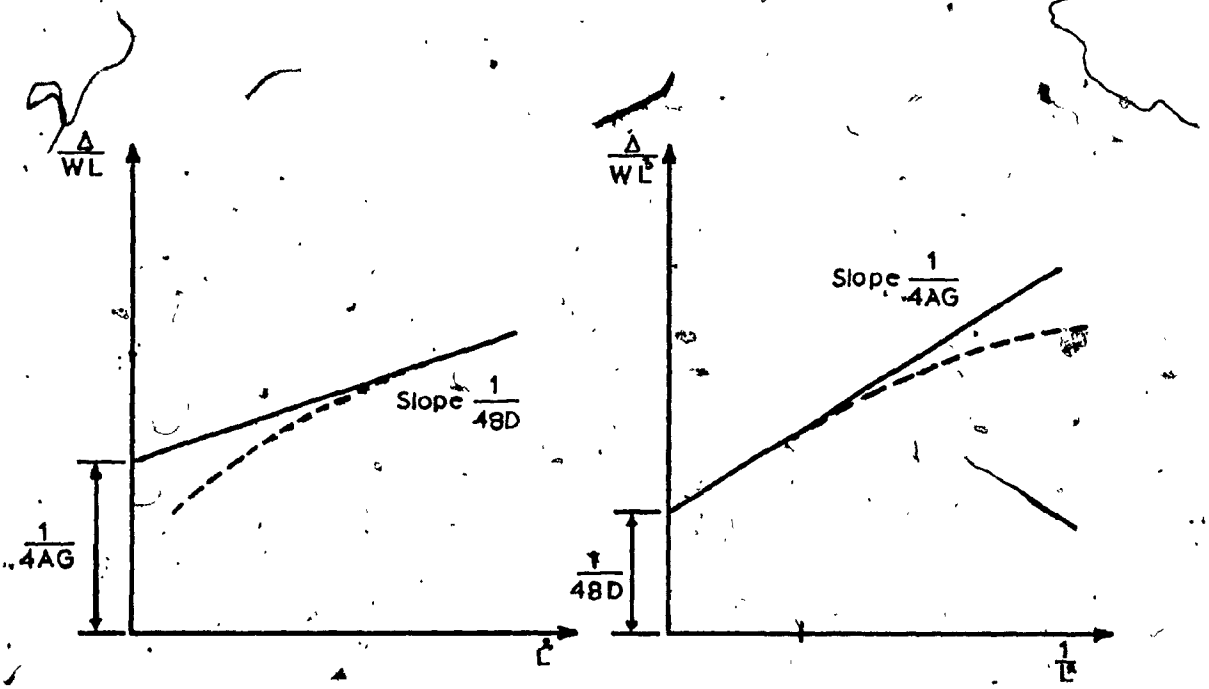

FIG. 5.2 DETERMINATION OF BENDING STIFFNESS (LEFT), AND SHEAR STIFFNESS (RIGHT), OF A SANDWICH BEAM. THE BROKEN CURVED LINES INDICATE THE DEVIATION (ERROR) WHEN STRONG AND THICK FACES ARE USED WITH A WEAK CORE

bending moment is increased by

$$\frac{W\Delta}{2} \tan\theta \ .$$

Two different spans, a large and a small, are usually enough in order to measure the deflections and then solve the resulting pair of equations from expression (5.13) for D and AG.

However, it is not so easy to decide that the span is large enough so that the deflection is free to pure bending, or that the span is small enough so that the measured deflection is mostly due to shear. The problem is satisfactorily solved by using a better method.

Equation (5.13) can be rearranged as follows:

$$\frac{\Delta}{WL} = \frac{L^2}{48D} + \frac{I}{4AG} \qquad (5.14)$$

$$\frac{\Delta}{WL^3} = \frac{1}{48D} + \frac{1}{4AG} \cdot \frac{1}{L^2} \qquad (5.15)$$

Plotting Δ/WL against L^2 in the first equation, the result is a straight line as shown by the full line in Fig. 5.2.

The second equation can also be represented as a straight line by plotting Δ/WL^3 against $1/L^2$, as shown by the full line in Fig. 5.2. The broken lines represent the category of sandwich panels with thick faces and very weak cores.

These descrepancies are due to the influence of local bending stiffness of the faces on the shear deflection. The problem is treated in reference [3], Section 2.5.

Therefore, if the load W and the corresponding deflection is measured for several spans the flexibility Δ/W of the beam is found and the straight lines in Fig. 5.2 may be plotted. The required stiffnesses D and AG can be obtained from the slopes and the intercepts, as shown in Fig. 5.2.

An accurate way to determine the flexibility of a certain span is to plot several deflections against their corresponding loads and use the slope Δ/W of the resulting straight line, as the flexibility of that particular beam.

The effect of the settlement at the supports due to crushing is minimized by measuring the settlement at points A and C at the top face of the beam and subtracting the mean from the central deflection.

CHAPTER 6

CONCRETE SANDWICH BEAMS WITH STYROPOR-FILLED LIGHTWEIGHT CONCRETE CORE

CHAPTER 6

CONCRETE SANDWICH BEAMS WITH STYROPOR-FILLED LIGHTWEIGHT CONCRETE CORE

6.1 DESIGN AND CONSTRUCTION

The cross-section of the test beams was designed for minimum weight based on bending strength.

From the best results in Table 2.2 (specimens C3 and C7) and from Table 3.2, we have:

	Material	Density(ρ)	Tensile Strength(σ)
Face:	LMC mortar	118 pcf(1890 kg/m^3)	1000 psi(70.3 kgf/cm^2)
Core:	Styropor-filled concrete	16.2 psf(260 kg/m^3)	-----

For a residential service load of 45 psf(720 kgf/m^2) and a span of 10 feet (approximately the length of the actual panels) the design moment for a simply supported beam is M_u = 956 in-lb/in.

The optimum value of d is (equation (5.3))

$$d = \sqrt{2B(\rho_f/\rho_c)} \quad \text{where} \quad B = \frac{M}{\sigma}$$

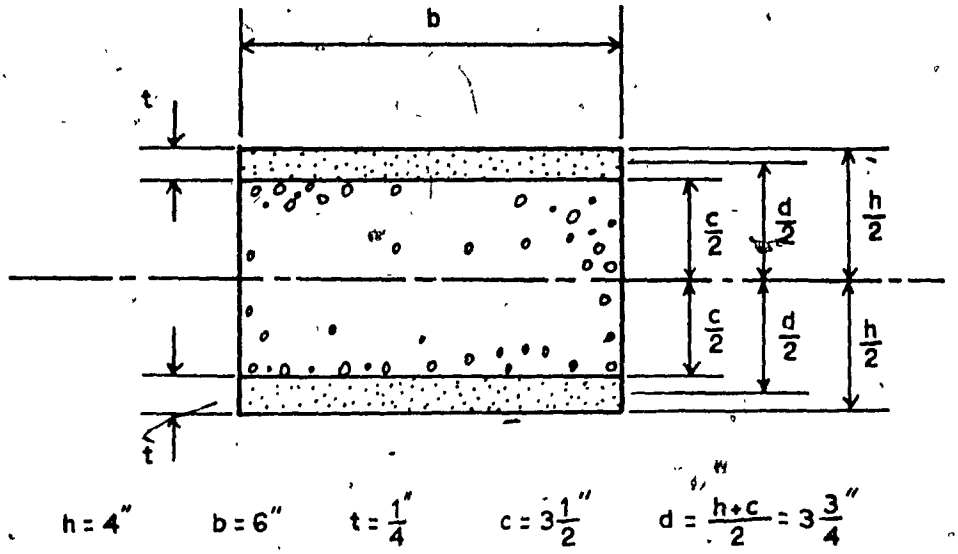

$h = 4''$ $b = 6''$ $t = \frac{1}{4}''$ $c = 3\frac{1}{2}''$ $d = \frac{h+c}{2} = 3\frac{3}{4}''$

FIG. 6.1 THE ADOPTED CROSS-SECTION FOR THE SANDWICH TEST BEAMS, WITH LMC MORTAR FACES AND STYROPOR-FILLED LIGHTWEIGHT CONCRETE CORE

The face mortar formulation was:

Washed Sand/Cement ratio	:	3:1
Latex Solids (% of wt. of cement)	:	16
Total Water/Cement ratio	:	30%

No Antifoam B was used in the mix.

Thus for

$$B = \frac{956}{1000} = 0.956 \text{ in}^2$$

$$d = \sqrt{2(.956)(118/16.2)} = 3.73 \text{ in}$$

A sandwich depth of 4" was adopted with ¼" thick faces. The cross-section of a 6" wide test beam is shown in Fig. 6.1.

The construction procedure for the test beams begins by casting the bottom face. An approximately 1/8" layer of LMC mortar was placed in 4" deep by 6" wide plywood forms and different lengths. Then a layer of BFG reinforcement was placed and leveled until cement paste passed through the "cloth", and another 1/8" layer of LMC mortar was added. At the same time a mix of polystyrene beads lightweight concrete was prepared and cast immediately after the bottom face was ready. The top face was placed on the core in a manner similar to the bottom face.

The specimens were left to cure in the open air for 14 days. Two sets of beam specimens were prepared with respect to the amount and position of BFG reinforcement. In the first set only one layer of BFG "cloth" was placed at the center of both mortar faces, while in the second set an additional layer was placed on the outside surface of the bottom face. The Latex content was also different in the two cores, 18% and 25% solids respectively. Washed sand was used in all face LMC mortars.

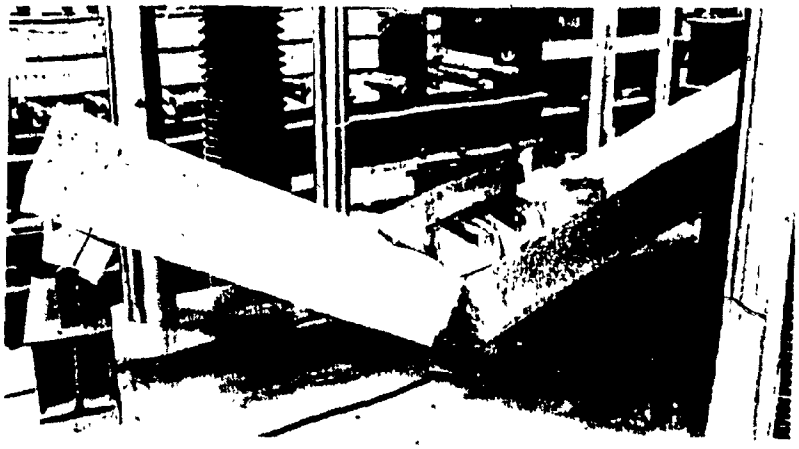

BEAM B1.1 IN TABLE 6.1

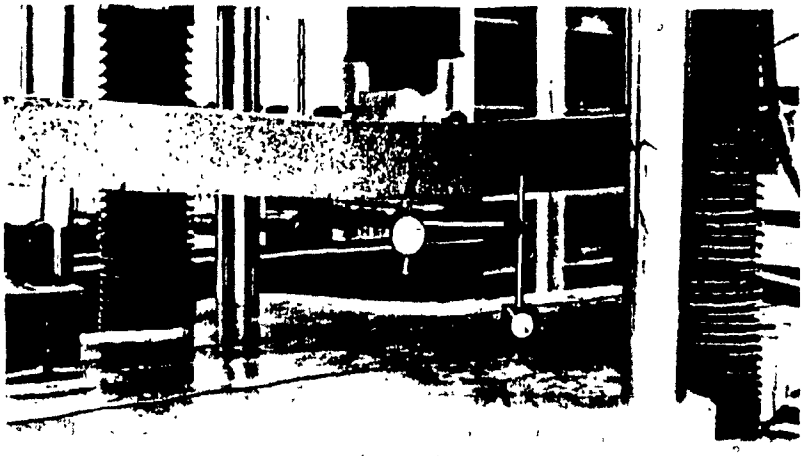

BEAM B2.1 IN TABLE 6.2

FIG. 6.2 TESTED CONCRETE SANDWICH BEAMS WITH STYROPOR-FILLED CONCRETE CORE

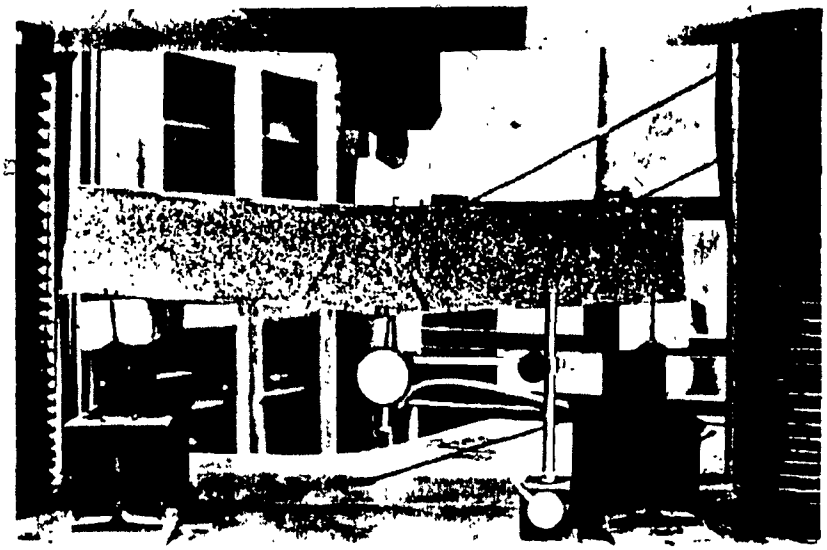

BEAM B_p^2.2 IN TABLE 6.2

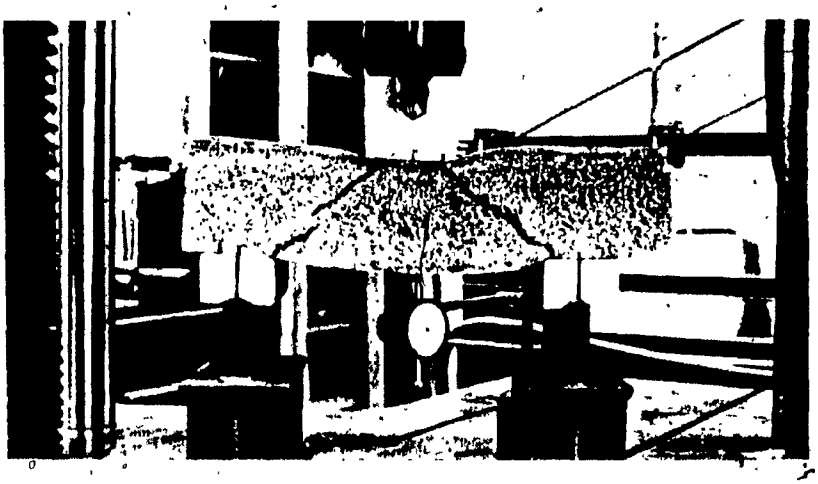

BEAM B_p^2.3 IN TABLE 6.2

FIG. 6.3 TESTED CONCRETE SANDWICH BEAMS WITH STYROPOR-FILLED CONCRETE CORE

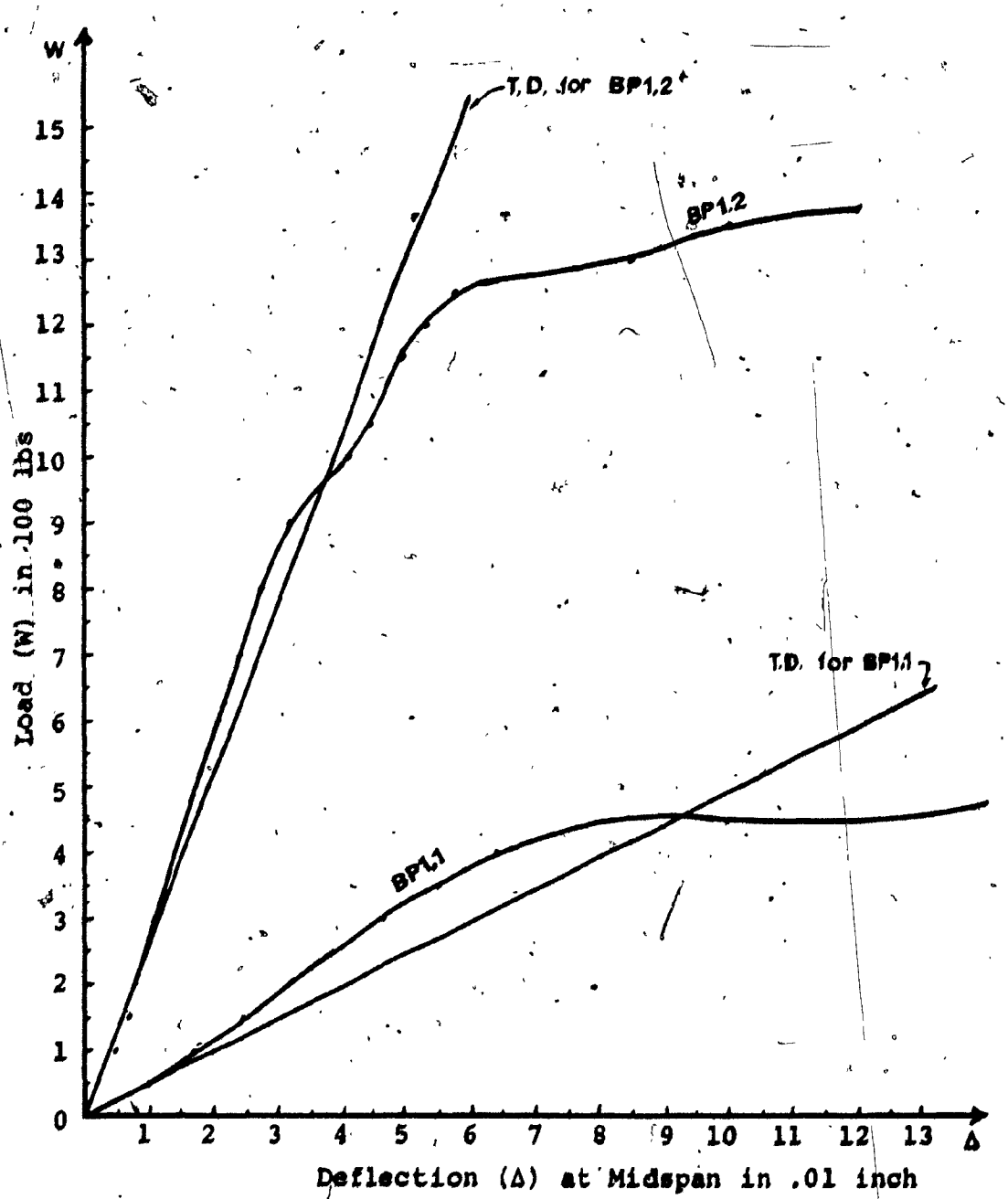

FIG. 6.4 THREE-POINT LOAD TEST : LOAD-DEFLECTION CURVES FOR BEAMS IN TABLE 6.1

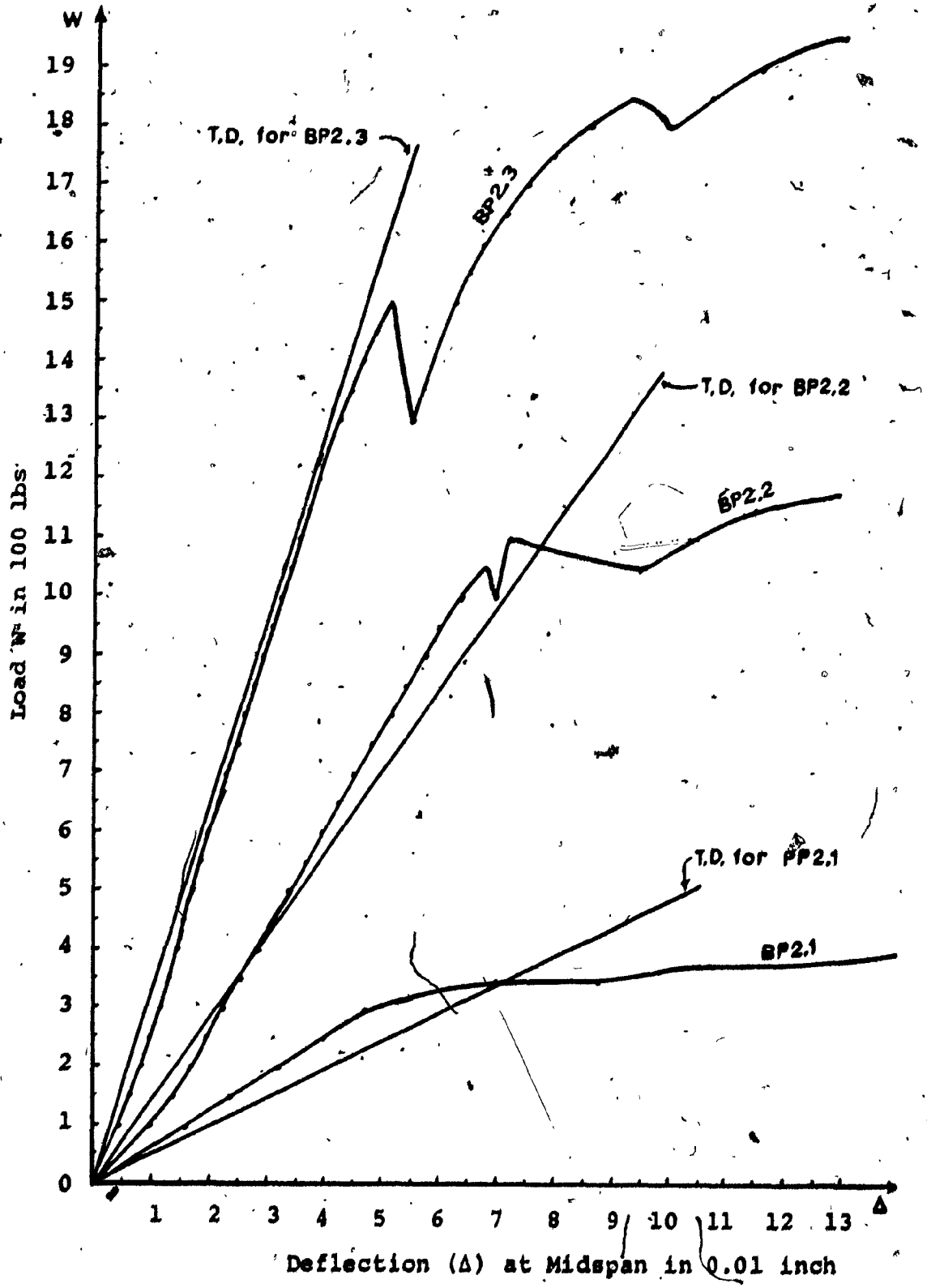

FIG. 6.5 THREE-POINT LOAD TEST: LOAD-DEFLECTION CURVES FOR BEAMS IN TABLE 6.2

Before testing, at 14 days, the specimens were weighed and showed an average weight of 10 psf (48.8 kg/m^2).

6.2 TEST RESULTS

The specimens were tested as simply supported centrally loaded beams. For the reaction supports and loaded area, 2½" wide by 6" long wooden blocks were used as shown in Fig.6.2 and Fig. 6.3, where tested specimens and their modes of failure are illustrated.

During the test, deflections were measured with dial indicators. The load (W) vs. Deflection (Δ) curves are plotted in Fig. 6.4 and Fig. 6.5.

The bending stresses (σ_f) and shear stresses (τ) at late stages of loading are given in Table 6.1 and Table 6.2, along with a description of the specimens. These stresses were calculated using equation (4.6a) for (σ_f) and equation (4.13) for (τ).

In Fig. 6.4 and Fig. 6.5, the theoretical deflections (T.D.) are plotted using the equation (4.20)

$$T.D. = \Delta_b + \Delta_s = \frac{WL^3}{48D} + \frac{WL'}{4AG} \qquad (6.1)$$

where

L' = L - (width of loaded area + width of support area + h)

= effective total length for shear deformation

In calculating bending stresses, shear stresses and deflections, the following constants were used:

LMC Mortar: $E_f = 1.9 \times 10^6$ psi (average from Table 2.2)

Styropor Filled Core: $E_c = 4400$ psi (Table 3.6)

Styropor Filled Core: $G = 2450$ psi (Fig. 3.7)

Bending Stiffness: $D = E_f(\frac{btd^2}{2} + \frac{bt^3}{6}) + E_c \frac{bc^3}{12} =$

$= 2.016 \times 10^7$ in^2-lbs

$A = \frac{bd^2}{c} = 24.1$ in^2

The agreement between theoretical and experimental load-deflection curves is considered to be reasonable in the elastic range in view of the nature of the materials used. A maximum face force of 362 lb/in(64.6 kgf/cm) and a maximum shear strength of 43 psi(3.04 kgf/cm^2) were obtained (specimens BP1.2 and BP2.3 respectively). The maximum local compressive stress on the core at the loaded zone at failure was 120 psi (8.43 kgf/cm^2), which is the compressive strength of similar

cores developed and tested earlier in the project.

6.3 OBSERVATIONS AND COMMENTS

The experimental deflections for both types of test beams were generally smaller than the theoretical ones in the elastic range. The average maximum differences being 17% for the first set of beams and 10% for the second set.

In spite of the additional layer of B.F.G. "cloth", the second set of beams showed higher flexibilities than the first set. This is possibly explained by the higher Latex content in the core (25% solids vs. 18% solids) which reduces the elastic modulus, as demonstrated in compression tests, and the fact that the additional B.F.G. "cloth" at the surface of the bottom face reduces the actual thickness of the mortar face.

The bending and shear strengths calculated from the test beams are in good agreement with the values obtained from the individual testing of the materials. It is important to note that creep deformations were initiated in the core at the top of the elastic range.

This might be due to poor compaction of the core material, the nature of the aggregates and the influence of the behaviour of the Latex; although no information came in the author's attention on the effect of Latexes in concretes under sustained loads.

TABLE 6.1

THREE-POINT LOAD TEST AT 14 DAYS, W_{PANEL} = 10.5 psf

Specimen No.	Load (W) (lbs) (kgf)	Deflection (Δ) in. (cm)	Bending Stress (σ_f) psi (kgf/cm^2)	Shear Stress (τ) psi (kgf/cm^2)	Remarks
BP1.1					
4" x 6" wide	400 (181.4)	0.062 (.157)	798 (56.1)	8.81 (.62)	
Span = 42"	450 (204)	0.10 (.254)	898 (63.1)	10.0 (.70)	
BFG cloth at centre of ½" thick faces	500 (226.8)	0.15 (0.381)	997 (70.1)	11.1 (.78)	First crack in bottom faces Core cracking at midspan
Face $\frac{P}{C}$ = 15% solids					
Core $\frac{P}{C}$ = 18% solids	550 (249.5)	0.36 (0.914)	1097 (77.13)	12.2 (.86)	
Beads Gradation "B"	550 (249.5)	1.00 (2.54)			Failure by rupture of lower face (Fig.6.2a)

(continued)

Specimen No.	Load (W) (lbs) (kgf)	Deflection (Δ) in. (cm)	Bending Stress (σ_c) psi (kgf/cm^2)	Shear Stress (τ) psi (kgf/cm^2)	Remarks
BP1.2					
Span = 17"	1100 (499)	0.047 (0.119)	888 (62.4)	24.4 (1.71)	
(Same as BP1.1)	1250 (567)	0.057 (0.144)	1009 (71)	27.7 (1.95)	Major crack in bottom face at mid-span
	1375 (624)	0.12 (.304)	1110 (78)	30.51 (2.15)	Core cracking at midspan
	1800 (816)	0.40 (1.016)	1453 (102)	40.0 (2.73)	Failure by rupture of lower face

TABLE 6.2

THREE-POINT LOAD TEST AT 14 DAYS, W_{PANEL} = 9.5 psf

Specimen No.	Load (W) (lbs) (kgf)	Deflection (Δ) in. (cm)	Bending Stress (σ_f) psi(kgf/cm^2)	Shear Stress (τ) psi(kgf/cm^2)	Remarks
BP2.1 h = 4" b = 6"					
Span = 40"	325(147.4)	0.06(.152)	617(43.4)	7.2 (.50)	
Additional BFG cloth at surface of bottom face	375(170.1)	0.10(.254)	712(50)	8.33(.58)	First crack in the core at mid-span
	400(181.4)	0.25(.635)	760(53.4)	8.8 (.62)	
Face $\frac{P}{C}$ = 15% solids Core $\frac{P}{C}$ = 25% solids Beads Gradation "B"	600(272.1)	0.73(1.854)	1140(80.1)	13.3(.94)	Slow BFG cloth failure with 1/4" crack (Fig. 6.2b) in lower face

(continued)

Specimen No.	Load (W) (lbs) (kgf)	Deflection (Δ) in. (cm)	Bending Stress (σ_f) psi(kgf/cm^2)	Shear Stress(τ) psi(kgf/cm^2)	Remarks
BP2.2					
Span = 20"	1100(499)	0.071(0.180)	1045(73.5)	24.4(1.71)	
	1150(522)	.115(.292)	1092(76.8)	25.5(1.79)	Major crack in the core at mid-span
	1250(567)	0.180(.457)	1188(83.5)	77.7(1.95)	
(Same as BP2.1)	1400(635)	0.400(1.016)	1330(93.5)	31.1(2.18)	Slow BFG cloth failure (Fig. 6.3a)
BP2.3					
Span = 12"	1500(680.4)	0.051(.129)	855(60.1)	33.3(2.34)	
(Same as BP2.1)	1600(726)	0.070(.177)	912(64.1)	35.5(2.5)	First diagonal crack in the core
	1950(885)	0.130(.330)	1111(78)	43.3(3.04)	Diagonal splitting (Fig. 6.3b)

CHAPTER 7

CONCRETE SANDWICH BEAMS WITH HONEYCOMB CORE

CHAPTER 7

CONCRETE SANDWICH BEAMS WITH HONEYCOMB CORE

7.1 DESIGN AND CONSTRUCTION

Due to the very large density difference of the mortar faces and kraft paper honeycomb core, the design for minimum weight based either on bending strength (σ) or bending stiffness (D) does not yield reasonable sections, so the same section as in Fig. 6.1 was adopted with honeycomb replacing styropor-filled lightweight concrete.

Two types of honeycomb were used in two sandwich beam thicknesses and cell orientation, shown in Fig. 3.7.

In all of the test specimens the core was first prepared by gluing to the two honeycomb faces one layer of BFG "cloth" using latex contact cement. The core was then laid on a 1/4" thick layer of LMC mortar in a plywood form and immediately after the top 1/4" thick face was placed and finished. The specimens were left to cure in the open air for 14 days. The average weight was found to be 5.0 psf which actually is the total weight of the mortar faces, as the weight of the core is negligible. This is one half the average weight of the styropor-filled core sandwich panels.

The sets of sandwich beams tested are identified as follows:

$BWT^{h}_{1 \text{ or } 2}$ - H - Honeycomb's WT-plane[1] parallel to the x-principal axis of the beam

$BST^{h}_{1 \text{ or } 2}$ - H or C = Honeycomb's ST-plane[1] parallel to the x-principal axis of the beam

h = the beam's thickness, either 4" or 5"

H = 3/4"-cell size kraft paper honeycomb (Fig. 3.7a)

C = 3/8"-cell size cormat paper (Fig. 3.7b)

1 = BFG "cloth" at face-core interface only,

2 = Additional layer of BFG "cloth" at the surface of bottom face

In addition to the above sets of test beams another set where the honeycomb was sprayed partially with polyester resin cut back with acetone, was tested.

The face mortar formulations were as in Chapter 6 specimens.

7.2 TEST RESULTS

All specimens were tested as simply supported centrally loaded beams using 2½" wide wooden blocks at the supports and

---

[1] See Figure 3.7 for definition and interpretation of W, S and T directions.

loaded area. Fig. 7.1 to Fig. 7.3 are photographs of the sandwich beams at failure.

The experimental load vs. deflection curves are plotted in Fig. 7.4 to Fig. 7.6 along with the theoretical deflections (T.D.).

The Theoretical Deflection (T.D.) curves were computed as in Chapter 6.

The constants used in computing the bending stresses, shear stresses and deflections were:

LMC mortar	:	$E_f = 1.9 \times 10^6$ psi (Table 2.2)
3/4"-cell Honeycomb	:	$G_{WT} = 625$ psi, $G_{ST} = 820$ psi (Fig. 3.8a)
3/8"-cell Cormat, ST-Plane	:	$G_{ST} = 720$ psi (Fig. 3.8b)
Bending Stiffness	:	$D = E_f(\frac{btd^2}{2} + \frac{bt^3}{6})$

The results of the Three-Point Load Test are given in Tables 7.1 through 7.5, along with a description of the specimens and their modes of failure.

Considering the experimental and theoretical deflections, the curves for the BWT_x^4-H specimens (Fig. 7.1, Table 7.1) are identical in the elastic range, while the experimental deflection curves for the BWT_1^5-H specimens (Fig. 7.2, Table 7.2) are not in very good agreement with the computed ones. Both of the above sets of test beams failed in shear and due to crushing of the core under the loaded area. The maximum shear strengths obtained at failure were 8.0 psi and

7.0 psi respectively for the two sets of beams, which are in agreement with the value (τ = 8.0 psi) determined earlier from the double-block shear test.

The local compressive stress on the core at the loaded zone at failure was 26.6 psi(1.87 kg/cm^2).

The experimental load-deflection curves for the specimens with their strong ST-plane (BST^h_x-H or C specimens) parallel to the principal x-axis of the test beams are in good agreement with the theoretical deflections (Fig. 7.4 to Fig. 7.6). The capacity however of these specimens was limited by the poor strength of the cement adhesive as is indicated in Tables 7.3 through 7.5.

7.3 OBSERVATIONS AND COMMENTS

Two main modes of failure were associated with the two WT- and ST-planes of the honeycomb and Cormat cores. The BWT^h_x-H specimens failed in shear of the core while the BST^5_1-H and BST^5_x-C specimens failed due to shearing failure of the bond at the core-face interface. The low shear strength of the WT-plane and the poor performance of the adhesive limited the bending stresses in the face to a maximum of 796 psi(56 kgf/cm^2) in $2BWT^4_2$-H and 975 psi(68.6 kgf/cm^2) in $1BST^4_2$-C. Both of these values are at least 50% below the strengths obtained in Chapter 6 where styropor-filled concrete core was used.

Thus, a stronger adhesive is needed for a higher and more consistent performance of this type of sandwich construc-

tion.

In all of the above tested specimens, creep deformations were initiated at the top of the linear range of the load-deflection curves. The reason may be the early and slow shear bond failure at the core-"cloth" interface.

(a) $1BWT^{4}_{1}$-H

Span = 42"

(b) $2BWT^{4}_{2}$-H

Span = 42"

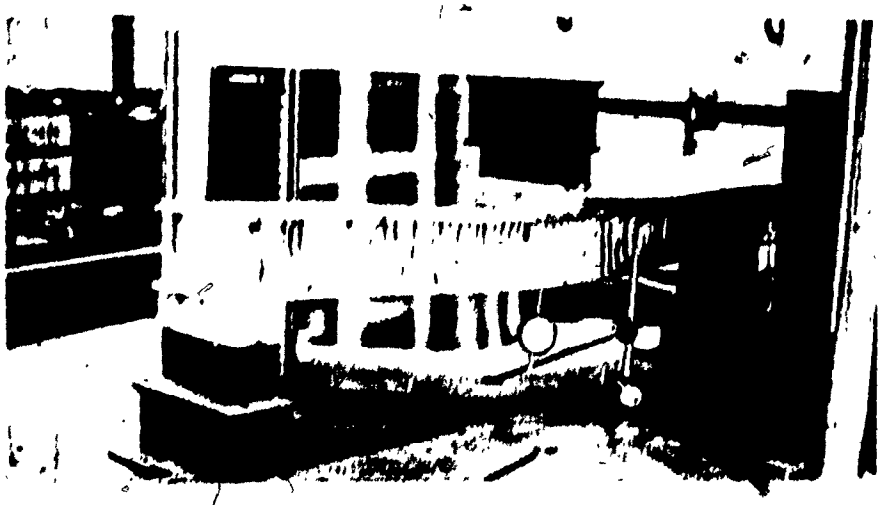

(c) $2BWT^{4}_{2}$-H

Span = 19"

FIG. 7.1 TESTED CONCRETE SANDWICH BEAMS WITH 3/4"-CELL HONEYCOMB CORE

(a) $1BWT_1^6$-H, Span = 42"

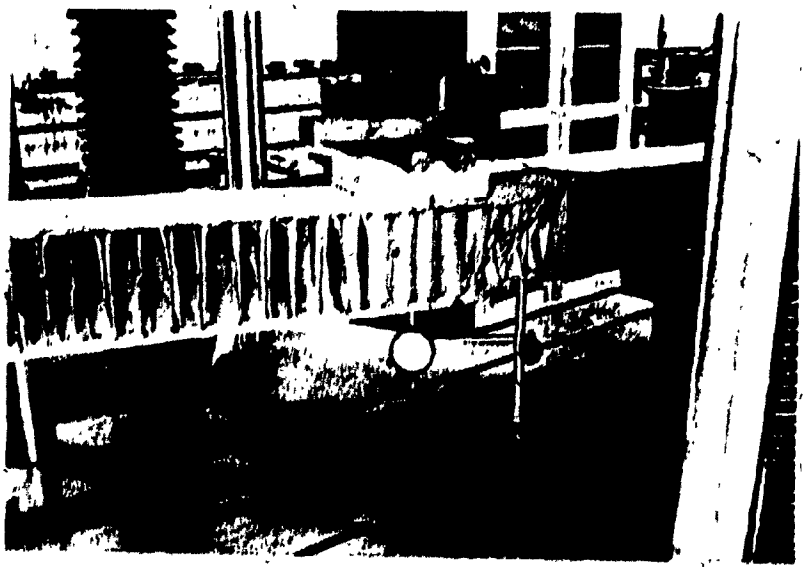

(b) $2BWT_1^6$-H, Span = 42"

FIG. 7.2 TESTED CONCRETE SANDWICH BEAMS WITH 3/4"-CELL HONEYCOMB CORE

(a) $1BST_2^{\frac{1}{2}}$-C, Span = 42"

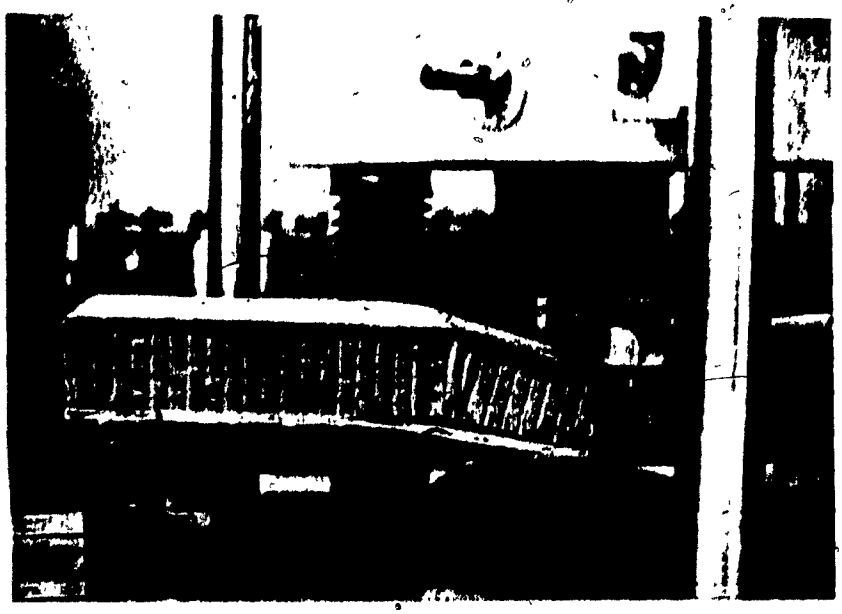

(b) $1BST_1^{\frac{1}{2}}$-C, Span = 42"

FIG. 7.3 TESTED CONCRETE SANDWICH BEAMS WITH 3/8"-CELL CORMAT CORE

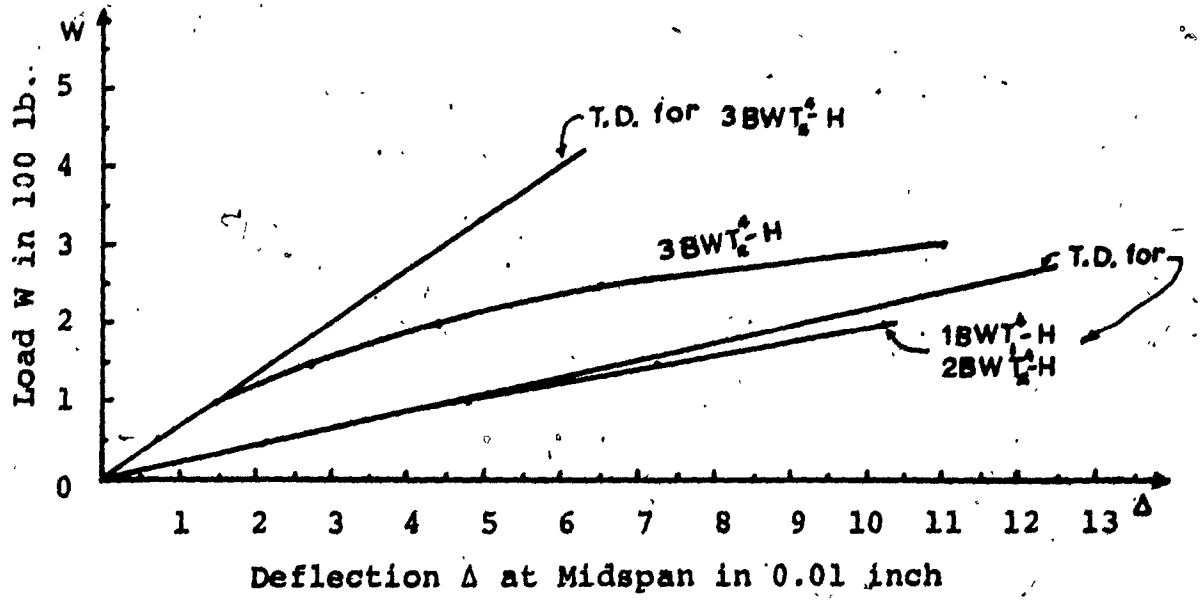

(a)

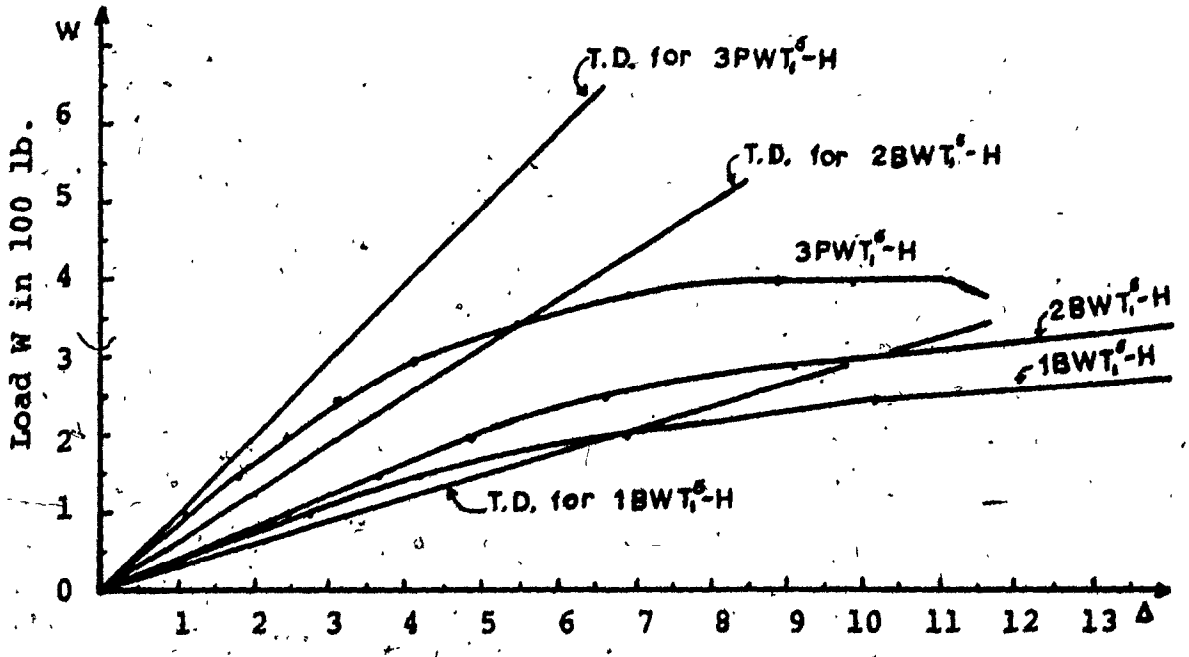

(b)

FIG. 7.4 THREE-POINT LOAD TEST : LOAD-DEFLECTION CURVES FOR (a) THE BEAMS IN TABLE 7.1, (b) THE BEAMS IN TABLE 7.2

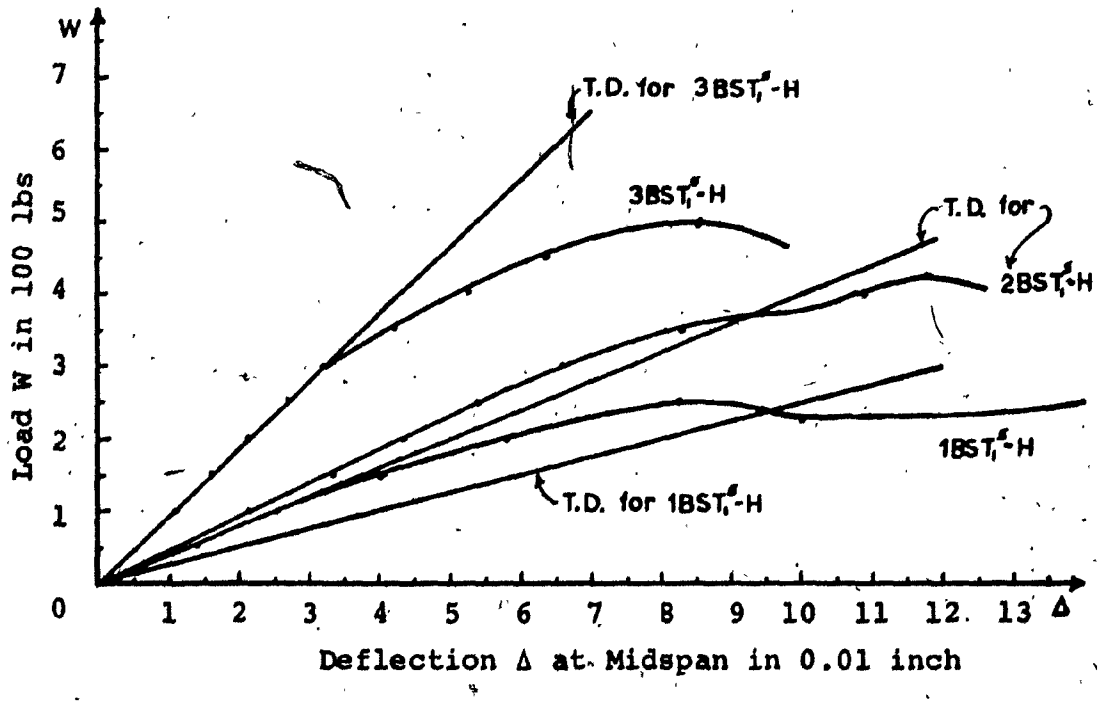

(a)

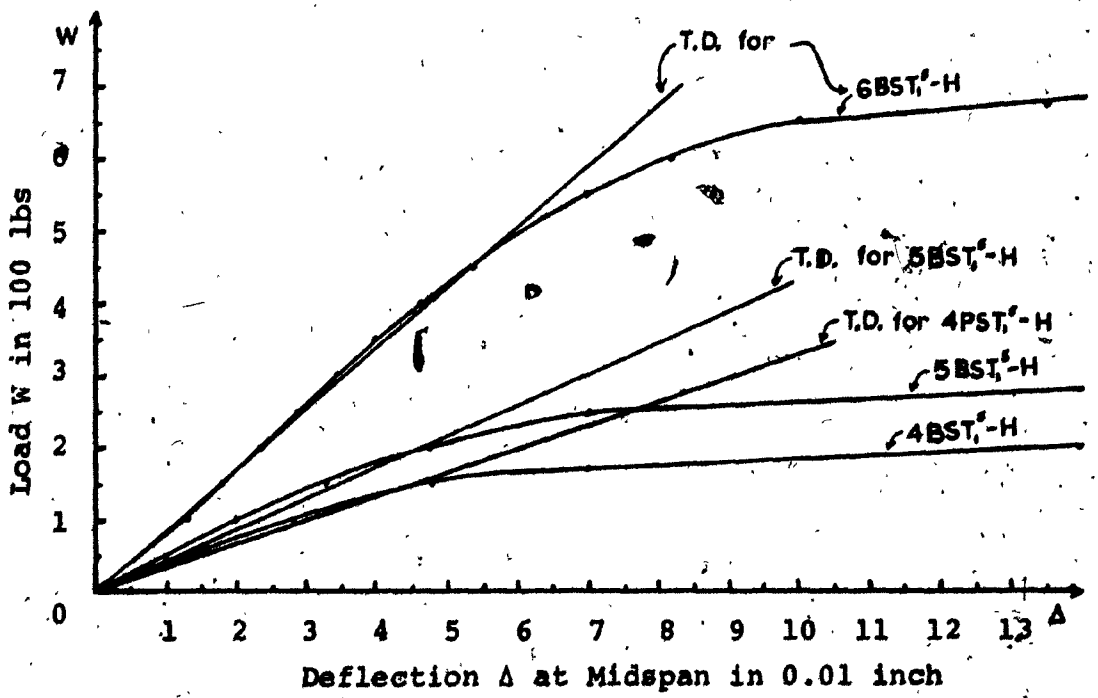

(b)

FIG. 7.5 THREE-POINT LOAD TEST : LOAD-DEFLECTION CURVES FOR (a) THE BEAMS IN TABLE 7.3, (b) THE BEAMS IN TABLE 7.4.

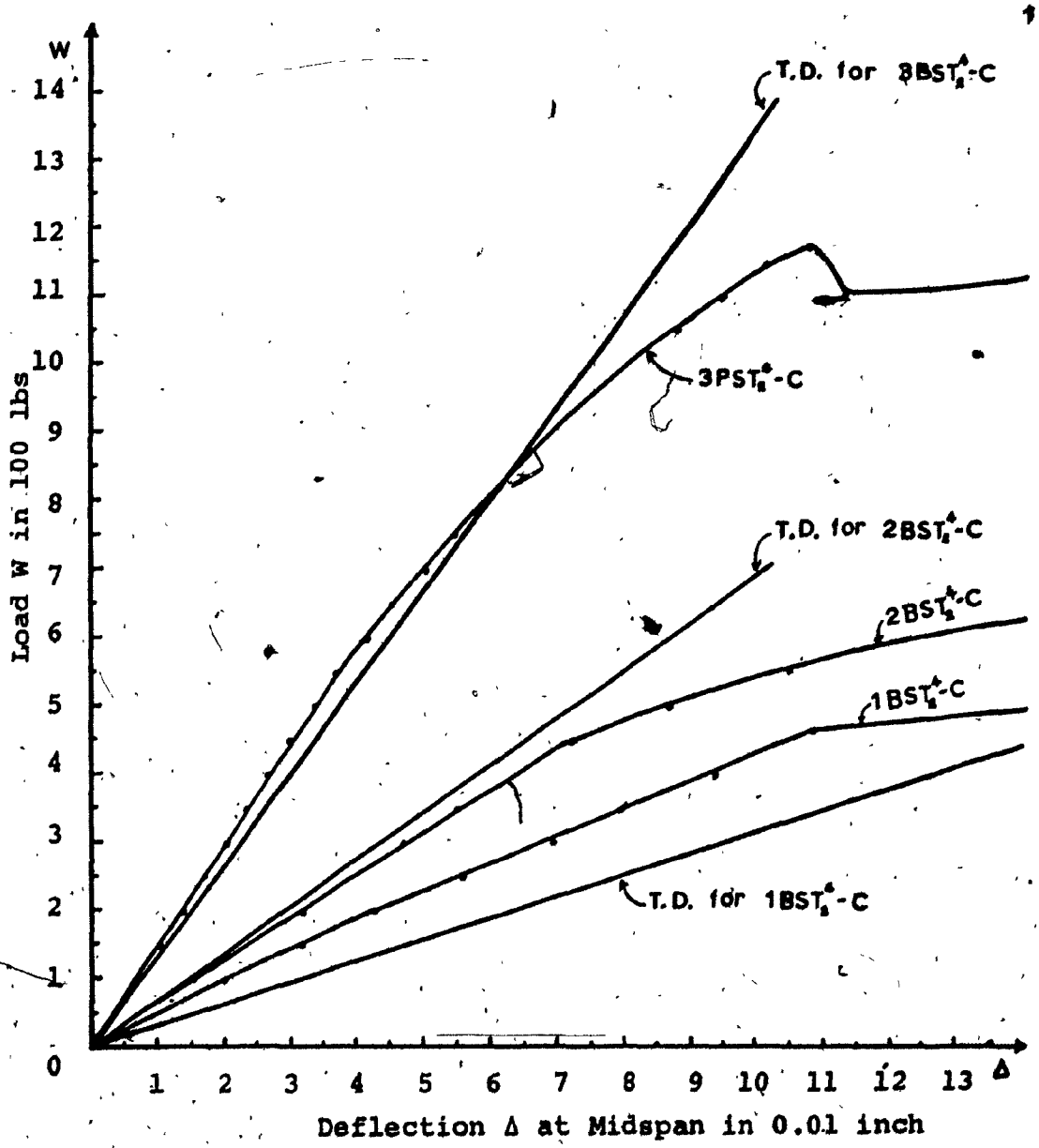

FIG. 7.6 THREE-POINT LOAD TEST : LOAD-DEFLECTION CURVES FOR THE BEAMS IN TABLE 7.5.

TABLE 7.1

THREE-POINT LOAD TEST AT 14 DAYS, W_{PANEL} = 5 psf

Specimen No.	Load (W) (lbs) (kgf)	Deflection (Δ) in. (cm)	Bending Stress (σ_f) psi(kgf/cm^2)	Shear Stress (τ) psi(kgf/cm^2)	Remarks
$\frac{1BWT_1^4-H}{}$ 6" wide Span = 42"	200(90.7)	.103(.26)	398(28)	4.4 (.31)	First crack at bottom face
BFG cloth at face-core interface	250(113.4)	.200(.50)	498(35)	5.5 (.39)	First crack at bottom face
Faces $\frac{P}{C}$ = 15% solids 3/4"-cell Honeycomb 1/4"-thick faces	280(127.0)	.80 (2.03)	557(39)	6.20(.44)	Core shear failure in left half of the beam (Fig.7.1a)

(continued)

Specimen No.	Load (W) (lbs) (kgf)	Deflection (Δ) in. (cm)	Bending Stress (σ_f) psi(kgf/cm^2)	Shear Stress (τ) psi(kgf/cm^2)	Remarks
2BWT$^{\frac{1}{2}}_{2}$-H					
Span = 42"	200(90.7)	.102(.25)	398(28	4.4 (.31)	
Same as	250(113.4)	.14 (.35)	398(35)	5.5 (.39)	
1BWT$^{\frac{1}{2}}_{1}$-H with additional BFG cloth at bottom face	400(181.4)	.35(.88)	796(56)	8.8 (.62)	Core shear failure (Fig. 7.16)
3BWT$^{\frac{1}{2}}_{2}$-H					
Span = 19"	200(90.7)	.044(.11)	180(13)	4.4 (.31)	
(Same as	350(158.7)	.76 (.40)	315(22)	7.7 (.54)	
2BWT$^{\frac{1}{2}}_{2}$-H	400(181.4)	.20 (.50)	360(25)	8.8 (.62)	Core shear failure (Fig. 7.16)

TABLE 7.2

THREE-POINT LOAD TEST AT 14 DAYS, W_{PANEL} = 5 psf

Specimen No.	Load (W) (lbs) (kgf)	Deflection (Δ) in. (cm)	Bending Stress (σ_f) psi (kgf/cm^2)	Shear Stress (τ) psi (kgf/cm^2)	Remarks
1BWT^5-H$_1$					
6" wide	250(113)	.102(.259)	388(27.3)	4.4 (.30)	
Span = 42"					
BFG cloth at face-core interface	275(125)	.14 (.355)	427(30.0)	4.8 (.34)	Local shearing of core
Faces $\frac{P}{C}$ = 15% solids	300(136)	.26 (.660)	465(32.7)	5.2 (.37)	Core shear failure (Fig. 7.2)
3/4"-cell Honeycomb					
1/4"-thick faces					

(continued)

Specimen No.	Load (W) (lbs) (kgf)	Deflection (Δ) in. (cm)	Bending Stress (σ_f) psi (kgf/cm^2)	Shear Stress (τ) psi (kgf/cm^2)	Remarks
$2BWT^5_1$-H					
Span = 24"	250 (113)	.07 (.177)	222 (15.6)	4.4 (.30)	
Same as	300 (136)	.101 (.256)	266 (18.7)	5.2 (.37)	
$1BWT^5_1$-H	360 (163)	.22 (.558)	319 (22.4)	6.3 (.44)	Core shear and crushing failure
$3BWT^5_1$-H					
Span = 12"	300 (136)	.042 (.106)	133 (9.3)	5.2 (.37)	
	400 (181)	.09 (.202)	177 (12.5)	7.0 (.49)	Core shear and crushing failure

TABLE 7.3

THREE-POINT LOAD TEST AT 14 DAYS, W_{PANEL} = 5 psf

Specimen No.	Load (W) (lbs) (kgf)	Deflection (Δ) in. (cm)	Bending Stress (σ_f) psi (kgf/cm^2)	Shear Stress (τ) psi (kgf/cm^2)	Remarks
IBST$^{fs}_{1}$-H					
6" wide	250 (113.4)	.082 (.20)	332 (23)	4.8 (.33)	
Span = 36"	300 (136)	.30 (.76)	398 (28)	5.7 (.40)	Shear bond failure at the core-"cloth" interface
BFG core at face-core interface	310 (141)	.46 (1.16)	412 (29)	5.9 (.41)	
Faces $\frac{P}{C}$ = 15% solids					
3/4"-cell Honeycomb					
1/4"-thick faces					

(continued)

Specimen No.	Load (W) (lbs) (kgf)	Deflection (Δ) in. (cm)	Bending Stress (σ_f) psi(kgf/cm^2)	Shear Stress (τ) psi(kgf/cm^2)	Remarks
$2BST^5_1$-H					
Span = 24"	300(136)	.066(.16)	266(18.7)	5.7 (.40)	
Same as	375(170)	.10 (.25)	332(23.3)	7.2 (.50)	Shear bond failure at the core-"cloth" interface
$1BST^5_1$-H	400(181.4)	.109(.27)	354(25)	7.6 (.54)	
$3BST^5_1$-H					
Span = 12"	300(136)	.033(.08)	133(9.3)	5.7 (.40)	
Same as	400(181.4)	.055(.14)	177(12.4)	7.6 (.54)	
$1BST^5_1$-H	500(227)	.085(.21)	221(15.6)	9.6(.67)	Crushing of core and top face under applied load

TABLE 7.4

THREE-POINT LOAD TEST AT 14 DAYS, W_{PANEL} = 5.5 psf

Specimen No.	Load (W) (lbs) (kgf)	Deflection (Δ) in. (cm)	Bending Stress (σ_f) psi(kgf/cm^2)	Shear Stress (τ) psi(kgf/cm^2)	Remarks
$4BST^5_1$-H					
6" wide	175(79.4)	.08(.20)	232(16.3)	3.3(.23)	
Span = 36"					
Same as	200(90.7)	.14(.35)	266(18.7)	3.8(.27)	Early shear bond failure at the core-"cloth" interface. Major crank at bottom face
$1BST^5_1$-H					
Core has been partially sprayed with polyester resin cutback with aceton					

(continued)

Specimen No.	Load (W) (lbs) (kgf)	Deflection (Δ) in. (cm)	Bending Stress (σ_f) psi(kgf/cm^2)	Shear Stress (τ) psi(kgf/cm^2)	Remarks
$5BST^5_1$-H					
Span = 30"	250(113.4)	.07(.17)	277(19.5)	4.8(.33)	
Same as $4BST^5_1$-H	300(136)	.14(.35)	332(23.3)	5.7(.40)	Early shear bond failure at the core-"cloth" interface
$6BST^5_1$-H					
Span = 20"	300(136)	.034(.08)	221(15.6)	5.7(.40)	
Same as $4BST^5_1$-H	450(204)	.054(.13)	332(23.3)	8.6(.60)	Early shear bond failure at the core-"cloth" interface
	675(306)	.135(.34)	498(35)	12.9(.91)	Crushing of the core under applied load

TABLE 7.5

THREE-POINT LOAD TEST AT 14 DAYS, W_{PANEL} = 6.5 psf

Specimen No.	Load (W) (lbs) (kgf)	Deflection (Δ) in. (cm)	Bending Stress (σ_f) psi(kgf/cm^2)	Shear Stress (τ) psi(kgf/cm^2)	Remarks
$\frac{1BST_2^{\frac{1}{2}}-C}{}$					
11" wide	400(181.4)	.093(.23)	434(30.5)	4.8(.34)	
Span = 42"					
Additional BPG cloth at bottom face	500(227)	.15 (.38)	542(38)	6.0(.42)	Shear bond failure at core-"cloth" interface. Crushing of core in the loaded zone (Fig. 7.3)
Faces $\frac{P}{C}$ = 15% solids	900(408)	.70(1.77)	975(68.6)	10.9(.76)	
3/8"-cell Honeycomb					
1/4"-thick faces					

(continued)

Specimen No.	Load (W) (lbs) (kgf)	Deflection (Δ) in. (cm)	Bending Stress (σ_f) psi(kgf/cm^2)	Shear Stress (τ) psi(kgf/cm^2)	Remarks
2BST$^{\frac{1}{2}}_{2}$-C					
Span = 24"	400(181.4)	.064(.16)	248(17.4)	4.8(.34)	
Same as 1BST$^{\frac{1}{2}}_{2}$-C	500(227)	.087(.22)	310(21.7)	6.0(.42)	Early shear bond failure at core-"cloth" interface.
	650(295)	.15 (.38)	402(28.3)	7.8(.55)	Crushing of core under applied load.
3BST$^{\frac{1}{2}}_{2}$-C					
Span = 12"	400(181.4)	.026(.066)	124(8.70)	4.8(.34)	
Same as	700(317)	.051(.129)	217(15.2)	8.5(.59)	Crushing of core and top face under applied load
1BST$^{\frac{1}{2}}_{2}$-C	1250(567)	.37 (.94)	387(27.2)	14.1(1.06)	

CHAPTER 8

DESIGN AND TESTING OF JOINTS

CHAPTER 8

DESIGN AND TESTING OF JOINTS

The design of CM panels requires a joint so that two or more panels can be joined together and perform as one continuous panel.

The strengths required are safe loads of approximately 500 lb/in. (89.3 kgf/cm) for the wheat container and 250 lb/in. (44.6 kgf/cm) for the housing module.

The joint in principal (J1) is shown in Figure 8.1. The machined aluminum pieces were held in place by two bolts 3/8" in diameter. Four variations were tested; the fifth variation, not yet tested, was adopted in the prototype model of the housing version.

In order to test the joint strength, avoiding secondary failures, the joint specimens were used to connect together sections of solid ~~LMC~~ mortar (except the first joint) to form simple centrally loaded beams.

The first variation (J1) supported a maximum load of 500 lbs (226.8 kgf) over a 21½" clear span resulting in an 89 lb/in (17.9 kgf/cm) force at the plates. Failure was due to the early bond failure between the bottom plate and the mortar.

The second variation (J2) is shown in Fig. 8.2, along with a picture of the tested specimen. At 14 days from

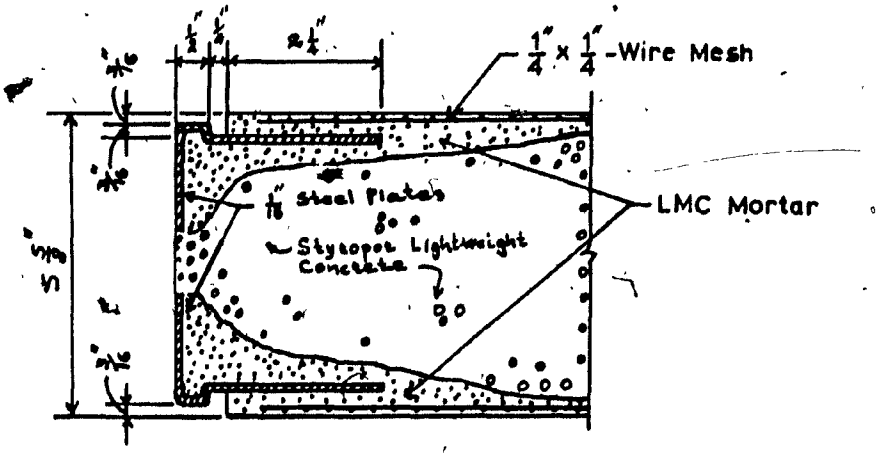

(a)

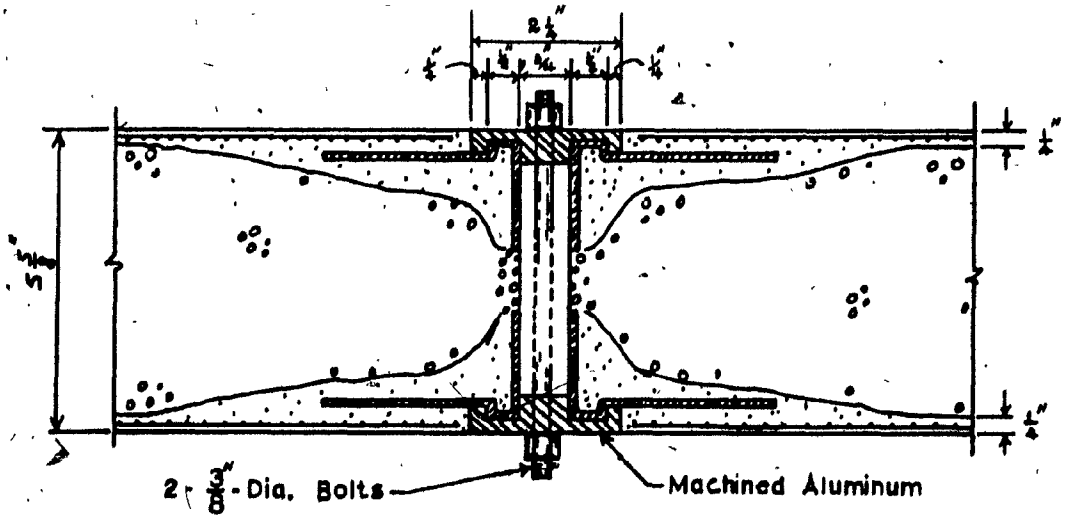

(b)

FIG. 8.1 DETAIL OF THE JOINT IN PRINCIPAL (J1). (a) EDGE DETAIL, (b) ASSEMBLY OF THE JOINT

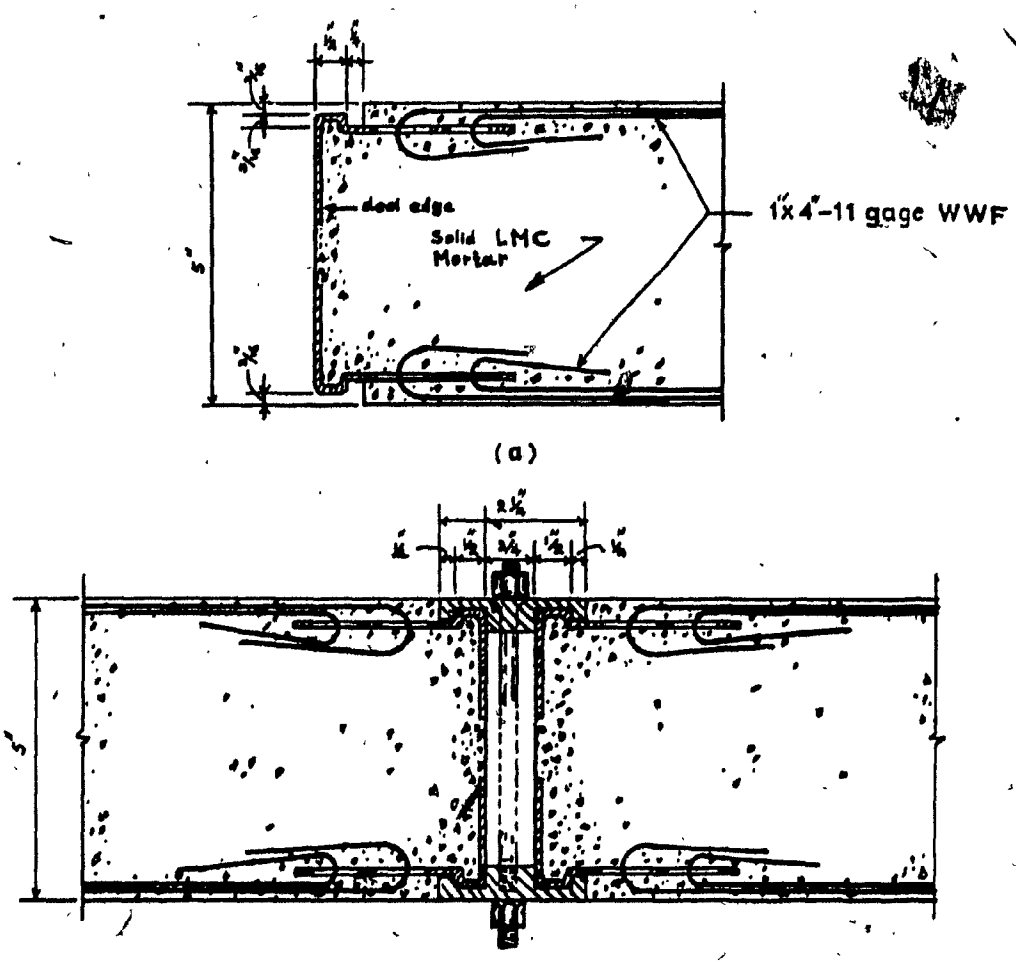

(a)

(b)

(c)

FIG. 8.2 JOINT VARIATION (J2). (a) EDGE DETAIL, (b) ASSEMBLY (c) TESTED SPECIMEN OVER A 20" CLEAR SPAN

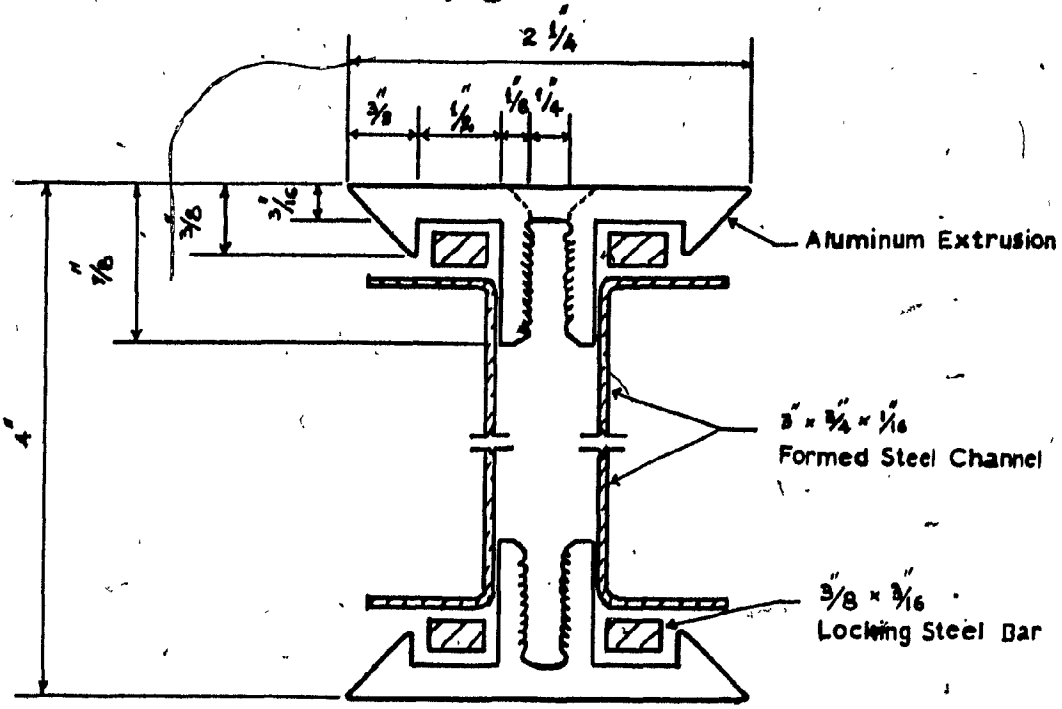

(a)

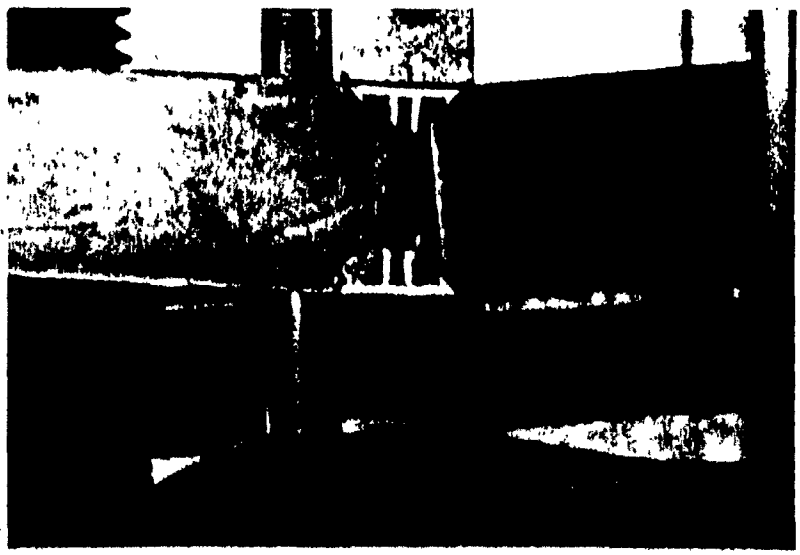

(b)

FIG. 8.3 JOINT VARIATION (J3). (a) COMPONENTAL DETAILING. THE BFG "CLOTH" AROUND THE LOCKING BARS AND THE TWO 1/4"-DIAMETER BOLTS ARE NOT SHOWN. (b) TESTED SPECIMEN OVER A 45½" CLEAR SPAN

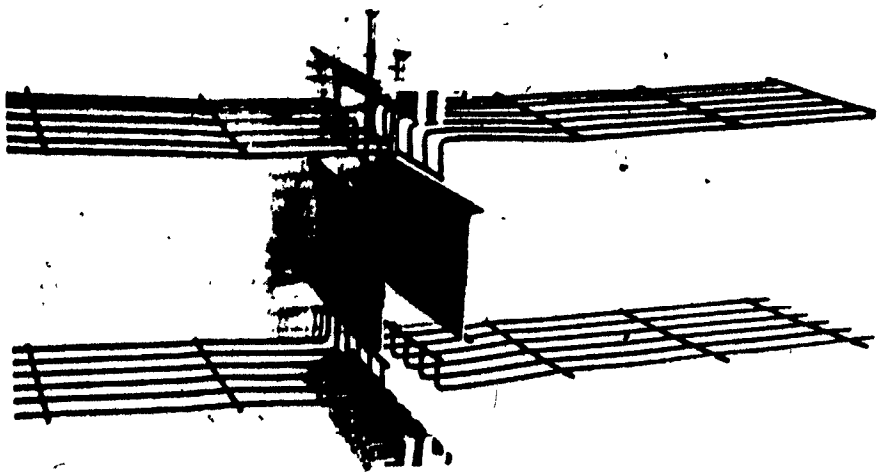

(a)

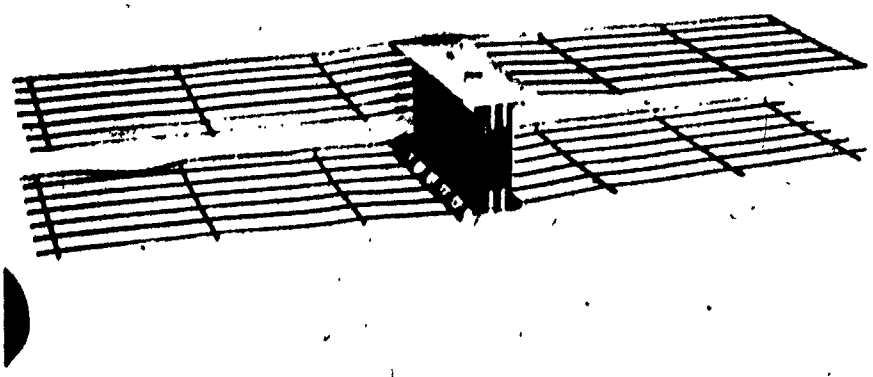

(b)

FIG. 8.4 JOINT VARIATION (J4). (a) COMPONENTAL DETAILING. (b) ASSEMBLY

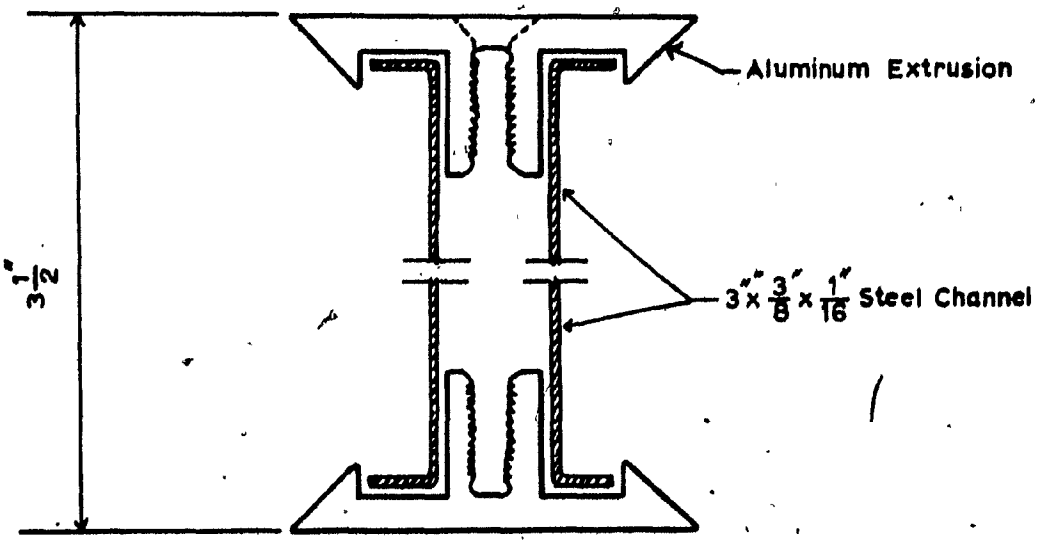

FIG. 8.5 JOINT VARIATION (J5). THE BFG "CLOTH" AROUND THE CHANNEL AND THE BOLTS ARE NOT SHOWN

casting, a maximum useful load of 6,600 lbs(2,994 kgf) was applied on a 20" span. The specimen failed at 7,000 lbs (3,175 kgf) giving a maximum moment of 35,000 lb/in(40,320 kgf/cm) or a resisting force of 1,296 lb/in(231.5 kgf/cm) in the reinforcement.

Failure occurred when the 1/4" layer of concrete below the bottom perforated plate peeled from reinforcement. The results of this test were very satisfactory, however, the formed profile could not be easily produced and a third variation (J3) shown in Fig. 8.3, was tested. In this joint, 3/8" x 3/16" "locking bars" with one layer of BFG reinforcement wrapped around, were glued to the flanges of a simple channel using 5-minute epoxy adhesive. The special aluminum extrusions (alloy AT 6351-T6) were held in place by one 1/4" in diameter bolt.

The central load at failure of the 45½" span specimen was P_{max} = 340 lbs(154 kgf) producing a moment of M_{max} = 3867 lbs-in (4,455 kgf-cm). Failure occurred in the BFG reinforcement at a tensile force of 215 lb/in(33.7 kgf/cm) or approximately 22 lb/thread(3.4 kgf/thread). It was noted that no damage occurred to the bond between the "locking bar" and the channel as it is technically unstressed. A picture of the failed specimen is shown in Fig. 8.3. By increasing the amount of reinforcement, the capacity of the joint would be increased proportionally.

The fourth type of joint (J4) was devised to make use of the existing extrusions and channels with steel mesh rein-

forcement, for a one-off prototype of the wheat container version.

The 4" x 1" - 11 gage welded wire fabric was bent around the channels as shown in Fig. 8.4a. Slots were milled in the aluminum extrusions to allow the steel wires to pass through and be secured as shown in Fig. 2.4b. No adhesive was involved.

The maximum centrally applied load was P_{max} = 1100 lbs (499 kgf) over a 40" span, giving a moment M_{max} = 11000 lb-in (12,674 kgf-cm) or a force of 611 lb/in. (109 kgf/cm) in the reinforcement, which is lower than the capacity of the wire mesh (840 lb/in). Failure occurred when the steel mesh slipped through the "leg" of the bottom extrusion and the channel. Increased capacity can be obtained by providing against slippage through better fitting or welding the wires to the channel.

In the joint (J5) used for the prototype demonstration model of the housing version (Fig. 8.5), BFG reinforcement is wrapped around the edge framing channels with the flanges of the channel used for anchorage as in J4. The exposed "cloth" along the non-connecting edges is of minor concern at this stage.

CHAPTER 9

PERFORMANCE OF CONCRETE SANDWICH PANELS

CHAPTER 9

PERFORMANCE OF CONCRETE SANDWICH PANELS

9.1 THE CONSTANT MODULE ELEMENT

The actual purpose of the research for a new combination of materials and subsequent investigation on sandwich beams, was the development and construction of the CONSTANT MODULE ELEMENT (CM panel). The individual element is a rigid unit consisting of a panel and two half-columns. Four such elements are combined to form a rigid structure (Fig. 9.1). The intended dual use of the MODULE (containerization and housing) requires performance capabilities meeting ISO standards and the National Building Code. The loads that must be sustained by the structure are given in Table 9.1.

A minimum panel weight of 10-12 psf(48.8 - 58.6 kg/m^2) required to resist safe bending loads of approximately 500 lb/in (89.3 kgf/cm) and 250 lb/in. (44.6 kgf/cm) for the wheat container and housing modules respectively was the initial objective.

The results in the previous Chapters indicated that the requirements can be met and full-size panels were fabricated for testing.

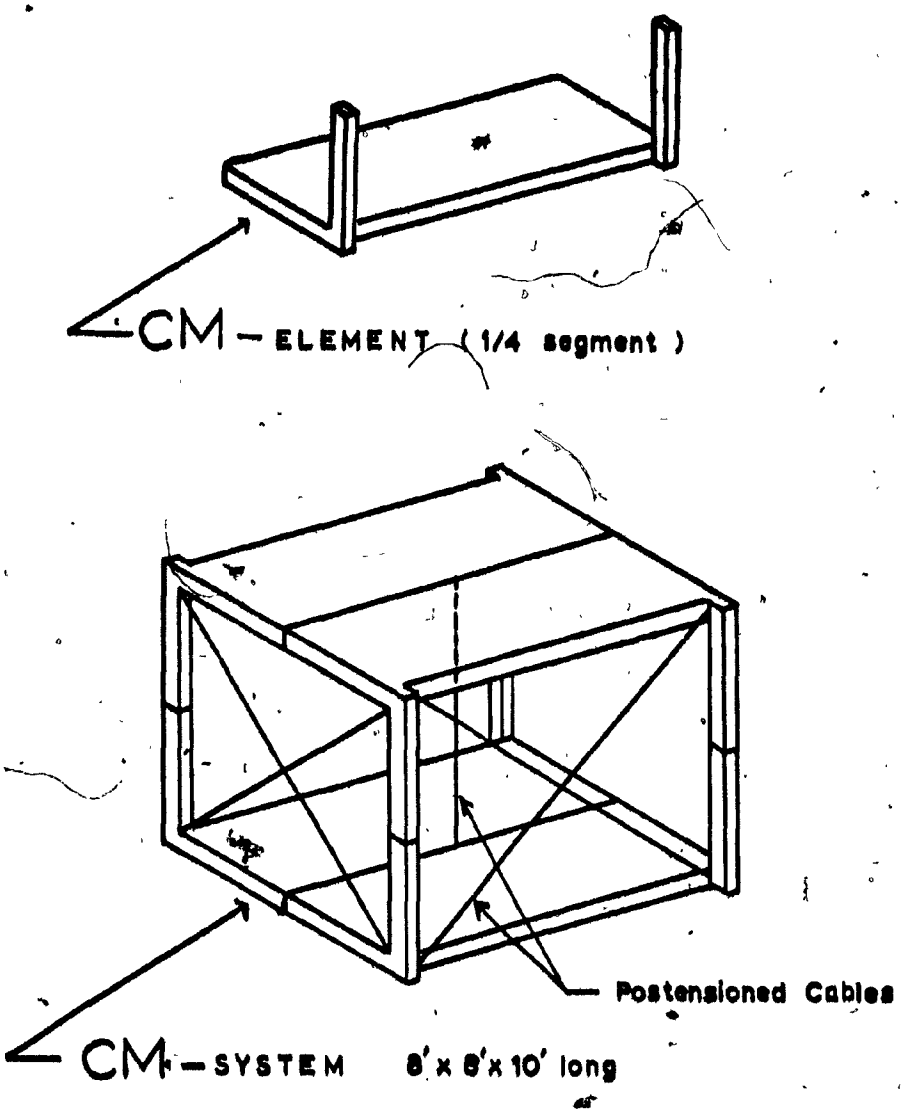

FIG. 9.1 THE CONSTANT MODULE (CM) SYSTEM IN PRINCIPAL

TABLE 9.1

LOADING REQUIREMENTS FOR CM SYSTEM

Description	Floor Load	Local Load	Lateral Load	Longitudinal Load	Column Load
Dwelling	50 psf	1000 lb on 30" x 30"	300 lb/ft	300 lb/ft	2000 lbs
Container	300 psf	600 lb on 22" x 22"	6 tons	24 tons	85 tons

In the meantime, two complete CM units, one for a wheat container and one for housing were manufactured and shipped for exhibiting at Habitat Forum in Vancouver, June 1976.

For the first set of CM panels only paper honeycomb was used as core material.

9.2 CONSTRUCTION AND TESTING OF CM PANELS

For the construction of the CM panels (container version, 5" thick) 3/4" cell size manually expanded honeycomb core, 4½" thick was used with one layer of Bobtex Fibre Glass reinforcement bonded on each face. The B.F.G. "cloth" was wrapped completely around the honeycomb and glued with commercial contact cement.

Three pieces of honeycomb[1] per CM panel of approximately 41" x 39" were used, leaving a 1/2" gap around the edge and two intermediate 1" gaps which were filled with LMC mortar.

The J3 type of joint was used with a 9" wide strip of B.F.G. "cloth" wrapped around the full length of the locking bar, so that an approximately 7" wide strip was left for splicing into the face. Half of the cross-section of the CM panel, is shown in Fig. 9.2.

---

[1] Unfortunately, due to dimension constraints, the WT-plane was used parallel to the long 10' spans.

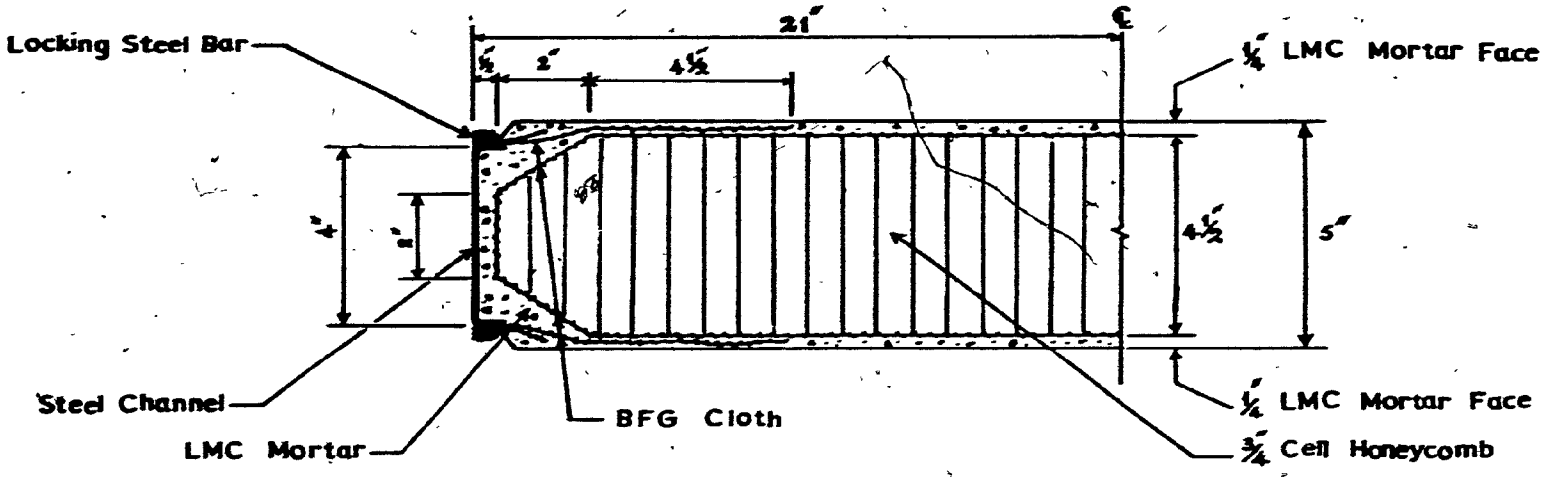

FIG. 9.2 DETAIL OF CM PANEL CROSS-SECTION (1/2-SPAN OF THE SHORT DIRECTION)

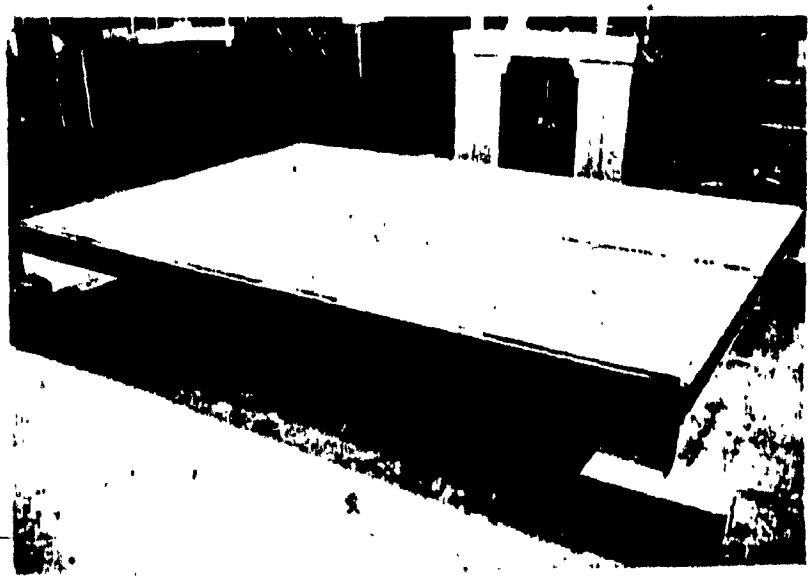

(a)

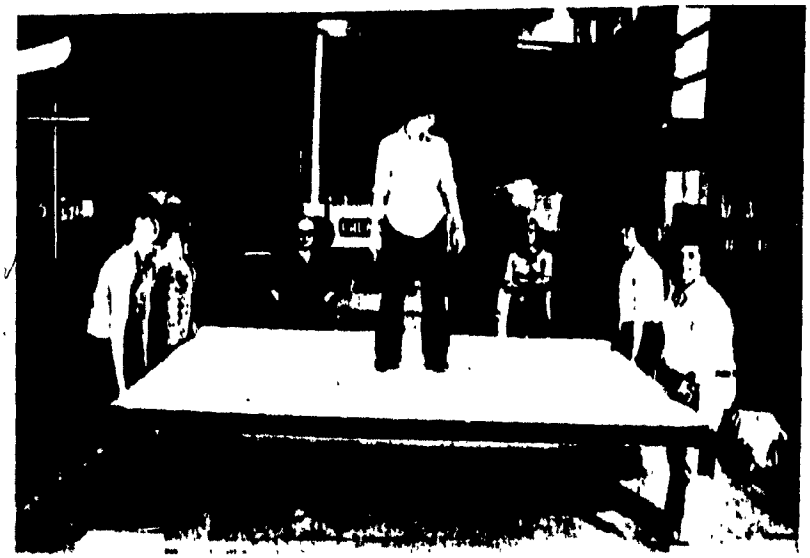

(b)

FIG. 9.3 TWO CM PANELS JOINED TOGETHER WITH JOINT J3. (a) THE SYSTEM IS SUPPORTED AT THE CORNERS BY 4 WELDED POSTS (3" x 3" ANGLES). (b) THE SYSTEM IS EASILY LIFTED BY 4 STUDENTS. THE WEIGHT OF EACH 42" x 119", 5" DEEP PANEL IS ESTIMATED TO BE 275 LBS (125 KG)

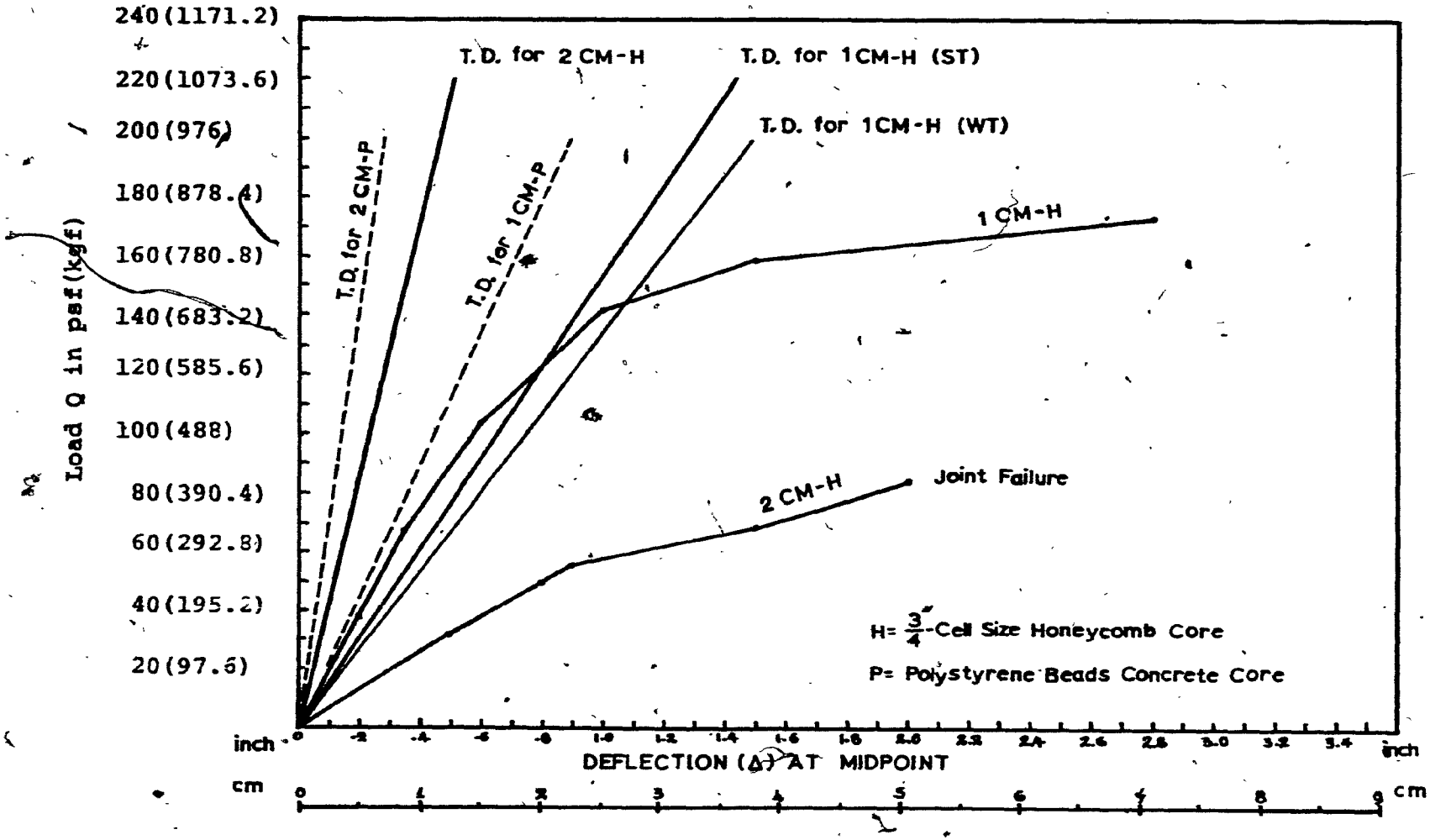

FIG. 9.4 LOAD-DEFLECTION CURVES FOR THE TESTED CM PANELS

(a)

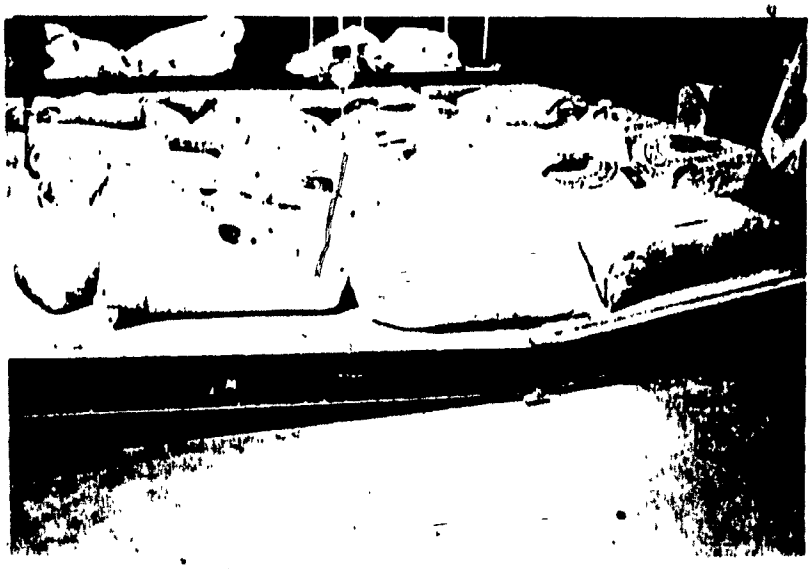

(b)

FIG. 9.5 TESTED CM PANELS. (a) LONG SIDE (b) FAILED JOINT SIDE

FIG. 9.6 SINGLE CM PANEL AT LAST STAGE OF LOADING (q = 173 psf). THE PANEL DID NOT FAIL COMPLETELY

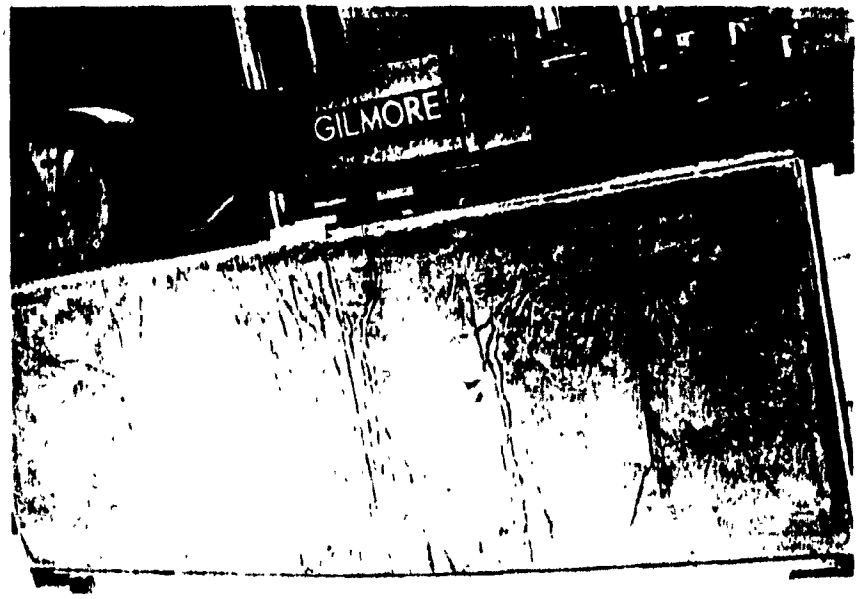

(a)

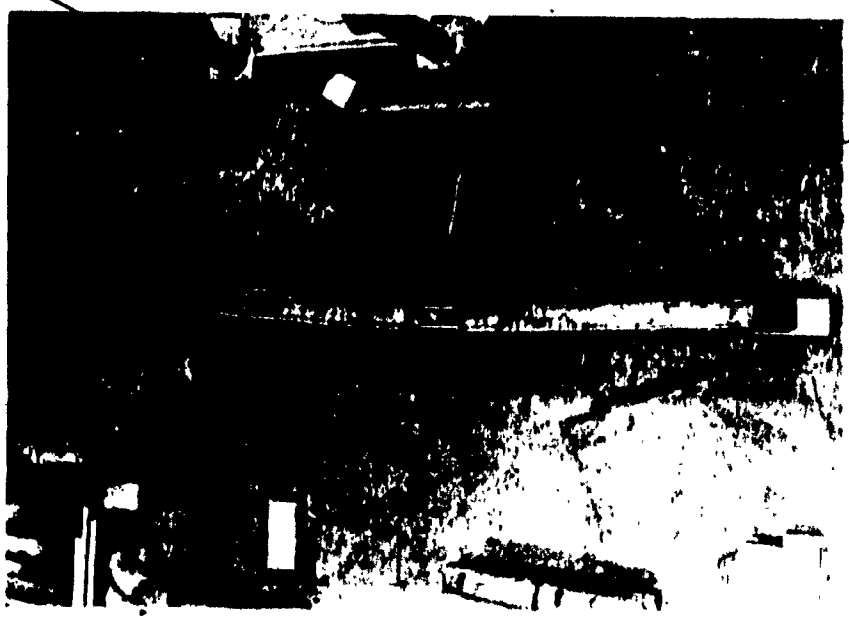

(b)

FIG. 9.7 (a) BOTTOM FACE OF SINGLE CM PANEL AFTER TESTING
(b) LONG SIDE ELEVATION SHOWS THE PERMANENT DEFORMATION

Four 10" x 42" "cloth" strips were placed at the faces above and below the two ribs to ensure continuity.

Two CM panels joined together weighed approximately 550 lbs(249 kgm) (Fig. 9.3a) easily lifted by 4 high-school students are seen in Fig. 9.3b. This demonstrates that the CM system can be handled manually.

The first test was performed at 14 days on the two CM panels of Fig. 9.3, supported on four corners. Cement bags, sand bags, shot bags and people were used for loading.

A 6-inch dial indicator was used to measure the deflections at midpoint of the panel. Fig. 9.4 shows the load-deflection curve obtained from the test, along with the computed deflections. The relatively large deflection (as compared to the theoretical, based on a 7' long by 1' wide beam) is believed to come from the slack and slipping in the joint. The system failed at a total load of 5800 lbs(2631 kgf) or 83 psf(405 kgf/cm^2). The two sides of the system after failure are shown in Fig. 9.5.

Failure was due to partial slip of the aluminum extrusions in the joint and tension failure in the B.F.G. reinforcement. The load in the joint at failure was 218 lb/in. (38.93 kgf/cm), which is approximately the capacity of the "cloth".

Then, the single undamaged panel was inverted, supported at four corners and loaded again. It took 6,000 lbs

(2732 kgf) or 173 psf(844 kgf/m^2) to reach the deformed position (Δ = 2.8" at midpoint) shown in Fig. 9.6. It can be seen in the same picture that the panel did not fail completely. The test was halted due to lack of additional load.

The experimental load vs. deflection curve for this panel is plotted in Fig. 9.4, which is in good agreement with the deflections in the linear range, computed using a 10' long by 1' wide uniformly loaded simply supported beam and equation (4.21). The maximum force in the face was 478 lb/in. (85.3 kgf/cm). It is noted that the share of the moment carried by the edge channels was not considered (5/8" x 1/16" thick flanges). The only visible damage was small cracking of the bottom face as shown in Fig. 9.7a. No visible deformation was observed in the short (42")direction of the CM panel as it can be seen in Fig. 9.7b, which also shows the permanent longitudinal deformation of the panel. This deformation is believed to be due to the permanent deformation of the main panel since no visible yielding of the steel edges was observed.

9.3 OBSERVATIONS AND COMMENTS

The theoretical deflections in the elastic range, for the single panel, are greater than the experimental deflections by a maximum of 15% (WT-Plane).

Deviation from linearity started at a load of approxi-

mately 70 psf, which gives a shear stress (although difficult to analyze) of approximately $\left(\frac{70 \text{ psf}}{12'' \times 4.75''}\right) \frac{10'}{2} = 6.2$ psi. This stress is close to the shear strength (8.0 psi) of the honeycomb in the WT-plane, determined by shear tests.

Creep deformations may be explained by the slow failure of the core at 70 psf of loading, and by the early failure of the adhesive. The maximum shear stress at failure must have exceeded $\left(\frac{173 \text{ psf}}{12'' \times 4.75''}\right) \frac{10'}{2} = 15.1$ psi (1.06 kgf/cm^2) which is approximately twice the shear strength of the honeycomb (WT-plane).

The total weight of the panels was estimated to be 7.8 psf(35 kgf/m^2). Based on a 10' long 1' wide beam with 3/4"-cell kraft paper honeycomb core, the shear deformations are 86% of the bending deformations or 46% of the total, with respect to the ST-Plane. These deformations are relatively high, which suggests that a better honeycomb with higher shear rigidity should be used.

CHAPTER 10

CONCLUSION

CHAPTER 10

CONCLUSION

Although there is no history of the use of concrete as 1/4" thick face material in lightweight sandwich construction, the present research and investigation showed that Latex Modified Concrete mortars can undoubtedly be used as a hard, strong and durable face material.

An expanded polystyrene beads-filled (styropor) lightweight concrete has the desired mechanical and physical properties for the core in sandwich construction. A 4" thick panel using this material, with 1/4" thick LMC mortar faces weighed 10 psf (48.8 kg/m^2).

The tests on simply supported sandwich beams with this core showed strengths similar to those obtained in independent tests on the skin and core. Shear deformations are relatively high. Based on a 10' long, 1' wide, 5" deep beam, shear deformation is 22% of the total.

Using paper honeycomb as the core material gave a weight for a 4" thick sandwich panel of 5 psf (24.4 kg/m^2). In this case, the shear strength was very much lower, between 15% and 25% of the styropor. This strength is sufficient for the housing module but may require improvement for the container module.

Panels with untreated 3/4" cell size honeycomb core, the weakest type, were constructed and tested. These provided overall bending strengths (478 lb/in) superior to that (240 lb/in) of individual 6-inch wide sandwich beams with no evidence of shear distress. This strength is 4% lower than the safe loads required for the container module, and 88% higher than those required for the housing module.

Assuming a limiting deflection $\frac{L}{360}$ = .33 inches, two CM rigidly connected concrete panels with honeycomb core, simply supported at four corners, can carry a load of 145 psf.

In the final design proposed for adoption the materials are Latex Modified Concrete for the 1/4" thick skin, Bobtex Fibre Glass, 3/4"-cell size resin impregnated kraft paper honeycomb, with a 1/16" thick steel channel frame.

Future work should involve investigation in firerating, durability, handling damage, long-term loading, preparing design tables and planning of production techniques.

Such a panel 119" x 42" x 5" thick weighed 7.8 psf (38 kg/m^2).

REFERENCES

REFERENCES

[1] Dow Latex 460 and 464 Improve the Properties of Portland Cement Mortars, Technical Sales Bulletin, The Dow Chemical Co., Midland, Michigan, (1973).

[2] Cook, D.J., "Expanded Polystyrene Beads as Lightweight Aggregate for Concrete", Precast Concrete, Vol.4, No.12, (December 1973), pp.691-693.

[3] Allen, H.G., Analysis and Design of Structural Sandwich Panels, Pergamon Press, (1969).

APPENDIX "A"

ADDITIONAL INFORMATION ON MECHANICAL AND PHYSICAL PROPERTIES OF LATEX MODIFIED CONCRETE MORTARS[1]

TABLE A1 - TYPICAL MECHANICAL PROPERTIES OF LMC MORTARS

TABLE A2 - COMPARISON OF LMC MORTARS MADE WITH TYPE I AND TYPE III PORTLAND CEMENT

TABLE A3 - ABRASION RESISTANCE OF LMC MORTARS

TABLE A1

TYPICAL MECHANICAL PROPERTIES OF LMC MORTARS

Sand/Cement = 3/1, Latex Solids as a % of weight of Cement with Antifoam B

Property and Cure Time	Dow Latex 460 Formulations			Unmodified Control[1]	Dow Latex 464 Formulations		
	10% Latex (psi)	15% Latex (psi)	20% Latex (psi)	(psi)	15% Latex (psi)	20% Latex (psi)	25% Latex (psi)
Compressive Strength							
2D	1940	1670	2080	1560	2330	3300	2420
7D	3380	3220	3360	3500	4300	5770	4400
14D	3730	3750	4150	4200	5160	7150	8000
28D	4000	4130	4800	4480	6180	8430	9670
28D/7W	2890	3000	3680	4430	3960	7150	7560
Tensile Strength							
2D	390	400	480	220	340	470	600
7D	550	670	750	320	670	810	880
14D	600	740	830	350	760	870	970
28D	630	790	870	380	820	910	1000

(continued)

Property and Cure Time	Dow Latex 460 Formulations			Unmodified Control[1]	Dow Latex 464 Formulations		
	10% Latex (psi)	15% Latex (psi)	20% Latex (psi)	(psi)	15% Latex (psi)	20% Latex (psi)	25% Latex (psi)
Shear Bond Strength							
2D	390	530	280	-	280	510	500
7D	620	> 650	> 650	-	530	> 650	> 650
14D	630	> 650	> 650	-	560	> 650	> 650
28D	630	> 650	> 650	50-200	> 650	> 650	> 650
28D/7W	300	330	370	50-200	400	> 650	> 650
Flexural Strength Modulus of Rapture							
2D	950	1080	1070	-	1040	1190	1280
7D	1090	1380	1510	660	1520	1550	1600
14D	1120	1520	1680	740	1710	1740	1770
28D	1130	1620	1730	820	1750	1820	1900
28D/7W	640	790	770	980	1200	1100	1150

(continued)

Property and Cure Time	Dow Latex 460 Formulations			Unmodified Control[1]	Dow Latex 464 Formulations		
	10% Latex (psi)	15% Latex (psi)	20% Latex (psi)	(psi)	15% Latex (psi)	20% Latex (psi)	25% Latex (psi)
Elastic Modulus ($\times 10^6$)							
2D	-	1.43	1.23	-	-	1.68	1.62
7D	-	1.72	1.42	2.85	-	2.10	1.77
14D	-	1.80	1.50	3.04	-	2.24	1.99
28D	-	1.92	1.56	3.40	-	2.52	2.25
28D/7W	-	1.40	0.66	3.74	-	2.44	1.98

D = Number of days dry cured at 73°F(23°C) and 50% relative humidity, tested dry.

28D/7W = 28 days dry cured at 73°F(23°C) and 50% relative humidity followed by 7 days water immersion at 75°F(24°C), tested wet.

[1] The unmodified control mortar has a sand-to-cement-to-water ratio of 3-to-1-to-0.50 by Weight.

These samples were cured at 73°F(23°C) and 100% relative humidity.

TABLE A2

COMPARISON OF LMC MORTARS MADE WITH TYPE I AND TYPE III PORTLAND CEMENT

(Polymer Content = 20% Dow Latex 464)

Property and Cure Time	Type I Cement (psi)	Type III Cement (psi)
Compressive Strength		
2D	3306	5060
7D	5770	7190
14D	7150	7610
28D	8430	8520
Tensile Strength		
7D	810	700
14D	870	950
28D	910	980
Shear Bond Strength		
7D through 28D	> 650	> 650
Flexural Strength		
7D	1550	1330
14D	1740	2130
28D	1820	2280

D Days dry cured at 73°F (23°C) and 50% relative humidity

TABLE A3

ABRASION RESISTANCE OF LMC MORTARS
(ASTM C241-51)

Dow Latex	% Weight Loss	
	Dry	Wet
None	4.80	3.50
15%-460	1.21	2.81
20%-460	1.00	2.70
20%-464	1.44	2.46
25%-464	1.16	2.20

CURE SCHEDULE:

Unmodified Dry Cure = Curing at 73°F and 100% relative humidity for 14 days followed by 14 days at 73°F and 50% relative humidity

Unmodified Wet Cure = 27 days at 73°F and 100% relative humidity followed by 1 day water immersion at 75°F

Modified Dry Cure = 28 days at 73°F and 50% relative humidity

Modified Wet Cure = 14 days at 73°F and 50% relative humidity followed by 13 days at 73°F and 100% relative humidity followed by 1 day water immersion at 75°F.

APPENDIX "B"

TERMS AND DEFINITIONS, ABBREVIATIONS

B1 TERMS AND DEFINITIONS

Antifoam "B" = A liquid agent used with Latexes to minimize the air content of Latex Modified Concrete mortars

Perm = The rate of water vapor transmission through a specimen caused by the vapor pressure difference across the specimen

MEL-lite = Rotary kiln expanded shale light-weight aggregate

Fineness Modulus = A number which determines the relative fineness or coarseness of fine aggregates. Allowable fineness modulus number range from 2.30 to 3.10.

Segregation = The separation of one-size particles or aggregates in excess, or due to large density difference

Core Shear Stiffness = $AG = \frac{bd^2}{c} G$

Thin Face = A face where I_f is negligible, however, not so thin that d and c can be equated

B2 ABBREVIATIONS

LMC	=	Latex Modified Concrete
WVTR	=	Water Vapor Transmission Rate
BFG	=	Bobtex Fibre Glass
$C_xL_yW_z$	=	Cement, Latex, Water contents in 1 cu.ft. of Styropor-Filled Concrete
T.D.	=	Theoretical Deflection of sandwich beams or panels
BWT-H	=	Beams with the weak direction of the honeycomb along the principal x-axis
BST-H or C	=	Beams with the strong direction of the honeycomb or cormat along the principal x-axis